Effect of Surface Oxygen Groups on Irreversible Adsorption of Volatile Organic Compounds on Beaded Activated Carbon

by

Nastaran Mosavari Nezamabad

A thesis submitted in partial fulfillment of the requirements for the degree of

Master of Science

in

Environmental Engineering

Department of Civil and Environmental Engineering

University of Alberta

ABSTRACT

Adsorption by activated carbons is a widely used method for controlling emission of volatile organic compounds (VOCs). However, accumulation of adsorbates and/or regeneration by-products (heel buildup) during cyclic process is a common challenge in this process. Irreversible adsorption restricts complete regeneration of adsorbent and reduces its capacity and lifetime. The objective of this research is to understand the impact of surface oxygen groups on heel build-up and adsorption capacity of activated carbon. For this purpose, the content of surface oxygen groups on beaded activated carbon (BAC) was modified by acid treatment and high temperature hydrogen treatment. The BET analysis showed that acid treatment and hydrogen treatment did not have a significant effect on pore size distribution and surface area. However, acid treatment increased the surface oxygen groups and hydrogen treatment decreased the surface oxygen groups' content of BAC. Then, five-cycle adsorption/regeneration tests with eight compounds with different functional groups were completed on prepared adsorbents. Based on mass balance and thermos-gravimetric analysis, heel build-up for hydrogen treated BAC (BAC-H-950) was similar to heat treated BAC (BAC-400), but lower than that of acid-treated BAC (BAC-O-400). For oxygen deficient samples, it can be concluded that adsorption was due to physisorption as most of adsorbates were desorbed during regeneration. For oxygen-rich samples, surface oxygen groups were consumed through reaction with adsorbates. Moreover, adsorbates with benzene ring formed stronger interaction with surface oxygen groups and showed higher heel relative to other tested adsorabtes. The results of this work will provide a better understanding of irreversible adsorption and its relation to surface chemistry of adsorbents.

DEDICATION

It would be my honor to dedicate this dissertation to my parents for their endless support throughout my life and encouraging me to pursue my goals.

ACKNOWLEDGMENTS

First and foremost, I would like to express my deepest appreciation to my supervisor, Dr. Zaher Hashisho, for supervision, guidance, and support during my studies. This work could not be accomplished without his expertise, knowledge, and passion.

I would like to acknowledge financial support from Ford Motor Company and the Natural Science and Engineering Research Council (NSERC) of Canada. Also, I acknowledge infrastructure and instrument grants from Canada Foundation for Innovation (CFI), NSERC, and Alberta Advanced Education and Technology.

I would like to thank my colleagues in air quality and control research characterization laboratory for their assistance, availability and suggestions in my experiments.

Table of Contents

List of Tables:

List of Figures:

List of Acronyms:

AC	Activated Carbon
BAC	Beaded Activated Carbon
BAC-H	Hydrogen-Treated BAC
BAC-O	Oxygen Functionalized BAC
BET	Brunauer-Emmett-Teller
DAC	Data Acquisition and Control
DTG	Derivative Thermo-Gravimetric
MFC	Mass Flow Controller
PSD	Pore Size Distribution
QSDFT	Quenched Solid Density Functional Theory
SCCM	Standard Cubic Centimeter per Minute
SOG	Surface Oxygen Group
SLPM	Standard Liter per Minute
TGA	Thermo-Gravimetric Analysis
VOC	Volatile Organic Compound
XPS	X-Ray Photoelectron Spectroscopy

1 INTRODUCTION

1.1 Volatile organic compounds (VOCs)

Volatile organic compounds (VOCs) are chemicals which have a boiling point less than or equal to 250 ºC in atmospheric pressure (101.3 Kpa). Most organic compounds with less than twelve carbon atoms usually are considered as VOCs [1]. The US environmental protection agency (EPA) define a VOC as "any compound of carbon, excluding carbon monoxide, carbon dioxide, carbonic acid, metallic carbides or carbonates, and ammonium carbonate, which participates in atmospheric photochemical reactions" [1]. They are usually emitted from automobile exhaust (i.e. 45%) and industries involving paints, varnishes, detergents, solvents, lubricants, thinners, and liquid fuels (i.e. 41%) [2]. According to Kim, about 6.58 kg of VOCs is used as paint solvents per vehicle in a typical automotive painting operation in North America [3].

Exposure to VOCs can cause eye irritation, nose irritation, throat irritation, headache, liver and kidney damage [4, 5]. Moreover, most of them have been identified as toxic and carcinogenic materials [6-8]. Concerns about negative impacts of VOCs on human and environmental triggered a lot of researches in developing treatment technologies to control or eliminate VOCs emission.

1.2 VOC abatement techniques

Different strategies are employed to control VOCs emission. These methods may be applied in two ways: improvements/redesign of processes or using additional control methods to control emissions. Modifying unit operations, such as increasing process yields, increasing separation levels, or simply decreasing fugitive emission are considered as improvement methods. Process redesign includes more significant changes in processes, such as switching from an organic phase to an aqueous phase, going from batch to continuous operation [2]. Although improving/redesigning methods are the most effective and efficient methods, their application is restricted since it is not always possible to adjust process or equipment. The second group includes techniques that add a treatment process to control or eliminate pollutant from off streams. A number of treatment techniques are available and they can categorized into two sub-groups, namely destructive and recovery methods [9]. In recovery methods, pollutants are removed from gas streams so that their nature and properties are preserved and they can be reused. Absorption, adsorption, condensation, and membrane separation for gaseous and liquid streams are example of recovery techniques [9, 10]. But, VOCs can also be converted to non-hazardous chemical compounds, often CO_2 and H_2O, using destructive methods such as catalytic/ thermal incineration and biological treatment [11].

Based on pollutant type, source, concentration, flow rate, presence of compounds other than VOCs, recovery potential, regulatory limits, fire and explosion hazards, location, cost, removal efficiency, and operation possibility of the selected technique, the best treatment method is chosen [10, 12, 13]. Khan and Ghoshal [9] classified the available VOCs removal techniques as shown in Figure 1-1.

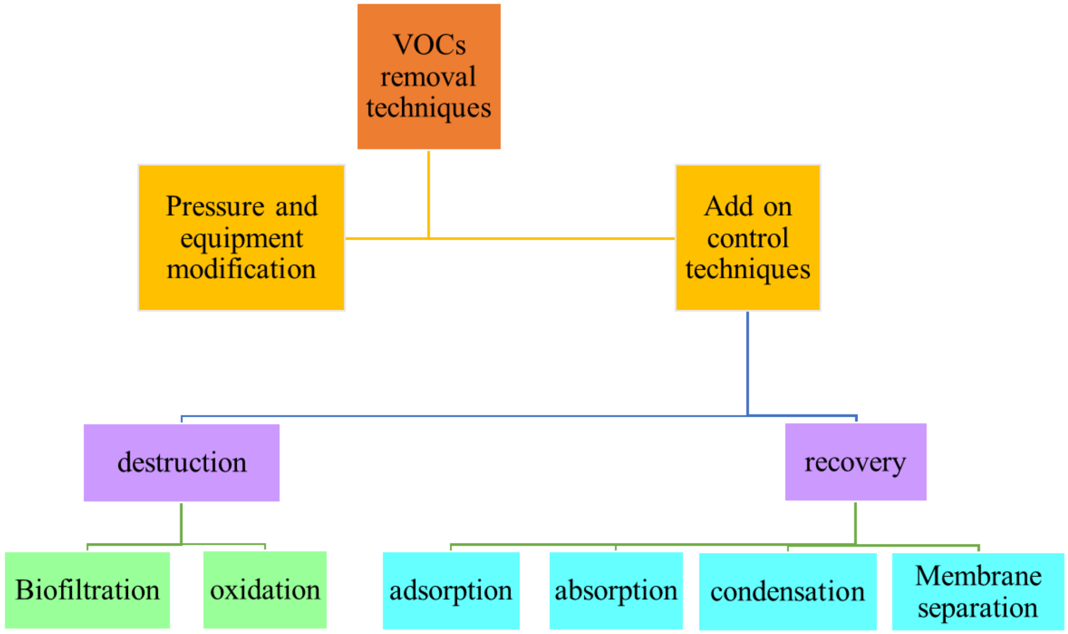

Figure 1-1. Classification of VOCs removal/ control techniques [9].

Among the methods listed in Figure 1-1, thermal/catalytic oxidation, condensation, absorption, biofiltration, and adsorption are common ones for VOCs abatement. Thermal oxidation is suitable for high concentration streams. As combustion may generate some noxious products, the outlet stream usually needs to be treated before release to atmosphere which restricts its applicability [9]. Catalytic oxidation is another method for VOCs removal but the catalyst should be compatible with the pollutant laden stream to prevent catalyst poisoning. Also, its energy recovery is moderate [9]. Condensation may be a feasible treatment for streams with high VOCs' concentration and low boiling point [9, 14]. However, its removal efficiency is usually low [9]. Catalytic/thermal oxidation and condensation methods are usually expensive treatment since they need high or low temperature for operation. Another method for VOCs abatement is biofiltration. It is economical and successful for low VOC concentration although its sluggishness, sensitivity to operating conditions, and selective destruction limit its commercial application [9, 14]. Absorption process can be used for VOC elimination from gas steams. It can be utilized for a wide range of concentrations and its process is simple with good efficiency. However, it has limited application since the method need some post-treatment such as distillation or extraction to remove pollutants from liquid phase, as well as high initial investment besides difficulties in design [9]. Adsorption is a low cost, high removal efficiency process for VOC control. It can be exploited for feed stream with high/low concentration, unsteady input concentration, and contaminants with a wide range of boiling point [9, 14].

1.3 Adsorption

Adsorption can be defined as the interaction between the field of forces of the solid surface and liquid or gas phase. The resultant forces from the field of forces attract and retain molecules, atoms, or ions of a fluid on the solid surface. This interaction appears when an unsaturated and unbalanced solid surface is brought in contact with a fluid. Hence, a higher concentration of the fluid is formed in the vicinity of the solid surface than in the bulk fluid phase [15].

Two types of forces may be involved in adsorption: physical forces which can be dipole moments and polarization forces, dispersive forces, or short-range repulsive interactions, and chemical forces which are valence forces resulting from redistribution of electron between solid surface and adsorbed atoms. Therefore, adsorption can be divided into two groups: physical adsorption and chemical adsorption based on the nature of involved forces [16-18].

In case of physical adsorption, van der walls forces, relatively weak forces, keep the adsorbate on the solid surface. On the other hand, chemisorption results from exchange or sharing of electrons between adsorbate molecules and adsorbent surface. The formed bond between the adsorbate and adsorbent is chemical bond and is much stronger than physisorption. In physical adsorption the enthalpy of adsorption is the same order as the heat of liquefaction and it is around 10-20 $kJ.mol^{-1}$, whereas in chemisorption the adsorption enthalpy is about 40-400 $kJ.mol^{-1}$[15]. The type of adsorption depends upon the nature of adsorbate and adsorbent, the surface reactivity, the surface area of adsorbate, and the temperature and pressure of adsorption [12, 15, 19].

Activated carbon, zeolite, or molecular sieve adsorbents are typical adsorbents for VOCs removal from gas and liquid streams, and their removal efficiency is usually more than 80% [15]. VOCs recovery may be possible when adsorption and regeneration process are coupled to each other [10, 20-22].

Activated carbon is extensively used as a media for removal of pollutants dissolved in aqueous/gaseous environment. The wide application of activated carbon results from its high surface area (500-1500 $m^2.g^{-1}$) and a well-developed internal microporosity structure [23]. The capacity and rate of adsorption of activated carbon depends upon its specific surface area, pore size distribution, and surface chemistry specifically presence of oxygen-containing groups [24, 25].

Activation process or post treatments can remove or form oxygen functional groups on surface of activated carbon [26, 27]. For example, heat treatment at high temperature in nitrogen or hydrogen environment can remove surface functional groups [28], while chemical oxidation process can add surface oxygen groups [26, 27]. The presence of surface oxygen functional groups has effect on adsorption capacity and irreversible adsorption characteristic of activated carbon. The extent of their influence on adsorption capacity and irreversible adsorption depends on adsorption media, adsorbate, and adsorbent characteristics.

1.4 Objective

The goal of this research is to determine the impact of activated carbon's surface oxygen groups on irreversible adsorption of volatile organic compounds, specially pollutants resulting from automotive painting. The adsorption behavior of activated carbon with surface oxygen groups (SOGs) has been well documented for removal of pollutant like phenol, methylene blue, or metals from liquid phase but there are a limited number research on the effect of SOGs on irreversible adsorption of organic compounds from gaseous phase. Hence, the main objective of this study is to investigate the effect of surface oxygen functional groups' content of beaded activated carbon on heel build-up from adsorption and desorption of organic vapors. A better understanding of heel formation and its relation to surface oxygen groups is essential to enhance adsorbent's lifetime and capacity. Increasing adsorbent lifetime results in a lot of saving for industries by reducing adsorbent consumption, disposal of spent adsorbent and labour cost.

1.5 Thesis outline

This thesis consists of five chapters which will contribute to fulfill the overall objective of this research. Chapter 1 provides an introduction about the background and purpose of the research. Chapter 2 is a literature review about adsorption, factors controlling adsorption, and activated carbon. The materials and methods used for completion of this research are explained in chapter 3. Experimental results and corresponding discussions are presented in chapter 4, and the research conclusion and recommendation for future work are provided in chapter 5.

2 LITERATURE REVIEW

2.1 Adsorption isotherm

The adsorption isotherm depicts adsorbate concentration on the adsorbent versus its concentration in liquid/gas phase. The capacity of adsorbents can be depicted by adsorption isotherms [12]. Adsorption isotherms can be classified in six main groups. Among them, type I, IV, and V are the most common for porous materials. Microporous adsorbents show a plateau at high concentration while mesoporous material have an ascending trend at high concentration [29]. Type I isotherms present microporous adsorbents when a monolayer coverage is formed at low adsorbate concentrations. Type II and type III isotherms are representative of multilayer adsorption on non-porous or highly macroporous adsorbents. Adsorbate –adsorbent interaction is stronger in type II than type III. In mesoporous material as a consequence of capillary condensation, a multilayer adsorption can occur (type IV). Type V presents adsorption behavior of porous material when the interaction between adsorbate and adsorbent is weak and similar to type III [15, 19]. Type VI is a rare one and a stepwise multilayer adsorption on a uniform non-porous surface. The slop of each step depends on the system and temperature [30].

34].

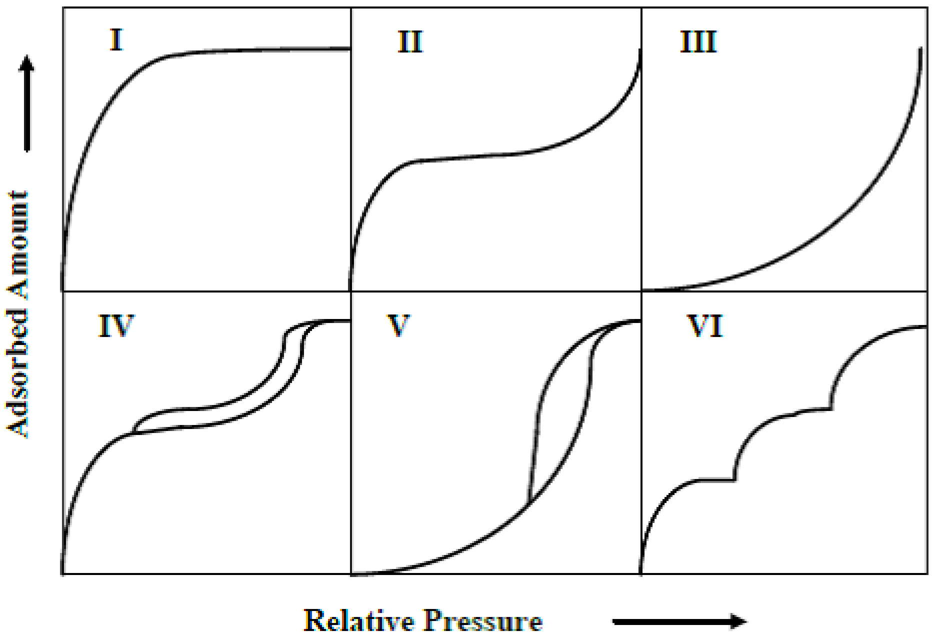

Figure 2-1. Adsorption isotherms in the IUPAC classification [31]

2.2 Adsorption's controlling elements

Many factors have effect on adsorption capacity, adsorption kinetic, and adsorbent regeneration. Understanding these factors and their impacts help to have a better control on adsorption process. These factors can be classified as adsorbent's physical and chemical properties, adsorbate characteristics, adsorption operating condition [32].

2.2.1 Adsorbent properties

Surface area, pore volume, pore size distribution, hydrophilicity/hydrophobicity, metal content, and surface functional groups have impact on adsorption ability of adsorbents [33, 34].

Typically, higher surface area corresponds to more adsorption sites for VOCs adsorption and higher adsorption capacity if there is an appropriate pore size for selected component [35, 36]. In addition to surface area of adsorbent, pore size distribution has significant influence on adsorption process. Lillo-Ro´ denas et al. [13] studied the effect of porosity on adsorption of toluene and benzene. They found that volume of narrow micropores governs adsorption at low VOCs concentration. The effect of pore size distribution on acetone and n-hexane's adsorption was considered by Huang et al. [32]. The difference in adsorption characteristic and diffusion of adsorbate was attributed to pore size distribution of adsorbent.

Although mesopores have more significant effect on adsorption capacity of VOCs at high concentration, it has been recognized that the volume of narrow micropores (<0.7 nm) is a governing factor in adsorption capacity and saturation time at low concentration of adsorbate [13, 29, 37]. Higher adsorption capacity of VOCs has been reported for activated carbon fiber compared to granular activated carbon due to higher volume of narrow micropores [38-40].

Other influential elements of adsorbent are surface accessibility, diffusion resistance and chemical properties. Sometimes, they are more decisive than surface area [32, 41].

2.2.2 Adsorbate properties

Physical and chemical properties of adsorbate have effect on its adsorption and regeneration. Molecular weight, size, structure, functional groups, polarity, and boiling point are the most important characters of adsorbate.

Li et al. (2012) found a linearly increasing relationship between adsorption capacity and molecular weight, size, boiling point, and density of adsorbate while pore size larger than the kinetic diameter of adsorbate are available.

As diffusion in adsorbent is controlling factor in adsorption rate, the molecular size of the adsorbate has critical role in adsorption/desorption rate [42, 43]. Adsorbates with large diameter are unable to enter narrow pores, which results in a lower adsorption capacity. Moreover, they have lower regeneration efficiency as they show low diffusion rate and may be trapped inside pores [44, 45]. Some adsorbents with limited pore size distribution can only adsorb molecules with specific range of kinetic diameters from a mixture. For a given pore size, the size and shape of adsorbate determine the amount adsorbed in a competitive adsorption mechanism [20, 46, 47].

Another important parameter is adsorbate polarity. Lee et al. [48] compared acetone (polar) and toluene (non – polar) adsorption on a hydrophobic adsorbent, and found that polar compounds presented higher affinity for hydrophilic adsorbent sites. So, adsorbate polarity is an influential factor on adsorption. However, Chiang et al. [49] reported that the surface area and pore volume are more critical on adsorption capacity than adsorbate polarity and functionality of the adsorbent.

In gas phase adsorption, adsorbate boiling point is important as activated carbon shows higher adsorption capacity for adsorbates with higher boiling point. Liang attributed it to easier condensation and liquefaction at higher boiling points while the physical adsorption of organic vapors on activated carbon is similar to gas liquefaction and condensation [50].

Kawasaki et al. [51] studied the effect of boiling point and molecular weight on adsorption behavior of toluene, benzene, and xylene. They found that the rate of adsorption of tested compounds depended on chemical properties and structure of adsorbate. Also, the adsorption kinetic constant depended on the difference between melting and boiling point of the adsorbates and adsorbate’s structure.

In adsorption of high boiling point compounds, the effect of adsorbate boiling point can be more significant as it was reported that compounds with higher boiling point than water can replace the water molecules already adsorbed on activated carbon [52].

2.2.3 Adsorption operating condition

2.2.3.1 Temperature

Adsorption is an exothermic process so increasing temperature decreases adsorption capacity [53]. However, increasing adsorption temperature increases diffusion rate which results in a faster adsorption kinetic [43, 54]. Then, breakthrough time and mass transfer zone are shorter at higher temperature [55]. Moreover, raising temperature can increase adsorbate and adsorbent interaction and may increase heel buildup [43, 56].

2.2.3.2 Adsorbate concentration

Adsorption capacity of adsorbent increases with rising input concentration as it increases driving force for adsorption. For mesoporous material, increasing inlet concentration develops intra-layer and intermolecular interactions so it increases adsorption capacity [57].

However, Fletcher et al. [58] reported a slower diffusion of water molecules into the activated carbon's pores due to higher surface coverage as result of high concentrations.

Also, bed fire is possible when a high concentration VOCs stream is adsorbed on activated carbon. Temperature increase usually observes for gas phase adsorption as liquids have greater heat capacity which damps the released heat [59, 60].

Gas flowrate in adsorption bed also affects adsorption capacity and kinetics. Higher flow rate increases adsorption kinetics [51]. In contrast, lower flow rates, because of increased contact time between adsorbate and adsorbent, can provide better diffusion and increase amount of adsorption [57].

2.2.3.3 Humidity

Water molecules can be adsorbed on activated carbon by physisorption or chemical interactions (e.g., hydrogen bonding) with surface functional groups [40, 61]. In competitive adsorption, water adsorption can hinder adsorption of VOCs. Also, adsorbed water molecules can form clusters and clog micropore entrances [62]. Therefore, most of times, relative humidity decreases adsorption capacity (Huang et al., 2003). However, in competitive adsorption, adsorbing compounds with higher adsorption energy than water can displace unwanted water molecules [52, 59, 63].

Hydrophobic adsorbents can be a good option to overcome the effect of humidity. Typically, carbonaceous materials with no surface oxygen groups and some of synthesized non-carbon based materials are hydrophobic and can employed for low concentration VOC adsorption from humid gas streams [10]. Occasionally, a low amount of humidity may be preferred to decrease temperature increment, associated with VOC adsorption, and fire hazard of activated carbon adsorption [59].

2.2.3.4 Oxic and anoxic conditions

An oxic or anoxic environment can also affect adsorption behavior. Most of studies considered the oxic and anoxic condition on adsorption in liquid phase. It has been reported that oxic condition increases irreversible adsorption of phenol in liquid phase as it increases phenol polymerization/oligomerization [33, 41].

2.2.3.5 Adsorption bed configuration

Configuration of the adsorption bed can affect adsorption capacity, kinetics, irreversibility, and regeneration efficiency. Two common adsorption bed configurations used in experimental and industrial processes are fixed, and fluidized bed. Adsorption kinetics, VOC removal efficiency, and regeneration conditions and efficiency are different for each configuration.

Fixed bed adsorber is the simplest configuration, and has the lowest operating cost. But, an inappropriate design can bring non-uniform gas distribution, gas channeling. Therefore, VOCs are adsorbed in zones with more contact between the adsorbate and adsorbent and may cause hot spots in these zones, and resulting in bed fires [60, 64, 65]. Also, a fixed bed system with impaired design may cause a high pressure drop which increases operational costs.

Fluidized bed adsorption configuration compared to a fixed bed configuration provides continuous processing of adsorption and desorption without process shut down, faster adsorption kinetic, sharper breakthrough curves, and lower pressure drop. Fluidized beds are especially applicable for treating large flow rates, consuming less energy and improving mass and heat transfer [60, 66-69].

2.3 Activated carbon

Activated carbon (AC) is one of the most common adsorbents in air and water treatment [41, 51, 70]. Activated carbons have a microporous structure which provide a highly developed porosity, a high surface area and a high degree of surface reactivity [15]. They are relatively cheap and can have high adsorption capacity for organic compounds [14, 41, 51, 70-74], also they have noticeable capacity for adsorption of metals and low molecular weight micro-pollutants in water and wastewater [20, 22]. Variety in physical forms of activated carbon, including fibers, powders, beads, monoliths, and granules, makes them usable in nearly every kind of reactors. Beside their good thermal stability in anoxic condition and regenerability, they can be modified to have desirable physical and chemical properties, and have good tolerance in acidic and basic conditions [75]. Therefore, they can be used for decolourization, deodorization, purification, separation to remove or modify the harmful constituents from gases and liquid solutions. So, many economic sectors and concern area as assorted as food, pharmaceutical, chemical, automobile, petroleum, and vacuum industries employ adsorption by activated carbons to treat their wastewaters and flue gases [15].

Activated carbon preparation involves two main steps: the carbonization of carbonaceous raw materials, such as Coal, wood, nutshells, bamboo, coconut shell, lignite, sawdust, petroleum coke, peat, synthetic polymers, biomass materials, and agricultural by – products [32, 36, 56, 76], at temperature below 800 ºC in an inert gas, and activation of carbonized material. The nature of carbonaceous material, activity agents, and process condition have a significant effect on the properties of prepared activated carbons [15].

During carbonization process, most of non-carbon elements such as oxygen, hydrogen, and nitrogen are removed by pyrolytic decomposition of raw materials. The residual carbon atoms group together as stocks of flat, aromatic sheets which are cross-linked in a random style. This type of structure provide a porous network which is occupied with tarry matter or products from decomposition or at least they are partially blocked [15].

Activation of char is carried out at high temperature (800-1000 ºC) in an atmosphere of air, CO_2, or steam. It can be done by physical or chemical treatments [32, 77, 78]. The activation process converts the carbonized material into a porous structure with a large number of randomly distributed pores in different sizes and shapes. The elemental composition of a typical activated carbon has been found to be 88% Carbon, 0.5% Hydrogen, 0.5% nitrogen, 1.0% sulfur, and 6 to 7% oxygen with the balance showing inorganic ash constituents. The oxygen amount in activated carbon can be different based on the type of source material and process conditions [15].

The pores in activated carbons are classified into three groups: the micropores with diameter less than 2 nm, mesopores with diameter between 2-50 nm, and macropores with diameter greater than 50 nm. About 95% of total surface area of activated carbon is related to micropores and around 5% of activated carbons' surface area is mesopores. The macropores contribution to surface area dose not typically exceed 0.5 m^2/g. they usually act as pathway and conduct adsorbate molecules into the micro- and mesopores [15].

The activation method and conditions (e.g., temperature and oxygen), and post – treatment reactions, and raw materials determine the porous structure and surface functional groups of activated carbons [35, 38, 74].

2.4 Activated carbon adsorption

The adsorption behavior of activated carbons cannot only be explained on the basis of surface area and pore size distribution as the chemical structure and the form of activities influence on its interaction with other atoms. The activated carbons prepared with different methods and treatment show markedly different adsorption properties although they might have similar surface area [15].

2.4.1 Chemical structure of the carbon surface

The chemical reactivity of carbon is significantly affected by its crystalline structure. The edge sites or defect positions have higher chemical reactivity than basal plane sites. Therefore, an amorphous carbon has higher reactivity than highly graphitized carbon with homogenous surface comprising mostly of basal planes. It has been reported by Grisdale [79] and Henning [80] that oxidation rate of carbon atoms at basal plane surface were 17 to 20 times lower than the edge sites. The presence of imperfect or partially burnt graphitic layers results in disturbances in elementary microcrystalline structure and variation in the electron clouds in carbon skeleton, so that it provides unpaired electrons and incompletely saturated valences which change the adsorption properties of activated carbons, especially for polar and polarizable compounds [15].

Along with physical and porous structure of activated carbon, its chemical structure is strongly influential. There are appreciable amounts of oxygen and hydrogen in activated carbons. Moreover, sulfur, nitrogen, and halogen atoms may be associated with them. These heteroatoms are derived from raw material or bonded during activation and subsequent treatments. The presence of these compounds alters the surface characteristics and properties of activated carbons [15].

2.4.2 Carbon-oxygen surface groups

Carbon-oxygen surface groups have been the most important surface groups with significant effect on the surface characteristic such as wettability, polarity, acidity and catalytic and chemical reactivity. For instance, the oxygen has effect on adsorption capacity of carbon for water and other polar gases and vapors, and on their ageing during storage [15]. Many of carbons' reaction result from their tendency to extend the chemisorbed oxygen layer. For instance, carbons are able to decompose oxidizing gases like ozone, and oxides of nitrogen, chemisorbing oxygen. Also, they can decompose aqueous solutions of silver salts, halogens, ferric chloride, potassium and ammonium persulphate, sodium hypochlorite, potassium permanganate, potassium dichromate, sodium thiosulphate, hydrogen peroxide, and nitric acid [15]. Furthermore, heat treatment in air, CO_2 or oxygen can be applied to oxidized carbons. In all cases, oxygen is chemisorbed and carbon-oxygen surface compounds are formed. The amount and nature of formed surface oxygen groups by different methods depend upon the nature of carbon surface, the history of its formation, its surface area, the nature of oxidative treatment and process temperature [15].

There are three types of carbon-oxygen surface groups: acidic, basic, and neutral. The acidic surface groups are developed when carbon is treated with oxygen at temperature below 400 ºC or by reaction with oxidizing solution at room temperature. They are mostly carboxylic, lactonic, and phenolic groups. Their thermal stability is not high so heat treatment in vacuum or in an inert gas in the temperature range of 350 to 750 ºC decompose them and resulting in evolving CO_2. The acidic surface groups make the carbon surface hydrophilic and polar [15].

The heat treatment of carbon surface in vacuum or in inert atmosphere at 1000 ºC, and cooling to room temperature in contact with oxygen gas results in formation of basic surface oxygen groups. They are usually decomposed at 900 to 1200 ºC. However, the structure of the basic surface oxygen groups is not well defined and needs more work [15].

Neutral surface oxygen groups are formed as a result of irreversible chemisorption of oxygen. They are more stable than acidic surface groups, and their decomposition begins in temperature range 500 to 600 ºC and a complete removal occurs at 950 ºC [15].

A lot of researches have been conducted to study the impact of surface oxygen groups on adsorption of different adsorbates such as phenol, methylene blue, benzene derivatives, and metals. Various hypothesises have been introduced about mechanism of adsorption and the effect of the surface oxygen groups on adsorption capacity. A brief review of some of the accomplished researches is provided here.

Terzyk [81] studied the effect of surface oxygen groups on phenol adsorption from aqueous solution by activated carbon. The author concluded that activated carbon become acidic as a result of carboxylic groups and those functional groups have less tendency for oxidative coupling. The enhancement in carboxylic group concentration decreased the oxidative coupling and adsorption capacity. However, Yonge et. al. [82] reported that saturated surface functional groups (e.g. methyl, ethyl, methoxy) increased oxidative coupling and enhanced irreversible adsorption.

Dąbrowski et al. [74] studied the adsorption of phenol and its derivative on activated carbon. Their results showed that adsorption capacity decreased on activated carbon with surface oxygen groups. They interpreted that oxygen bond on carbon surface localized electron and removed them from π-electron system of basal plane, which caused a weaker $\pi - \pi$ interaction. In a study by Mattson [83], the adsorption of phenol, m-nitrophenol, and p-nitrophenol was attributed to "donor-acceptor complex" mechanism which carbonyl surface oxygen group acts as electron donor and the aromatic ring of solute acts as electron acceptor.

Alvarez et. al. [22] showed that acidic functional groups on activated carbon decreased dispersive interactions by removing π-electrons from carbon, forming water cluster in pores which prevents phenol diffusion, and promoted phenol chemisorption on carbonyl and carboxylic groups. The net impact of these mechanisms decreased the overall irreversible adsorption because the main contributor, oxidative coupling, was hindered.

Magne and Walker [84] also mentioned that irreversible adsorption of phenol decreased as consequence of acidic surface functional groups. This was attributed to hydration of surface functional groups, where the probability of oxidative coupling is reduced by higher water adsorption. They suggested that a mild oxidation of activated carbon and lower temperature during adsorption and lower time laps between adsorption and regeneration make easier the regeneration of activated carbon.

In another study, physisorption and surface polymerization are stated as the main mechanism in adsorption of phenol from aqueous solution [33]. Furthermore, the interaction between phenol and carbon's basal planes and surface oxygen groups were reported as the controlling parameter in phenol adsorption. Increase in the amount of carboxylic groups decreased adsorption capacity as dispersion interactions with basal planes got weakened. Acidic oxygen groups on activated carbons reduce the surface polymerization under oxidic conditions, though basic oxygen groups raise polymerization and increase irreversible adsorption.

Soudani et. al. [85] explored the effect of nitric acid on olive stone-based activated carbon. They tried different acid concentration (2, 3, 4, and 5 mol.L^{-1}) for treatment. Higher acid concentration resulted in lower surface area and pore volume, which was more obvious for concentration higher than 3 mol.L^{-1}. Also, they found that acid concentration increment did not change the amount of phenolic groups but it increased the amount of carboxylic groups, specifically for concentration higher than 3 mol.L^{-1}.Acid treatment caused a reduction in adsorption capacity of phenol but an increase in methylene blue adsorption. Acid treatment strongly charged the carbon surface so adsorbed methylene blue on surface arranged in vertical orientation instead of flat position. Vertical orientation allowed more adsorption and enhanced methylene blue adsorption. However, for phenol adsorption, the oxidation process facilitated water attachment and inhibited the phenol adsorption, and reduced dispersive interaction which is the main mechanism in phenol adsorption. Moreover, phenol is a weak acid (pK=9.95) and it is undissociated at pH< pKa. Hence, its adsorption became unfavourable with acidic groups' enhancement.

Wang et. al. [86] studied the physical and surface chemical characteristic of activated carbon. They found that acid treatment extremely changed the chemical surface properties while it had little impact on carbon textural characteristic. However, it had negative effect on adsorption of methylene blue. The acid treatment of activated carbon reduced adsorption capacity of methylene blue by about 10%. The lower adsorption capacity of treated activated carbon compared to virgin activated carbon was attributed to electron extraction from π bond of the carbon by acidic oxygen groups which reduced the interaction between the methylene blue molecules and carbons.

El-Hendawy [87] investigated the effect of oxidation by nitric acid on the structure and adsorption properties of corncob-based activated carbons. The strong oxidation of HNO_3 decreased the surface area of activated carbon due to destruction of some micropores and blockage of some narrow pores as consequence of introduction of oxygen groups. Because of pore widening, the removal efficiency of methylene blue from aqueous solution improved by oxidation. Moreover, generation of oxygen functionalities on surface notably increased lead uptake. Nevertheless, phenol adsorption capacity of oxidized activated carbon decreased or did not change, depending on activation precursor.

In another study, Gokce and Aktas [88] investigated the impact of surface oxygen groups on adsorption of methylene blue and phenol from aqueous solution. Their results showed that modification of activated carbon has different effects on adsorption capacity of methylene blue and phenol. The adsorption of methylene blue increased due to the introduction of surface oxygen groups, however, the phenol adsorption decreased. They attributed this behavior to the interaction between electrostatic and dispersion forces. Formation of surface oxygen groups resulted in extraction of electrons from π bond of aromatic groups on basal planes which weakened the dispersion forces and reduced phenol adsorption since phenol adsorption is mostly controlled by dispersion forces. On the other hand, dispersive forces were not a key factor in removal of methylene blue. Electrostatic forces were responsible for methylene blue's adsorption since these forces arranged methylene blue molecules in vertical axis which caused a rise in adsorption capacity.

Jiang et. al. [25] modified activated carbons by sulfuric acid (96%). The modification increased the mesopore volume from 0.24 ml/g to 0.45 ml/g hence the surface area increased from 393 m^2/g to 745 m^2/g. Furthermore, acidic surface oxygen groups increased from 0.07 meq/g to 1.99 meq/g in comparison to unmodified activated carbons. It was reported that modification with concentrated acid have positive effect on adsorption of large molecules such as methylene blue and dibenzothiophene. Nevertheless, the adsorption capacity for smaller molecules, like iodine, was reduced. They attributed this decrease to the smaller influence of mesopores on iodine adsorption. Hence, the enhancement in mesopores' volume did not have any impact on the adsorption capacity of iodine.

The impact of acid treatment of activated carbons on dye adsorption was explored by Wang and Zhu [89]. The results showed a decrease in dye adsorption for activated carbons modified by HNO_3. Activated carbon treated by HCl showed higher adsorption capacity for larger molecules, like methylene blue, although it was lower than virgin activated carbon. Nitric acid treatment resulted in more acidic oxygen groups such as carboxyl and lactone which brought a drop in the adsorption of dyes. However, HCl treatment generated lower acidic functionalities, hence the HCl-treated activated carbon had higher adsorption capacity.

Valdes et. al. [90] reported that the adsorption of methylene blue decreased when activated carbons were treated by ozone. Formation of surface oxygen groups by oxidation prevented diffusion in some pores and reduced the available surface area.

Arafat et. al. [24] investigated the adsorption of aromatic compounds on oxygenated activated carbon in aqueous and non-aqueous media. They expressed that the adsorption capacity decreased for all tested components in aqueous phase since the H-bonding between treated activated carbon surface and adsorbates was limited due to competitive water adsorption. But, the adsorption capacity for phenol and aniline in cyclohexane medium increased linearly with surface oxygen groups' concentration. This was not seen for non-H-bonding compounds, benzene and nitrobenzene.

Lillo-Ro´ denas et al. [13] found that adsorption capacity of benzene and toluene were higher on activated carbon with low oxygen content. They explained that removal of surface oxygen groups enrich graphene layer with π-electron, and bring a stronger interaction between adsorbate and carbon surface. Also, their results showed that benzene adsorption has correlation with volume of narrow micropores. However, adsorption capacity of toluene was governed by both volume of narrow micropores and total volume.

Jahangiri et al. [91] explored adsorption of benzene, toluene, and xylene on different nanostructure adsorbent. Multiwall carbon nanotube with surface oxygen group (MWCN-COOH) had lower adsorption capacity than Multiwall carbon nanotube (MWNT) due to decreased surface area, reduced hydrophobicity, promoted diffusion resistance, and accessibility reduction.

The influence of oxygen surface groups on adsorption of benzene derivatives from aqueous solution was studied by Marczewska et. al. [92]. The adsorption capacity declined by increasing the surface oxygen groups, but the extent of reduction depended on adsorbate 's solubility, and the adsorbate ‘s functional groups

Rodriguez-Reinoso et. al. [93] studied the adsorption of polar molecules on microporous activated carbon with different amount of surface oxygen groups. They found that for non-polar molecules the adsorption mainly depended on porous structure but the influence of surface oxygen groups became significant for polar molecules.

Furmaniak [94] considered the impact of porosity and surface oxygen groups on activated carbon adsorption, for a simple polar volatile organic component (acetonitrile). Their simulation results showed that a decrease in the pore size and an increase in oxygen surface groups resulted in a rise in adsorption energy and provided more accessible volume which can be filled in the low-pressure part of the isotherm.

Also, Bohi and Quederni [95] studied the effect of oxygen containing functional groups on removal of heavy metals. Hydrophilicity of activated carbon increased by modification and resulted in more adsorption of Co(II), Cu(II), and Ni(II) from single aqueous solution in comparison to starting material.

Gotzias et. al. [96] modeled adsorption of N_2 and CO_2 in micro and mesoporous slit carbons with oxygen surface functionalities. They concluded that the adsorption is strongly affected by surface oxygen groups. However, this effect is merely observed during monolayer formation of adsorbate molecules, since monolayer adsorption typically occurrs at low concentration of adsorbate. The presence of surface oxygen groups caused a rise in adsorption energy and a smoother isotherm.

Ledesma et al. [97] investigated thermal regeneration of activated carbons saturated with *p*-Nitrophenol. As the regeneration efficiency of adsorbent decreased after every use, they concluded that the remaining fraction of adsorbate on carbon surface is chemisorbed species. Moreover, progressive deterioration of porosity and surface area reduction were attributed to continual pore widening, pore erosion, and levelling off effects.

Cuervo et al. [98] studied the effect of chemical activation by HNO_3 on adsorption capacity of carbon nanofiber. They found that both adsorption capacity and strength of adsorption were reduced for chlorinated compounds, however, the presence of surface oxygen groups does not have any effect on adsorption of n-alkane and aromatic compounds. Oxidation of nanofiber caused steric limitation of adsorption. This limitation has negative effect on adsorption of aromatic and chlorinated compounds. It was explained that the nucleophilic interactions between aromatic rings and surface oxygen groups can compensate for the steric limitation and keep adsorption capacity the same. But, the adsorption capacity of chlorinated compounds decreased as there are not any nucleophilic groups to aid their adsorption. Steric limitation was not found important in adsorption of linear hydrocarbon. It was concluded that geometrical factors, such as structure and kinetic diameter, have key role in adsorption of n-alkane.

As it is observed, oxidation of activated carbon can have different effects on the adsorption capacity and activated carbons' texture which depends on pore size distribution of activated carbons, oxidation method and its severity, and adsorbate characteristics such as hydrophilicity, polarity. In addition, most of the studies were done on adsorption from aqueous media. There is a limited research on the effect of activated carbon treatment on activated carbon adsorption from gas phase. Moreover, the unwanted accumulation of adsorbate and by-products from adsorption process, or heel buildup, is a challenge in adsorption process as it reduces the adsorbent's capacity and lifetime. Therefore, exploring the influence of surface oxygen groups is very important. It is expected that surface oxygen groups change regeneration efficiency and heel buildup since they affect adsorption capacity and adsorption mechanism. However, up to the best of our knowledge, there is little or no detailed information about the effect of surface oxygen groups on irreversible adsorption and heel buildup resulting from adsorption of volatile organic compounds on activated carbon. Therefore, additional research is required to understand better the effect of surface oxygen groups on reversible/irreversible adsorption on carbonaceous material, specifically for adsorption in gas phase.

3 MATERIALS AND METHODS

3.1 Adsorbent preparation

The activated carbon used in all experiments was pitch-based BAC (G-70R; Kureha Corporation). The BAC is characterized by its high microporosity, attrition-resistance, and narrow particle size distribution (average particle diameter of 0.70 mm, 99% by mass between 0.60 and 0.84 mm) [99].

Hydrogen treated BAC was prepared by exposing virgin BAC to hydrogen at 950ºC. Accordingly, virgin BAC was placed in a quartz boat in a tube furnace equipped with a quartz tube. The quartz tube was purged with nitrogen at 200 standard cubic centimetres per minute (SCCM) while temperature was increased from room temperature to 200 ºC. Then, it was purged with 200 SCCM hydrogen gas for 2 hours while its temperature kept constant at 200 ºC. After purging for 2 hours at constant temperature (200 ºC), the temperature was raised to 950 ºC at 10 ºC/min, and kept for 3 hours at 950 ºC. Then, heating was stopped and the BAC sample was allowed to cool to 100 ºC while the hydrogen gas flowed through the quartz tube. After reaching 100 ºC, the purge gas was switched to nitrogen and the sample was allowed to cool to room temperature. The final sample was referred to as hydrogen treated BAC and labeled as BAC-H-950.

Acid treated BAC was prepared by exposing virgin BAC to nitric acid. Virgin BAC was mixed with 5.3 molar (M) nitric acid and stirred for 17 hours. Afterward, BAC was drained and washed with deionized water till neutral pH, and dried in 150 ºC oven to remove water. The prepared sample was heated at 400 ºC for 3 hours while it was purged with 1 SLPM nitrogen gas to remove adsorbed nitrate groups [26]. It was referred to as acid treated BAC and labeled as BAC-O-400.

For consistency with BAC-O-400, virgin BAC was heated at 400 ºC under 1 standard liter per minute (SLPM) N_2 for 3 hours before characterization and application. It was referred to as heat-treated BAC and labeled as BAC-400.

3.2 Adsorbate

The tested adsorbates represent different organic groups commonly present in automotive paint solvents. The adsorbates were tested individually, at an inlet concentration of 500 ppm_v. The properties of the tested adsorbates are presented in Table *3-1*.

Table 3-1. Adsorbate properties

Compounds	**Structure**	**Boiling point (°C)***	**Kinetic diameter (Å) [3, 27, 100]**	**Molar mass (g/mol)**
p-xylene (Acros Organic, 99%)	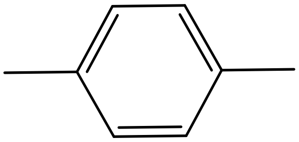	138	5.9	106.16
1,2,4 trimethylbenzene (TMB) (Acros Organic, 98%)	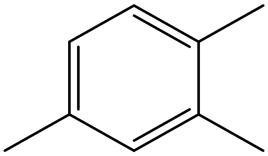	171	6.8	120.19
Ethylbenzene (Fisher Scientific, certified)	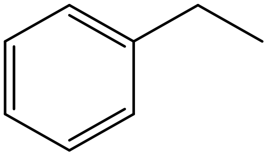	136	6.0	106.16

Compounds	Structure	Boiling point (°C)*	Kinetic diameter (Å) [3, 27, 100]	Molar mass (g/mol)
n-decane (Fisher Scientific, 99.5%)		174	4.3	142.29
2-heptanone (Acros Organic, 98%)	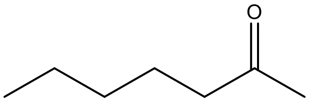	151	-	114.18
n-butyl acetate (Acros Organic, >99%)	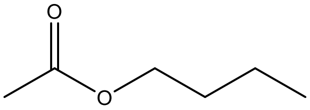	126	-	116.16
n-butanol (Fisher Scientific, 99.5%)	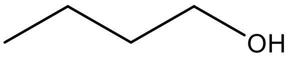	118	4.3	74.12
2-butoxyethanol (Acros Organic, >99%)	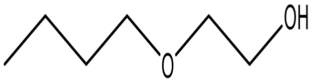	168	-	118.17

*from compound's datasheet

3.3 Experimental setup and methods

The experimental setup (Figure 3-1) consisted of an adsorption-regeneration reactor, an adsorbate generation system, a gas detection system, a power application module, and a data acquisition and control (DAC) system.

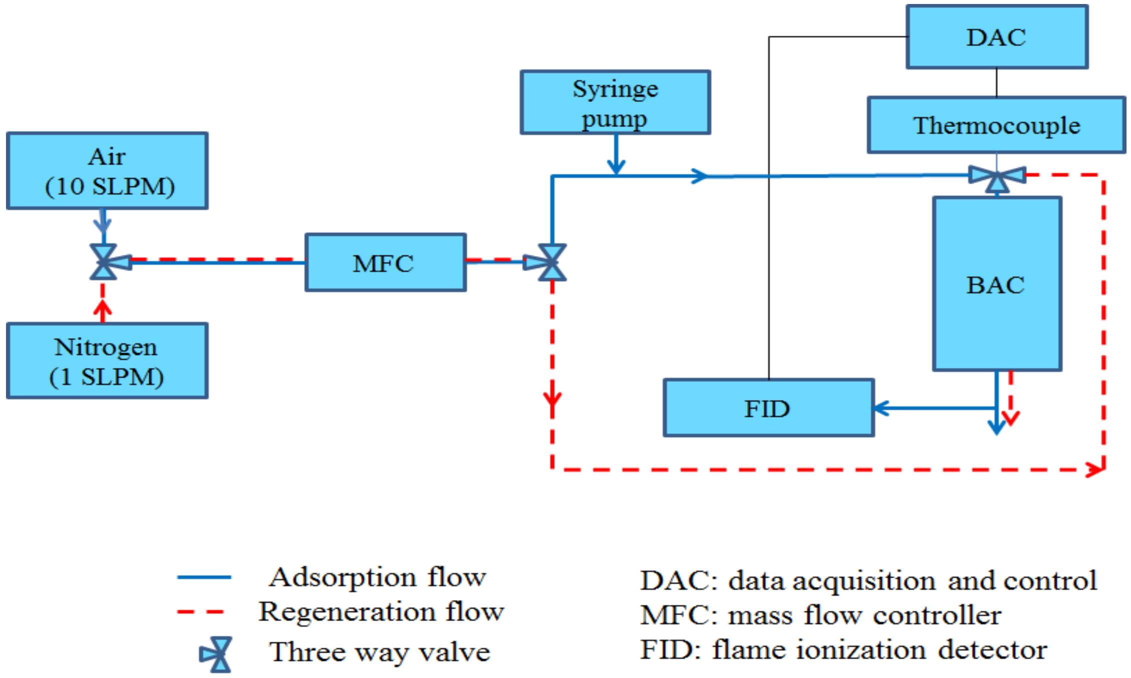

Figure 3-1. Schematic diagram of adsorption and regeneration setup.

The adsorber consisted of a stainless steel tube with 1.44 cm inner diameter, and 15.24 cm long containing 4.0 ± 0.1 g of BAC. Glass wool was used as a support for the BAC bed at the bottom and top of the tube.

The adsorbate generation system consisted of a syringe pump (KD Scientific, KDS-220) which injected liquid organic compound into a dry air stream. A mass flow controller (Alicat Scientific) adjusted the air flowrate to 10 SLPM (standard conditions are 25 ºC and 1 atm). A heating tape was wrapped around injection point to keep inlet temperature constant (about 23 ºC) and help vaporise the injected VOC. The inlet concentration of different adsorbates was 500 ppm$_v$.

A flame ionization detector (FID, Baseline-Mocon Inc., series 9000) was used to measure VOC concentration. The FID was calibrated before each adsorption test using the same gas generation system. The VOC concentration at the adsorber's outlet stream was measured continuously during adsorption (1 min sampling frequency).

Adsorption experiments were completed at room temperature (about 23 ºC) using 4.0 ± 0.1 g of dry adsorbent, and lasted to saturation. The adsorber was weighed before and after adsorption to determine the adsorption capacity, as follows:

$$\textbf{Adsorption capacity}\ \% = \frac{\mathbf{W_{AA}-W_{BA}}}{\mathbf{W_{BAC}}}\times\mathbf{100} \qquad \textbf{Equation 3-1}$$

Where W_{AA} is the adsorber’s weight after adsorption cycle, W_{BA} the adsorber’s weight before adsorption, and W_{BAC} is the initial BAC weight.

Heating and insulation tapes (Omega) were wrapped around the adsorption tube during regeneration. A type K thermocouple (1.6 mm outer diameter, ungrounded, Omega) was used to measure the temperature at the center of adsorber bed during adsorption and regeneration. The Data Acquisition and Control (DAC) system consisted of a LabVIEW program (National Instruments) and a data logger (National Instruments, Compact DAQ) equipped with analog input/output modules. The DAC was interfaced to the thermocouple to record temperature during adsorption/regeneration.

Regeneration tests were performed for 3 hours by heating at 288 ºC which was chosen to simulate industrial operation conditions [3, 27, 101]. This condition provides an optimum desorption of adsorbate and minimizes potential damages to the adsorbent structure as consequence of high temperature [101]. During regeneration, 1 SLPM nitrogen gas was passed through the adsorber to sweep desorbed compounds. After heating for 3 hours at 288 °C, it was cooled to ambient temperature under 1 SLPM flow of nitrogen.

Heel build-up after 5 adsorption and regeneration cycles, was calculated as follows:

$$\textbf{Cumulative heel}\ \% = \frac{\mathbf{W_{AR}-W_{BA}}}{\mathbf{W_{BAC}}}\times\mathbf{100} \qquad \textbf{Equation 3-2}$$

Where W_{AR} is the adsorber's weight after the fifth regeneration cycle, W_{BA} the adsorber's weight before first adsorption, and W_{BAC} is the initial BAC weight. The heel after 5 adsorption and regeneration cycles was referred to as cumulative heel.

3.4 BAC characterization

Treated BACs were characterized before adsorption/regeneration cycles by Boehm titration, x-ray photoelectron spectroscopy (XPS, AXIS 165 spectrometer, Kratos Analytical), thermo-gravimetric (TGA/DSC 1, Mettler Toledo), and micropore surface analyzer (Autosorb iQ2MP, Quantachrome).

3.4.1 Boehm titration

Boehm titration was used to assess the concentration of different acidic groups (carboxylic, lactonic, and phenolic groups) on carbon surface [102-104]. 50 mg of BAC sample was mixed with 0.05 M NaOH, $NaHCO_3$, Na_2CO_3 in three separate vials and shaken for 24 hours using wrist shaker (Burrell Scientific). Then, BAC was drained and solutions were back titrated with 0.05 M NaOH solution till reaching a faint and permanent pink color as phenolphthalein was used as indicator. The consumed amount of NaOH is used to determine the remaining concentration of NaOH, $NaHCO_3$, Na_2CO_3. The hypothesis of Boehm titration is that NaOH neutralizes carboxylic, lactonic, and phenolic groups, $NaHCO_3$ neutralizes carboxylic groups, and Na_2CO_3 neutralizes carboxylic and lactonic groups [104]. Based on this assumption, the amount of each group was determined.

3.4.2 Thermo-gravimetric analysis

Thermo-gravimetric analysis (TGA/DSC 1, Mettler Toledo) was performed to assess the thermal stability of BAC samples and accumulated heel. Each run consisted of a temperature ramp from 25 ºC to 900 ºC at 2 ºC/min under 50 SCCM N_2 purge flow to prevent oxidation and undesired reaction. TGA instrument continuously weighs sample as it is heated. As the temperature increases, various components of the sample are decomposed and the resulting mass change is measured. Plotting the mass loss vs temperature or first derivative can help to assess the stability and strength of physical/chemical bond between adsorbate and adsorbent.

3.4.3 X-ray photoelectron spectroscopy analysis

X-ray photoelectron spectroscopy (AXIS 165 spectrometer, Kratos Analytical) was used to determine elemental composition of carbon, oxygen, and nitrogen on adsorbent surface. It can identify elements and the quantity of those elements which are within the top 1-12 nm of the sample surface. High resolution scans (with signal to noise ratio of >10) were collected for binding energy spanning from 1,100 eV to 0 eV with analyzer pass energy of 20 eV and a step of 0.1 eV. “Casa XPS” Software was used to process the scans and the results were presented in terms of atomic concentration.

3.4.4 Micropore surface analysis

Pore size distribution and BET surface area were obtained using a micropore surface analysis system (Autosorb iQ2MP and Autosorb MP, Quantachrome) with N_2 ($10^{-7} < P/P_0 < 1$) adsorption at -196 °C. About 40 mg of BAC was placed in a 6 mm cell, and degassed at 150°C for 5 h to remove moisture. BET surface area and micropore volume were determined in relative pressure ranges of 0.01 – 0.07 and 0.2 – 0.4, respectively. The V-t model was used to calculate micropore volume. Pore size distributions were obtained using the quenched solid density functional theory (QSDFT) [100].

4 RESULTS AND DISCUSSION

4.1 BAC characterization

Treated activated carbon samples were characterized before cyclic adsorption-regeneration experiments (Table 4-1). Acid treatment or hydrogen treatment, which adds or removes surface oxygen groups, did not result in a large change in surface area (< 5%), micropore volume, and total pore volume in comparison to heat treated BAC.

Table 4-1. Physical and chemical properties of treated BAC before adsorption/regeneration cycling.

Carbon Sample	Physical Properties			Surface Composition		
	BET Surface Area (m^2/g)	Micropore Volume (cm^3/g)	Total pore Volume (cm^3/g)	C (%)[a]	O (%)[a]	N (%)[a]
BAC-O-400	1288	0.47	0.56	83.9	16.1	0.0
BAC-H-950	1296	0.47	0.55	97.6	2.4	0.0
BAC-400	1353	0.50	0.54	94.6	5.4	0.0

[a] Relative atomic percentages (%C + %O + %N = 100); Other elements were not considered in surface composition

Nevertheless, treatments altered the amount of oxygen on BAC surface, as determined by XPS. Acid treated BAC had more than three times as much surface oxygen group as heat treated samples (Table 4-1).

Pore size distribution for all treated BAC were determined (Figure 4-1). The pore size distributions of unused (before adsorption) acid/hydrogen treated BAC (BAC-O-400 and

BAC-H-950) were similar to heat treated BAC (BAC-400). The heat treated BAC showed a little higher pore volume but the pore volume difference between acid/ hydrogen treated and heat treated BAC was less than 5%. Micropore volume was more than 80% of total pore volume which allows a higher affinity for volatile organic compounds adsorption [44]. These characteristics, i.e. similar porosity and different content of surface oxygen groups, is needed to investigate the effect of surface oxygen groups on adsorption and irreversible heel formation.

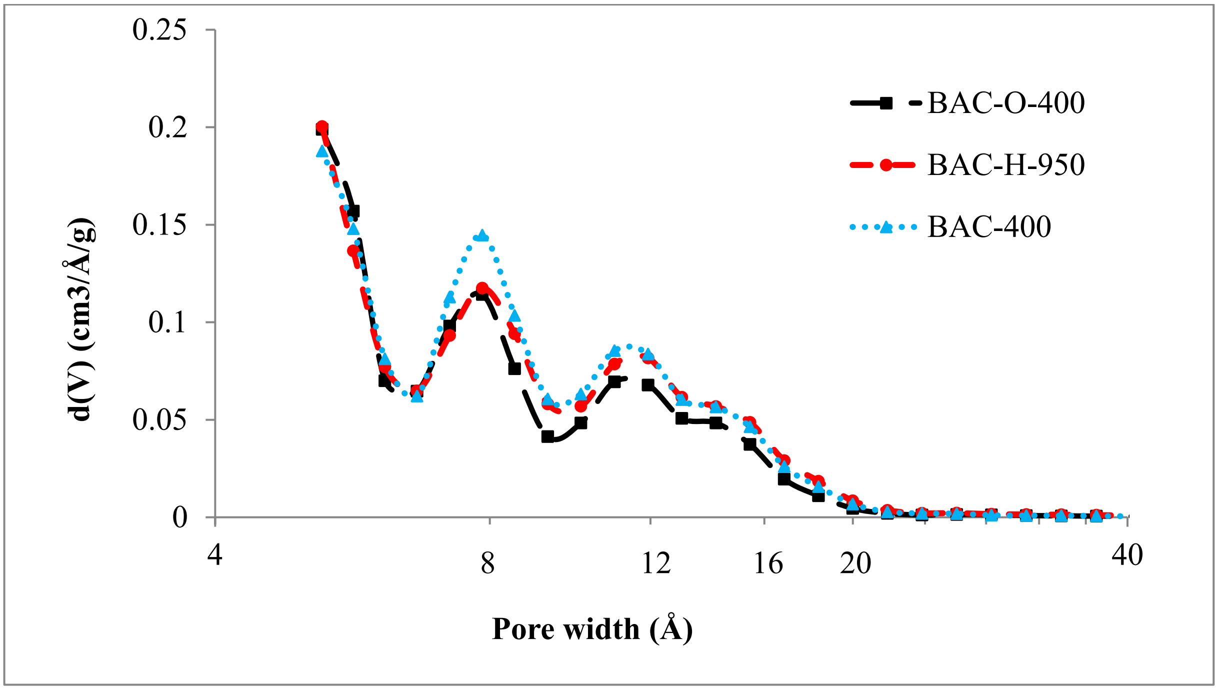

Figure 4-1. Pore size distributions of unused BAC.

DTG analysis was used to characterize thermal stability of the 3 types of BAC as well as to provide a qualitative description of surface oxygen groups (Figure 4-2). The first peak in DTG plot is related to water removal since water vapor can be adsorbed before analysis [71]. This peak is a little higher for acid-treated samples as acid treatment increases hydrophilicity of activated carbon [40]. There was not any specific mass loss until 400ºC because all samples were preheated at this temperature. For acid treated BAC, a large and wide peak was observed which shows removal of surface oxygen groups from carbon surface [105]. This statement can be confirmed by the DTG analysis result for heat treated BAC and hydrogen treated BAC as these samples did not show any peak before carbon decomposition which begins around 700 ºC [27].

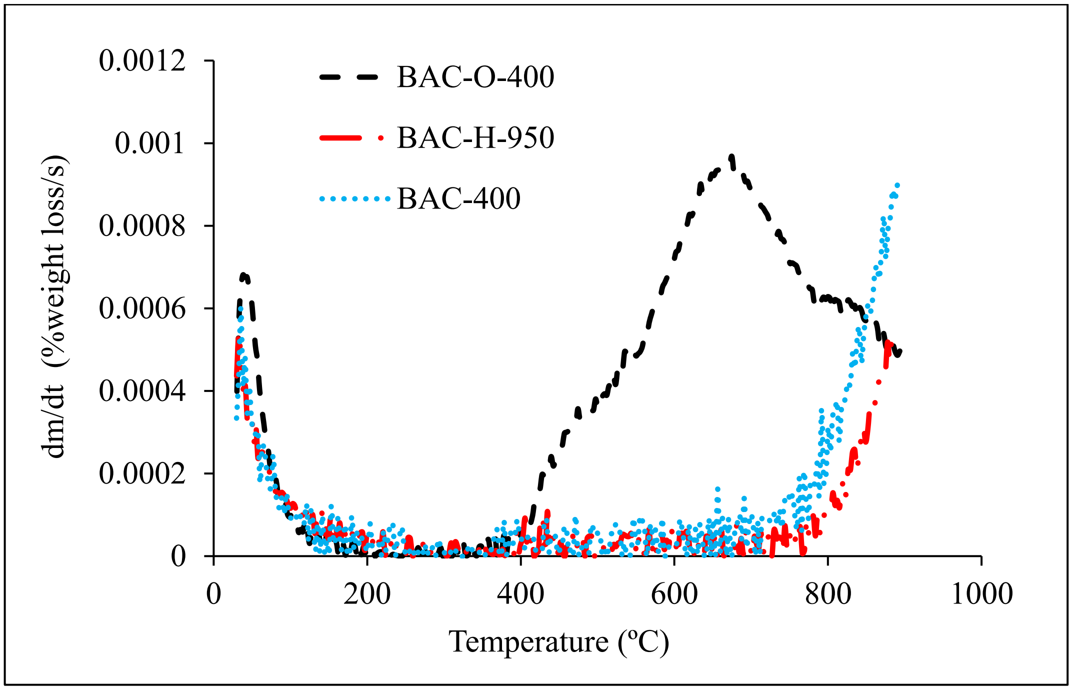

Figure 4-2. DTG analysis of unused BAC.

The concentration of different acidic oxygen groups on the carbon surface was determined by Boehm titration (Figure 4-3). Hydrogen treatment removes acidic surface oxygen groups and acid treatment increases the amount of acidic surface oxygen groups, specifically it increases the amount of carboxylic and lactonic groups. Based on Boehm titration results, the phenolic groups are the only oxygen groups on the surface of heat treated BAC. Hydrogen treatment removed about 67 percent of phenolic groups. This was expected since hydrogen treatment was performed at 950 ºC which is higher than decomposition temperature for phenol groups (around 550 ºC) [106]. As shown in Figure 4-3, about 50% of acidic groups are carboxylic groups. The higher percentage of carboxylic groups can be attributed to their higher stability during preheating and formation of carboxylic anhydrides [107].

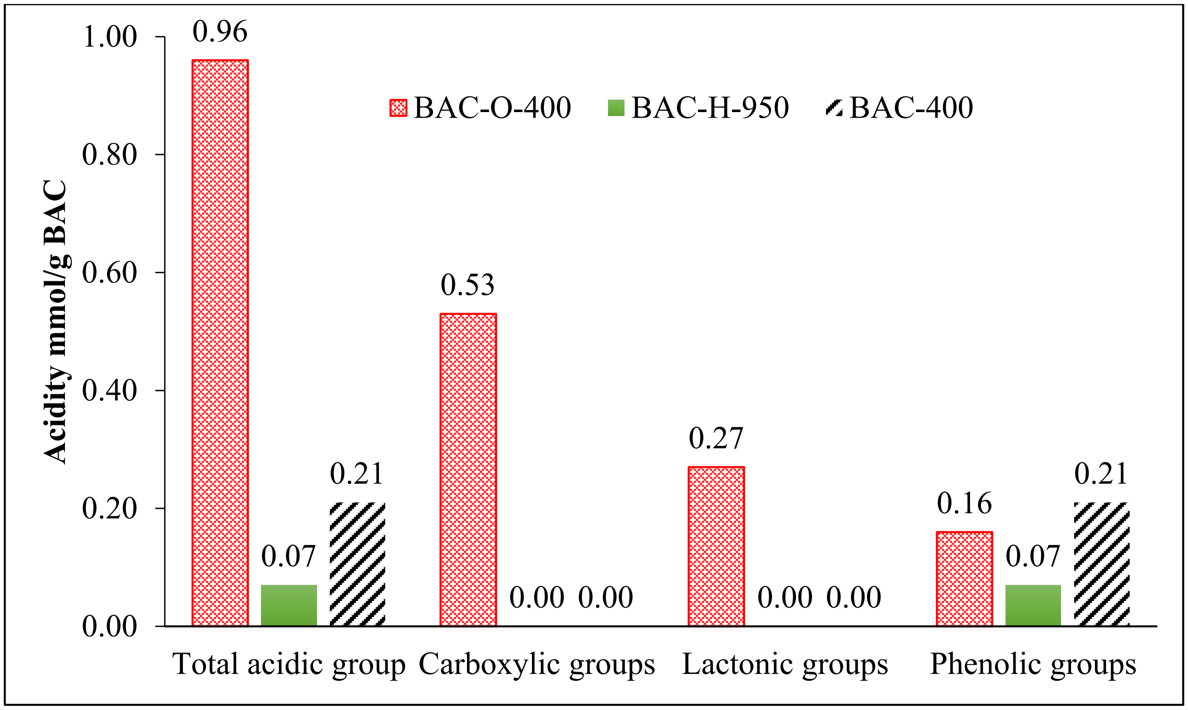

Figure 4-3. Contribution of various SOGs based on Boehm titration.

4.2 Cyclic adsorption and regeneration

Treated BACs were used in five adsorption/ regeneration cycles. The cumulative heel after five cycles is presented in Table *4-2*. The breakthrough curves and detailed mass balance for heel buildup and adsorption capacity during 5 cycle adsorption and regeneration for each adsorbate can be found in Appendix A and B.

The presence of surface oxygen groups resulted in higher heel for acid treated BAC in comparison to heat treated BAC and hydrogen treated BAC. This can be attributed to stronger interactions between surface oxygen groups and adsorbates. Another reason can be related to the location of surface oxygen groups on carbon surface. These groups may partially block the pores' entrance which prevents diffusion of adsorbate [108] and its removal.

The amount of accumulated heel on hydrogen treated BAC and heat treated BAC were similar. The heat-treated BAC did not have any carboxylic or lactonic oxygen surface groups and the only difference between heat treated BAC and hydrogen treated BAC is the amount of phenolic surface groups (Figure 4-3). It can be interpreted that these groups with this concentration do not have a specific effect on adsorption capacity or irreversible heel formation.

These results suggest that tailoring activated carbon surface to increase oxygen surface groups worsened the activated carbon performance. Moreover, hydrogen treatment does not have a significant effect on adsorption capacity and irreversible heel of Kureha BAC for tested adsorbates.

Table 4-2. Mass balance of cumulative heel after 5-cycle adsorption/regeneration

Description		**Cumulative Heel (%)**	**Adsorption Capacity (%)**
P-xylene	BAC-H-950	0.6	38.4
	BAC-400	0.4	40.7
	BAC-O-400	3.3	36.5
ethylbenzene	BAC-H-950	0.0	38.5
	BAC-400	0.2	40.5
	BAC-O-400	1.4	38.1
1,2,4-TMB	BAC-H-950	0.3	41.5
	BAC-400	0.7	45.1
	BAC-O-400	4.5	40.1
n-butanol	BAC-H-950	0.3	35.2
	BAC-400	0.3	36.3
	BAC-O-400	0.6	33.8
2-butoxyethanol	BAC-H-950	0.7	41.5
	BAC-400	1.1	44.3
	BAC-O-400	1.6	40.9
n-decane	BAC-H-950	0.7	34.5
	BAC-400	0.7	36.2
	BAC-O-400	1.2	33.6
2-heptanone	BAC-H-950	0.3	36.9
	BAC-400	0.5	39.4
	BAC-O-400	2.2	35.9
n-butyl acetate	BAC-H-950	0.1	39.7
	BAC-400	0.2	41.6
	BAC-O-400	0.4	39.1

Aromatic adsorbates showed higher heel on acid treated BAC in comparison to heat treated BAC or hydrogen treated BAC. The oxygen surface functional groups have a major effect on the irreversible heel build-up for aromatic compounds. This effect indicates to stronger interactions of aromatic adsorbate with surface oxygen groups. The donor–acceptor mechanism between acidic groups and the π –electron of benzene ring may be the reason for this behavior [109]. Moreover, oxidation of carbon surface increases the electrophilic character of surface and reduces its nucleophilic character. Therefore, it results in a stronger interaction between activated carbon surface and nucleophilic adsorbate like double bond and aromatic structure [98]. Any of these mechanisms or both of them can be the reason for higher heel build-up for aromatic compounds on acid treated adsorbent compared to heat treated samples.

1,2,4-trimethylbenzene showed the highest heel build-up among tested aromatic compounds. It can be attributed to the higher kinetic diameter, boiling point, and molar mass of 1, 2, 4 trimethyl benzene compared to the two other aromatic adsorbates, ethylbenzene and p-xylene. The lowest heel formation among tested aromatic components was related to ethylbenzene although both ethylbenzene and p-xylene have similar boiling point and kinetic diameter and the same molar mass. Since methyl group has higher stability than ethyl group [110, 111], one possible hypothesis is that the ethyl group can be broken down during regeneration and ethylbenzene is converted to benzene which has smaller kinetic diameter and better diffusion [112]. A smaller size and higher diffusion rate can allow for a better regeneration and less heel build-up.

In addition, boiling point and molecular weight of adsorbate have important impact on irreversible heel formation. Compounds with higher boiling point and molecular weight showed higher heel. The adsorption capacity of activated carbon decreased with increasing saturation vapor pressure as adsorption of components with lower boiling point/ higher vapor pressure is difficult in pore spaces [50]. Also, adsorbates with lower boiling point can be easily removed during regeneration as they require less energy to overcome internal and interfacial forces and leave adsorbent’s surface.

Moreover, adsorption capacity decreased during cyclic adsorption/regeneration, which is consistent with occurrence of heel formation. Heel build-up results in pore blockage and reduces available adsorption sites. As accessible sites decrease, adsorption capacity decreases.

4.3 BET surface area and pore volume

The BET surface area and pore size distribution of BAC before and after 5 adsorption/regeneration cycles were measured to find the effect of irreversible adsorption on surface area and pore size distribution. After adsorption and regeneration, some of adsorption sites became inaccessible for adsorbate's molecules as they were occupied by heel. Therefore, the number of available sites for next adsorption cycle would decrease. The effect of irreversible adsorption on total and micropore volume was similar to its impact on surface area.

Table 4-3. Surface area and pore volume for treated BAC after 5 cycle adsorption/regeneration.

Description		**BET Surface Area (m^2/g)**	**Micropore Volume (cm^3/g)**	**Pore Volume (cm^3/g)**
P-xylene	BAC-O-400	1174	0.41	0.51
	BAC-H-950	1223	0.45	0.52
	BAC-400	1399	0.51	0.58
ethylbenzene	BAC-O-400	1219	0.43	0.53
	BAC-H-950	1242	0.45	0.53
	BAC-400	1349	0.49	0.55
1,2,4-TMB	BAC-O-400	1148	0.42	0.49
	BAC-H-950	1234	0.47	0.50
	BAC-400	1277	0.48	0.51
n-butanol	BAC-O-400	1246	0.45	0.53
	BAC-H-950	1234	0.45	0.53
	BAC-400	1307	0.45	0.57
2-butoxyethanol	BAC-O-400	1183	0.43	0.50
	BAC-H-950	1210	0.44	0.52
	BAC-400	1283	0.47	0.52
n-decane	BAC-O-400	1210	0.44	0.51
	BAC-H-950	1149	0.43	0.47
	BAC-400	1288	0.47	0.53
2-heptanone	BAC-O-400	1170	0.42	0.48
	BAC-H-950	1220	0.46	0.50
	BAC-400	1316	0.49	0.54
n-butyl acetate	BAC-O-400	1319	0.48	0.55
	BAC-H-950	1224	0.45	0.52
	BAC-400	1391	0.51	0.57

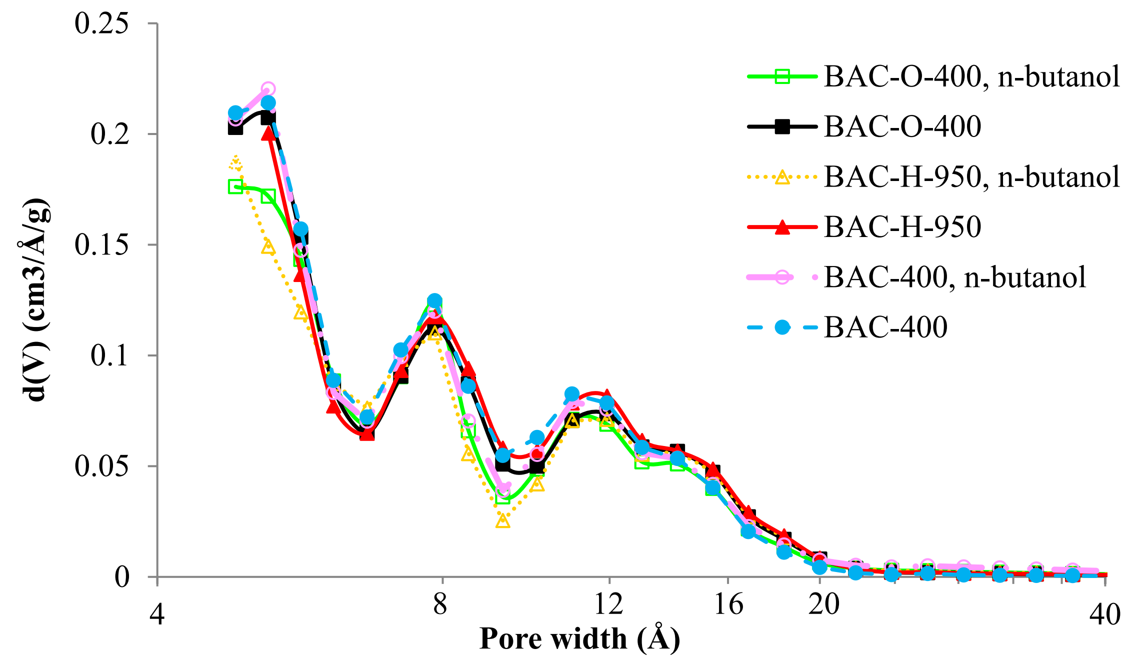

Figure 4-4. PSD of treated BAC after 5cycle adsorption/regeneration of n-butanol.

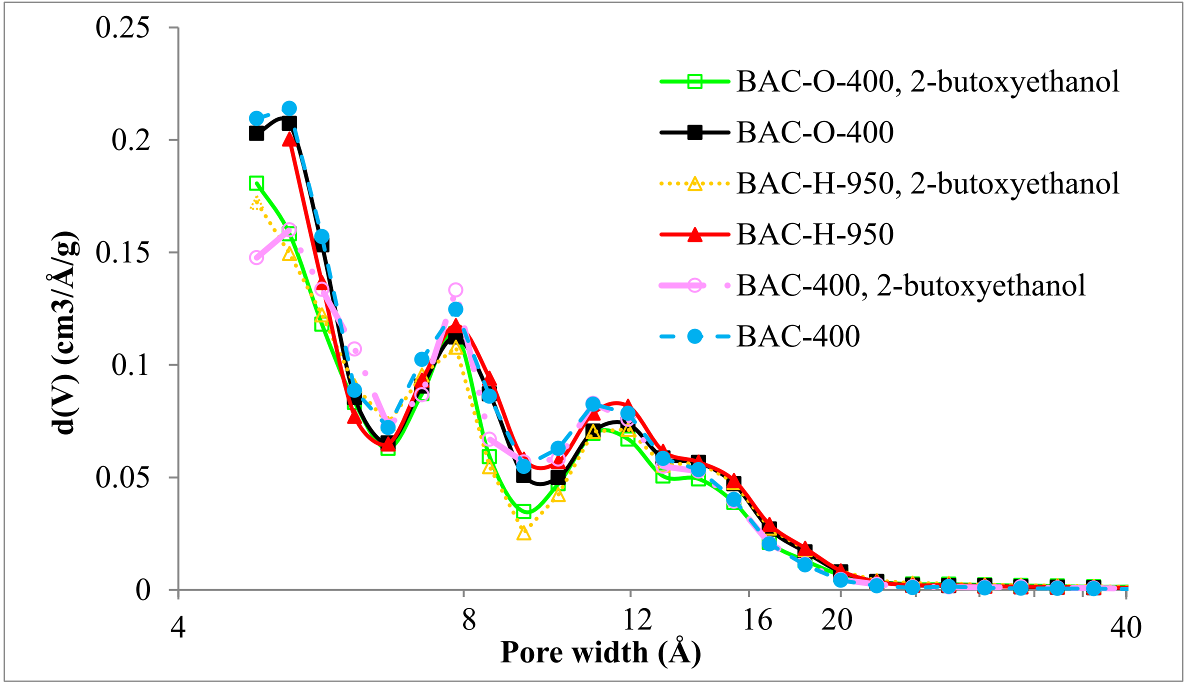

Figure 4-5. PSD of treated BAC after 5cycle adsorption/regeneration of 2-butoxyethanol.

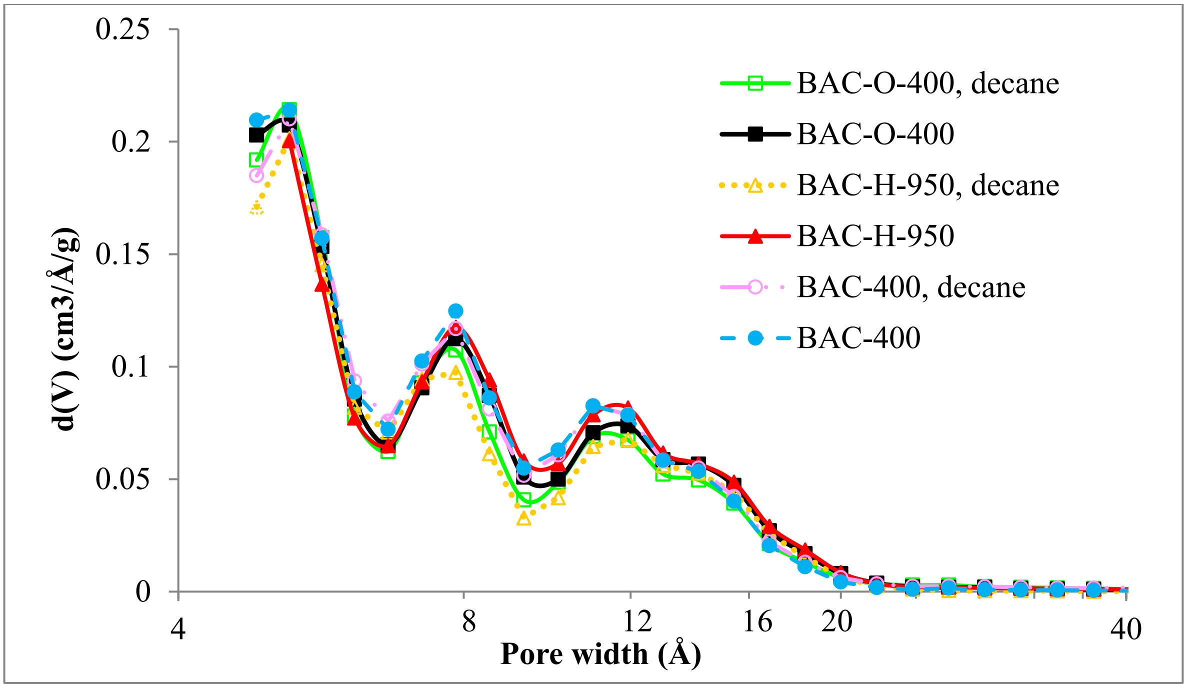

Figure 4-6. PSD of treated BAC after 5cycle adsorption/regeneration of n-decane.

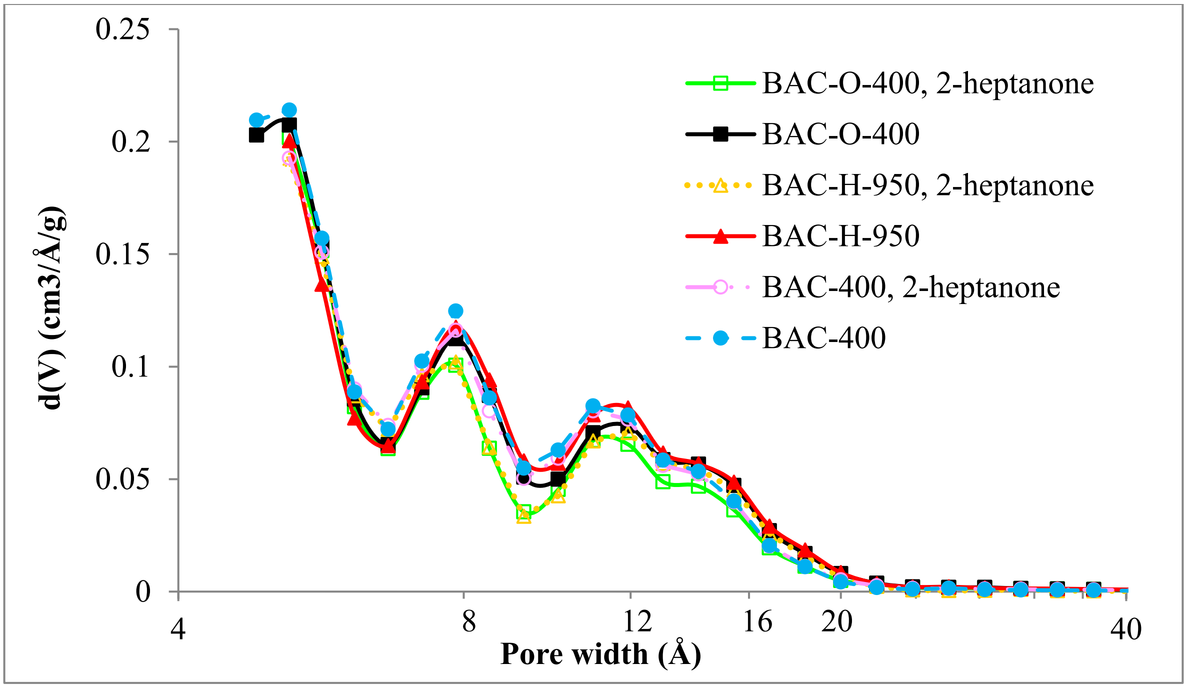

Figure 4-7. PSD of treated BAC after 5cycle adsorption/regeneration of 2-heptanone.

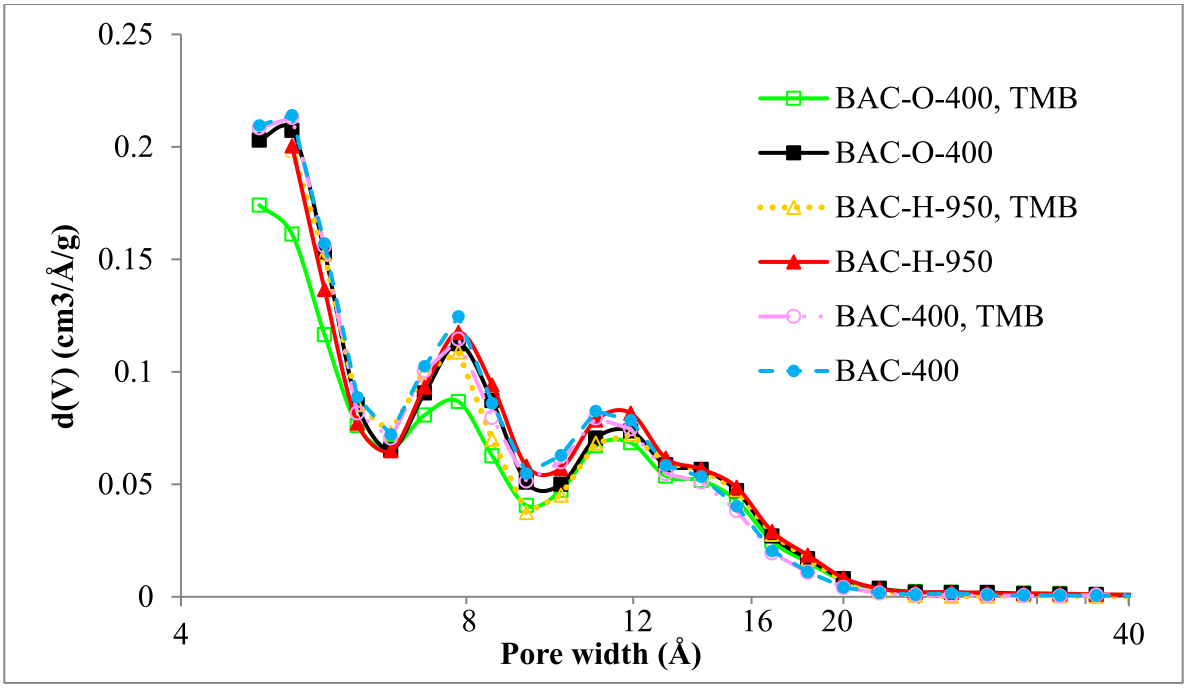

Figure 4-8. PSD of treated BAC after 5cycle adsorption/regeneration of 1,2,4-trimethylbenzene.

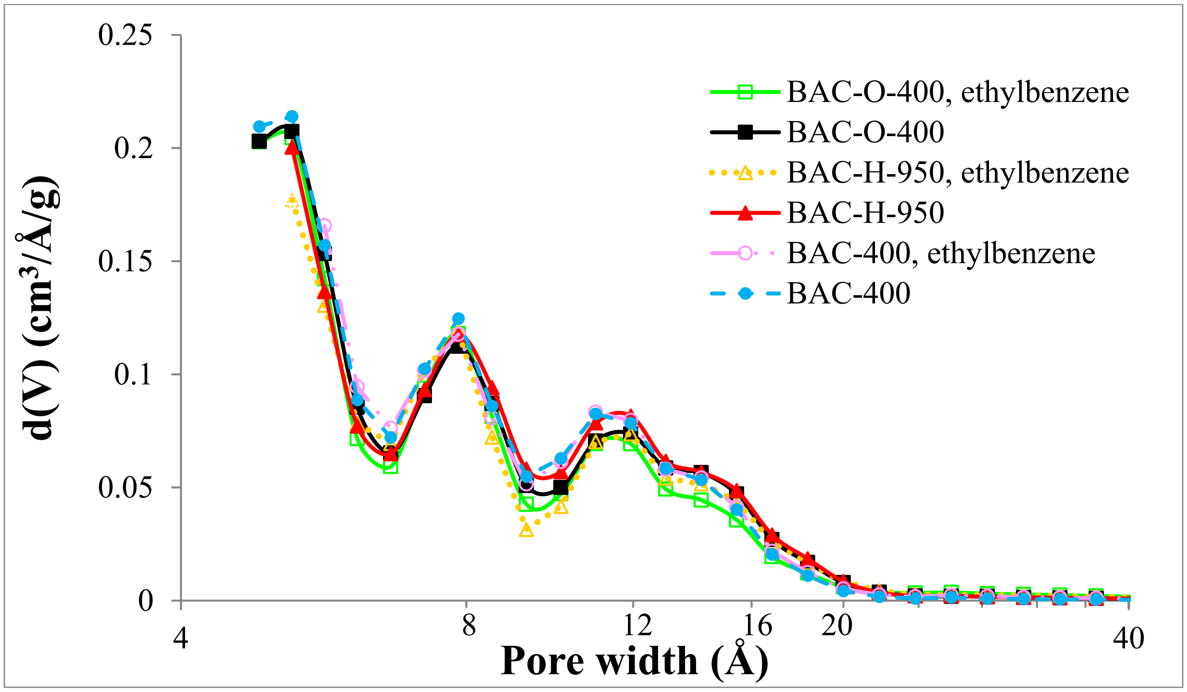

Figure 4-9. PSD of treated BAC after 5cycle adsorption/regeneration of ethylbenzene.

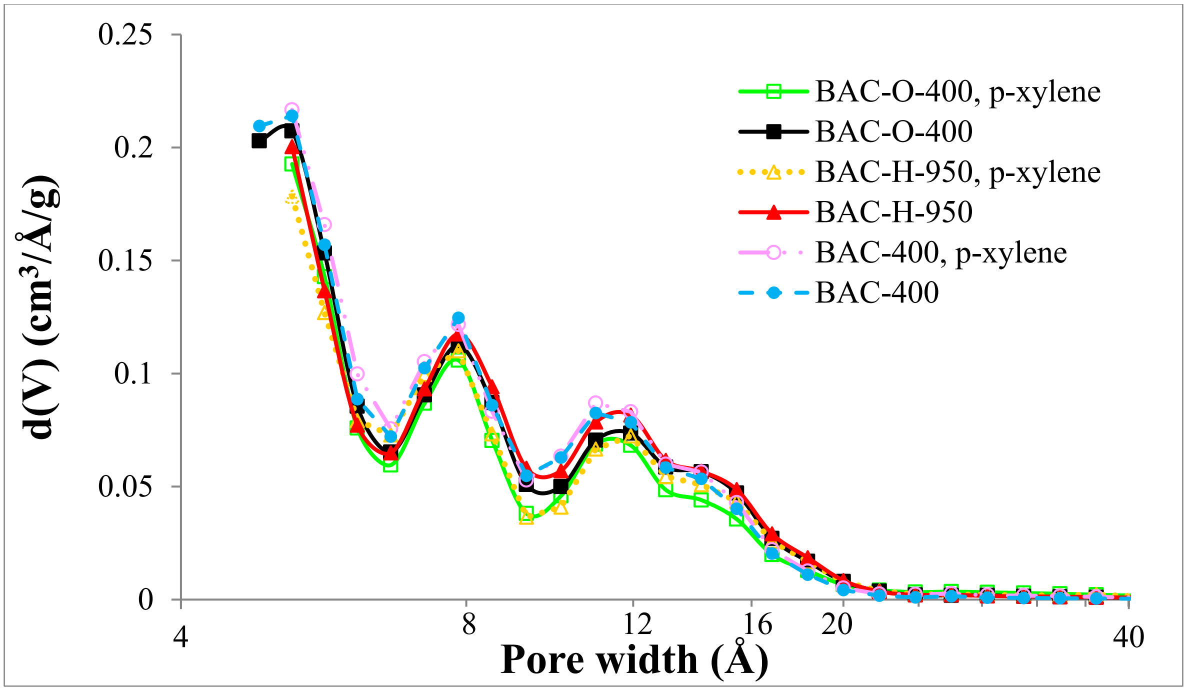

Figure 4-10. PSD of treated BAC after 5cycle adsorption/regeneration of p-xylene.

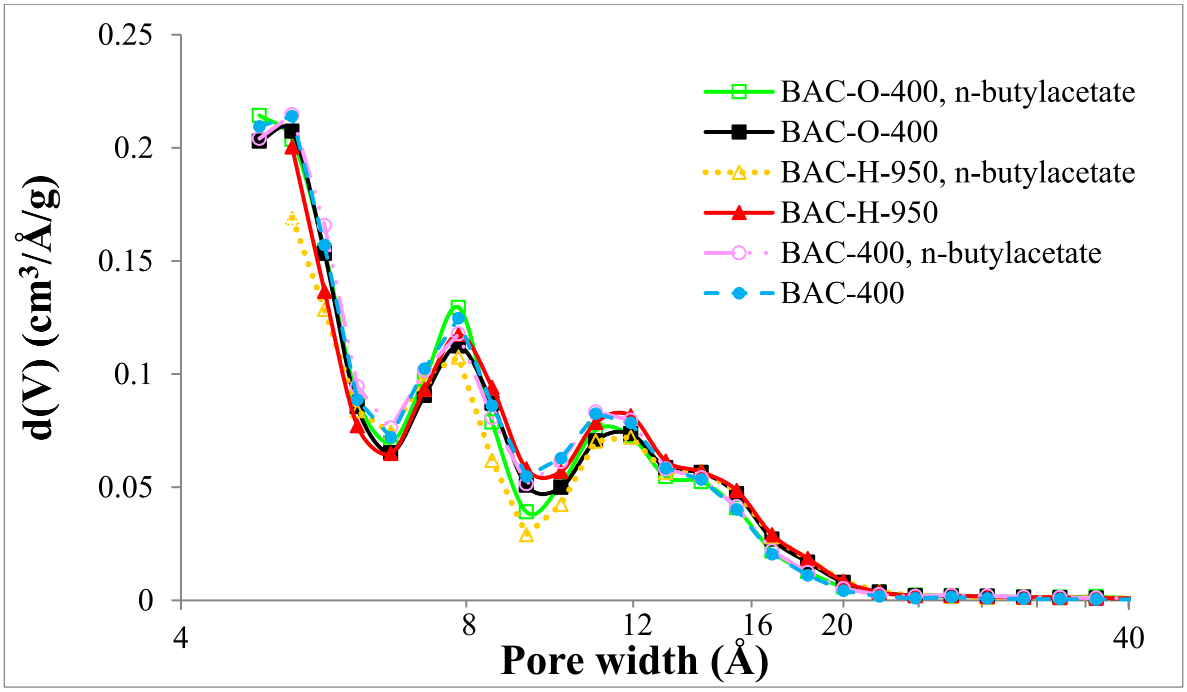

Figure 4-11. PSD of treated BAC after 5cycle adsorption/regeneration of n-butylacetate.

The effect of heel build-up on the surface area and pore volume is small as the percent of accumulated heel after 5 cycle adsorption/regeneration is between 0-4.5%. The reduction in BET surface area of acid treated BAC after cycling was less than 5% except for TMB, 2-heptanone, p-xylene. Acid treated BAC showed the highest surface area reduction for TMB, 2- heptanone, p-xylene (around 10%) compared to others, which is consistent with higher heel formation.

Pore size distribution (Figures 4-4 to 4-11) of adsorbents after regeneration reveals the location with higher potential for heel formation. The pore size distribution indicates that the irreversible adsorption has more effect on micropores. Obviously, the effect of heel formation will be more explicit for compounds with higher heel build-up. Pore size distribution for TMB showed that micropores in the range of 7 to 9 Å, have more tendency for heel build-up. It is possible that large physisorbed species were trapped in these pores. Depending on the size of adsorbed compound, either oligomerized adsorbates or chemisorbed by-products, the interfacial forces from pores' wall can hinder a complete regeneration of adsorbents and hold adsorbate or oxidation by-products insides micropores.

Also, the most reduction in pore volume is related to acid treated activated carbon. For acid treated carbon, this reduction can be attributed to higher irreversible heel formation as the pore volume related to acid treated samples before adsorption is similar to heat treated BAC before adsorption.

4.4 DTG analysis

Thermal analysis is used to obtain the DTG profiles for regenerated samples after 5 adsorption/regeneration cycles. A low heating rate (2 ºC per minute) was applied to allow a high resolution DTG profile. Figure 4-12 shows DTG analysis for different adsorbates on treated BAC. Multiple peaks at different temperatures are attributed to strength of adsorption and physisorption/chemisorption [113]. Based on the strength of interaction between adsorbent and adsorbate, the adsorbates will be desorbed at different temperatures, for example chemisorbed adsorbates are desorbed at higher temperature than physisorbed components as more energy is required to break down the formed bond between adsorbate and adsorbent.

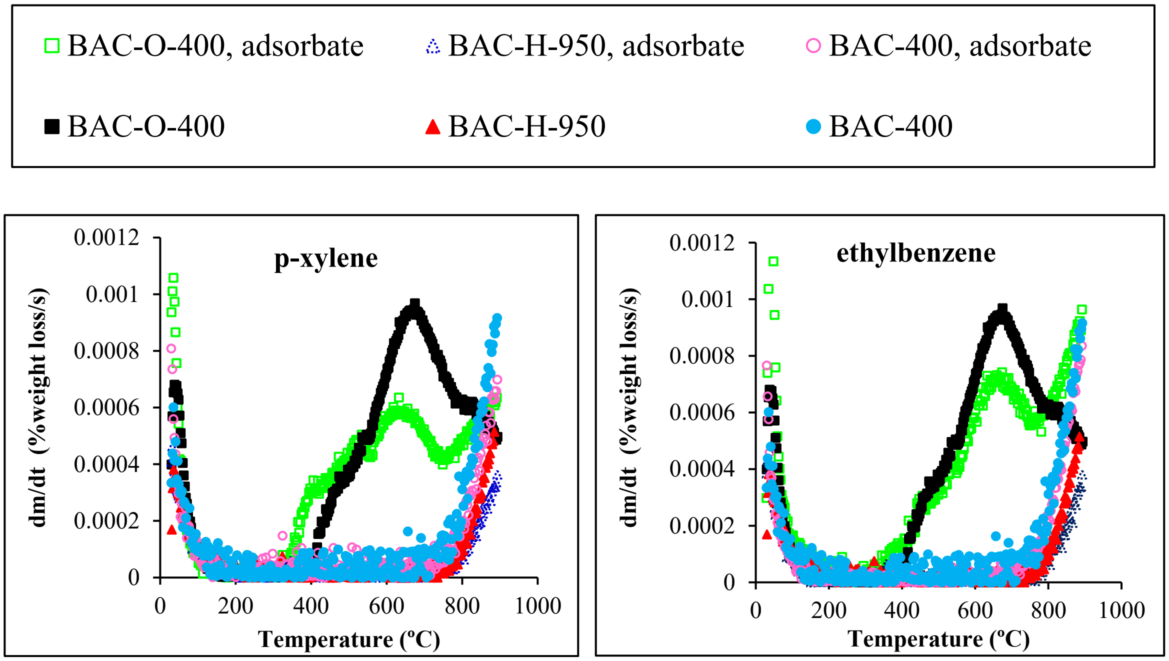

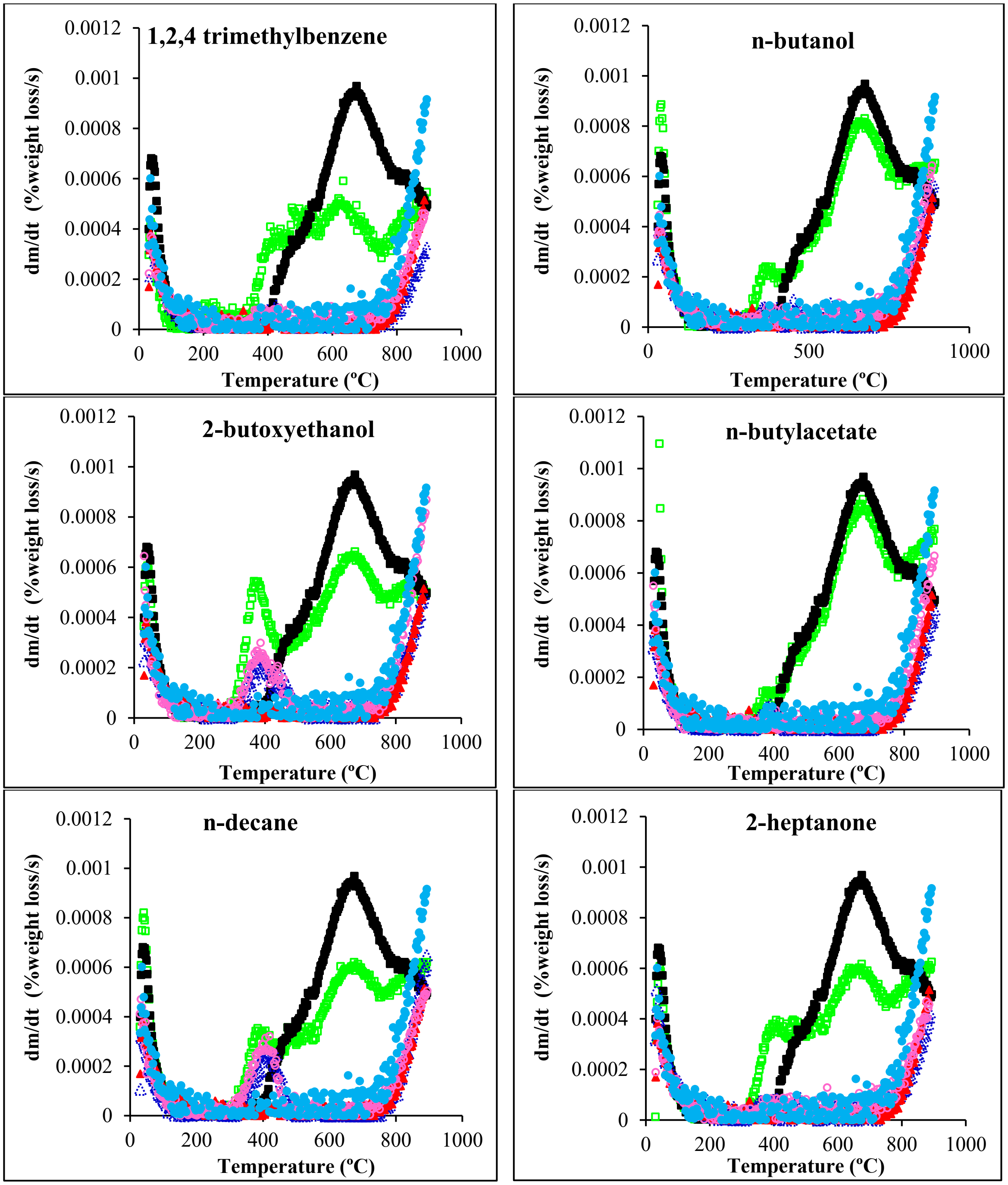

Figure 4-12. DTG analysis of treated BAC as prepared and after 5-cycle adsorption/desorption with indicated adsorbate.

The first peak in DTG plot is related to water removal since some water vapor can be adsorbed before analysis [71]. This peak is slightly higher for acid-treated samples as acid treatment increases hydrophilicity of activated carbon [40].

Except the first peak which appeared at temperature lower than 100 ºC, all acid treated BAC loaded with adsorbate showed a lower mass loss at 600-700 ºC compared to unused acid treated BAC. This behavior can be due to surface oxygen groups’ consumption. During adsorption, some of the surface oxygen groups react with adsorbate and form physi/chemisorbed by-products; hence some of surface oxygen groups are consumed [27]. The reaction by-products may be desorbed during regeneration at 288 ºC or in thermal analysis at higher temperature upon their boiling point and the type of interaction with adsorbent surface.

For most adsorbates, there was a low mass loss for heat treated BAC and hydrogen treated BAC in comparison to unused samples. Weak Van der Waal’s forces are mostly responsible for adsorption of tested adsorbates on heat treated BAC and hydrogen treated BAC. Hence, most of adsorbate molecules can be removed during regeneration process. Beside the strength of adsorbate-adsorbent interaction, boiling point and size of adsorbate have significant and direct influence on the heel accumulation and resulting mass loss peak in DTG profiles.

Among physisorbed adsorbates on heat treated or hydrogen treated BAC, non-aromatics species with short chain such as butanol, n-butyl acetate, and 2-heptanone can be removed during regeneration at 288 ºC. Therefore, mass balance showed a minute accumulated heel. However, compounds such as 2-butoxyethanol, and n-decane were not completely removed during regeneration since they have higher boiling point, longer chain or benzene ring. Limitation in diffusion and entrapment in pores or stronger interaction with adsorbent surface prevent a thorough desorption which results in higher heel compared to other tested adsorbates, and presence of a mass loss peak in DTG profiles. Another possible premise for higher heel formation for 2-butoxyethanol can be the hydrogen bonding. The hydrogen in hydroxyl group (-OH) can be involved in hydrogen bonding with the polar oxygen on the surface of activated groups [24, 61].

Overall, it can be said that the peak around 400 ºC, which is higher than boiling point of tested adsorbates and regeneration temperature, can be attributed to accumulated physisorbed adsorbates. In small pores, both diffusion limitation and interfacial forces from pores' wall have critical influence on preventing complete regeneration of the BAC. In narrow pores of adsorbent, the removal of physisorbed adsorbates can be difficult due to limited diffusion, specifically for bulky adsorbates [43]. In small pores (< 7 ºA) comparable to kinetic diameter of tested adsorbates, the interaction between adsorbate molecules and pores' wall is higher and prevents an easy and complete removal of physisorbed species during regeneration cycles at 288 ºC. Therefore, a higher energy is required to overcome these interfacial interactions and removes most of physisorbed components, which can be provided at 400 ºC [44]. Therefore, a complete regeneration cannot be attained during regeneration periods. This peak is so obvious for high boiling components like n-decane and 2-butoxyethanol as they have a longer chain.

5 CONCLUSION AND RECOMMENDATIONS

5.1 Conclusion

The impact of activated carbon's surface oxygen groups on irreversible adsorption of volatile organic compounds commonly present in paint booth air streams was investigated. For this purpose, three types of adsorbents were used. Beaded activated carbon' surface was tailored to have similar pore size distribution but different content of surface oxygen groups. Adsorbates with different functionality were chosen to study the interaction of different compounds with surface oxygen groups. Important findings of this research are:

- Adsorption capacity decreased after 5-cycle adsorption-regeneration as a consequence of heel formation.
- For all samples, acid-treated samples showed higher heel build-up compared to hydrogen-treated or heat treated BAC.
- Cumulative heel buildup for hydrogen treated and heat treated BAC were similar.
- From derivative thermo-gravimetric analysis, it can be inferred that both chemisorption and physisorption are responsible for heel formation on acid-treated BAC. A hypothesis was introduced that surface oxygen groups are consumed during adsorption/regeneration. The products of this consumption reaction may be removed during regeneration or thermogravimetric analysis [27].
- Among tested adsorbates, aromatic adsorbates showed higher heel on acid-treated BAC in comparison to hydrogen-treated and heat treated BAC.

- Compounds with higher boiling temperature and longer chain showed higher heel as they need more energy to overcome interfacial forces or they are bulkier and may be trapped in small pores.

5.2 Recommendations for future research

This study explored the impact of surface oxygen content on irreversible heel formation. The following recommendations can be considered for future works:

- The presence of water vapor during adsorption of volatile organic compounds can be studied as off gas streams from different industries usually contain water vapor. The presence of water vapor results in a competitive adsorption, which will affect the adsorption capacity and heel build-up.

- High purity nitrogen was used as regeneration purge gas in this research. Alternative purge gases, such as $N_2 + H_2O$, and flue gas ($N_2 + CO_2 + H_2O$) can be employed to reduce the operational cost and consider the effect of regeneration gas on irreversible adsorption on treated activated carbon.

- Since surface oxygen groups are removed during hydrogen treatment, it would be interesting to investigate the effect of hydrogen treatment on activated carbons with different precursors and activation method, which results in different amount of surface oxygen groups. The BAC used in this study contains a low amount (5.6%) of surface oxygen groups. The effect of hydrogen treatment on irreversible heel build-up may be highlighted for activated carbon with higher amount of surface oxygen groups.

- The influence of adsorbent porosity on irreversible adsorption of organic vapors on acid/hydrogen treated activated carbon can be investigated since porosity of adsorbent is one of the controlling factors in irreversible heel formation. Activated carbon with different pore size distribution can be used to consider the impact of porosity along with acid/hydrogen treatment.

- In this research, a mild acid treatment was done to avoid large change to the adsorbent's porosity. Higher acid concentration can be employed to study the effect of higher oxidation condition on activated texture and its impact on irreversible heel build-up and adsorption capacity since more concentrated acid results in lower surface area, pore widening and higher surface oxygen groups, which may block the entrance of some pores.

- The effect of regeneration temperature can be considered for future work. At higher temperature, the possibility of side reaction increases and it will have influence on heel formation and adsorption capacity. In contrast, regeneration at lower temperature will reduce operating cost and cause less adsorbent destruction but it is necessary to consider regeneration efficiency.

REFERENCES

[1] US Environmental Protection Agency (EPA). https://www.epa.gov/indoor-air-quality-iaq/technical-overview-volatile-organic-compounds#EPA%20Regulatory%20Definition, 2016 (accessed 06/09/2016.2016).

[2] P. Hunter, Control of volatile organic compound emissions : conventional and emerging technologies, in: S.T. Oyama (Ed.) John Wiley & Sons, New York, 2000.

[3] B.R. Kim, VOC emissions from automotive painting and their control: A review, Environmental Engineering Research 16 (2011) 1-9.

[4] M. Kampa, E. Castanas, Human health effects of air pollution, Environmental Pollution 151(2) (2008) 362-367.

[5] G.B. Leslie, Health risks from indoor air pollutants: public alarm and toxicological reality, Indoor and Built Environment 9(1) (2000) 5-16.

[6] F. Pariselli, M.G. Sacco, J. Ponti, D. Rembges, Effects of toluene and benzene air mixtures on human lung cells (A549), Experimental and Toxicologic Pathology 61(4) (2009) 381-386.

[7] L.A. Wallace, Human exposure to environmental pollutants: a decade of experience, Clinical & Experimental Allergy 25(1) (1995) 4-9.

[8] N. Ramírez, A. Cuadras, E. Rovira, F. Borrull, R.M. Marcé, Chronic risk assessment of exposure to volatile organic compounds in the atmosphere near the largest Mediterranean industrial site, Environment International 39(1) (2012) 200-209.

[9] F.I. Khan, A. Kr. Ghoshal, Removal of volatile organic compounds from polluted air, Journal of Loss Prevention in the Process Industries 13(6) (2000) 527-545.

[10] G.R. Parmar, N.N. Rao, Emerging control technologies for volatile organic compounds, Critical Reviews in Environmental Science and Technology 39(1) (2008) 41-78.

[11] A. Berenjian, N. Chan, H.J. Malmiri, Volatile organic compounds removal methods: a review, American Journal of Biochemistry and Biotechnology 8(4) (2012) 220-229.

[12] C.D. Cooper, F.C. Alley, Air pollution control : a design approach, in: F.C. Alley (Ed.) Waveland Press, Long Grove, Ill, 2011.

[13] M.A. Lillo-Ródenas, D. Cazorla-Amorós, A. Linares-Solano, Behaviour of activated carbons with different pore size distributions and surface oxygen groups for benzene and toluene adsorption at low concentrations, Carbon 43(8) (2005) 1758-1767.

[14] Z. Hashisho, H. Emamipour, M.J. Rood, K.J. Hay, B.J. Kim, D. Thurston, Concomitant adsorption and desorption of organic vapor in dry and humid air streams using microwave and

direct electrothermal swing adsorption, Environmental Science & Technology 42(24) (2008) 9317-9322.

[15] R.C. Bansal, Activated carbon adsorption, in: M. Goyal (Ed.) Taylor & Francis, Boca Raton, 2005.

[16] K.P. Singh, D. Mohan, G.S. Tandon, G.S.D. Gupta, Vapor-phase adsorption of hexane and benzene on activated carbon fabric cloth: equilibria and rate studies, Industrial & Engineering Chemistry Research 41(10) (2002) 2480-2486.

[17] R.T. Yang, Gas separation by adsorption processes, Imperial College Press, London, 1997.

[18] M. Suzuki, Adsorption engineering, Kodansha, Tokyo, 1990.

[19] E.J. Bottani, J.M.D. Tascón, Adsorption by carbons, in: E.J. Bottani, J.M.D. Tascón (Eds.) Elsevier, Amsterdam ;, 2008.

[20] Q. Lu, G.A. Sorial, A comparative study of multicomponent adsorption of phenolic compounds on GAC and ACFs, Journal of Hazardous Materials 167(1–3) (2009) 89-96.

[21] G. Busca, S. Berardinelli, C. Resini, L. Arrighi, Technologies for the removal of phenol from fluid streams: A short review of recent developments, Journal of Hazardous Materials 160(2–3) (2008) 265-288.

[22] P.M. Álvarez, F.J. Beltrán, V. Gómez-Serrano, J. Jaramillo, E.M. Rodríguez, Comparison between thermal and ozone regenerations of spent activated carbon exhausted with phenol, Water Research 38(8) (2004) 2155-2165.

[23] C.Y. Yin, M.K. Aroua, W.M.A.W. Daud, Review of modifications of activated carbon for enhancing contaminant uptakes from aqueous solutions, Separation and Purification Technology 52(3) (2007) 403-415.

[24] H.A. Arafat, F. Ahnert, N.G. Pinto, On the adsorption of aromatics on oxygenated activated carbon in nonaqueous adsorption media, Separation Science and Technology 39(1) (2005) 43-62.

[25] Z. Jiang, Y. Liu, X. Sun, F. Tian, F. Sun, C. Liang, W. You, C. Han, C. Li, Activated carbons chemically modified by concentrated H2SO4 for the adsorption of the pollutants from wastewater and the dibenzothiophene from fuel oils, Langmuir 19(3) (2003) 731-736.

[26] G.G. Stavropoulos, P. Samaras, G.P. Sakellaropoulos, Effect of activated carbons modification on porosity, surface structure and phenol adsorption, Journal of Hazardous Materials 151(2–3) (2008) 414-421.

[27] M. Jahandar Lashaki, J.D. Atkinson, Z. Hashisho, J.H. Phillips, J.E. Anderson, M. Nichols, The role of beaded activated carbon's surface oxygen groups on irreversible adsorption of organic vapors, Journal of Hazardous Materials 317 (2016) 284-294.

[28] Z. Hashisho, M.J. Rood, S. Barot, J. Bernhard, Role of functional groups on the microwave attenuation and electric resistivity of activated carbon fiber cloth, Carbon 47(7) (2009) 1814-1823.

[29] J. Carratalá-Abril, M.A. Lillo-Ródenas, A. Linares-Solano, D. Cazorla-Amorós, Activated carbons for the removal of low-concentration gaseous toluene at the semipilot scale, Industrial & Engineering Chemistry Research 48(4) (2009) 2066-2075.

[30] M.B. Yahia, Y.B. Torkia, S. Knani, M.A. Hachicha, M. Khalfaoui, A.B. Lamine, Models for type vi adsorption isotherms from a statistical mechanical formulation, Adsorption Science & Technology 31(4) (2013) 341-358.

[31] K.S. Sing, Reporting physisorption data for gas/solid systems with special reference to the determination of surface area and porosity (recommendations 1984), Pure and applied chemistry 57(4) (1985) 603-619.

[32] M.C. Huang, C.H. Chou, H. Teng, Pore-size effects on activated-carbon capacities for volatile organic compound adsorption, AIChE Journal 48(8) (2002) 1804-1810.

[33] C.C. Leng, N.G. Pinto, Effects of surface properties of activated carbons on adsorption behavior of selected aromatics, Carbon 35(9) (1997) 1375-1385.

[34] A. Chakma, A. Meisen, Activated carbon adsorption of diethanolamine, methyl diethanolamine and their degradation products, Carbon 27(4) (1989) 573-584.

[35] H.L. Chiang, C.P. Huang, P.C. Chiang, The surface characteristics of activated carbon as affected by ozone and alkaline treatment, Chemosphere 47(3) (2002) 257-265.

[36] J.-H. Tsai, H.-M. Chiang, G.-Y. Huang, H.-L. Chiang, Adsorption characteristics of acetone, chloroform and acetonitrile on sludge-derived adsorbent, commercial granular activated carbon and activated carbon fibers, Journal of Hazardous Materials 154(1–3) (2008) 1183-1191.

[37] M.A. Lillo-Ródenas, D. Cazorla-Amorós, A. Linares-Solano, Benzene and toluene adsorption at low concentration on activated carbon fibres, Adsorption 17(3) (2011) 473-481.

[38] B. Boulinguiez, P. Le Cloirec, Adsorption on activated carbons of five selected volatile organic compounds present in biogas: comparison of granular and fiber cloth materials, Energy & Fuels 24(9) (2010) 4756-4765.

[39] D. Das, V. Gaur, N. Verma, Removal of volatile organic compound by activated carbon fiber, Carbon 42(14) (2004) 2949-2962.

[40] P.D. Sullivan, B.R. Stone, Z. Hashisho, M.J. Rood, Water adsorption with hysteresis effect onto microporous activated carbon fabrics, Adsorption 13(3) (2007) 173-189.

[41] Ö. Aktaş, F. Çeçen, Effect of type of carbon activation on adsorption and its reversibility, Journal of Chemical Technology and Biotechnology 81(1) (2006) 94-101.

[42] F. Salvador, C.S. Jiménez, A new method for regenerating activated carbon by thermal desorption with liquid water under subcritical conditions, Carbon 34(4) (1996) 511-516.

[43] M.J. Lashaki, M. Fayaz, H. Wang, Z. Hashisho, J.H. Philips, J.E. Anderson, M. Nichols, Effect of adsorption and regeneration temperature on irreversible adsorption of organic vapors on beaded activated carbon, Environmental Science & Technology 46(7) (2012) 4083-4090.

[44] M. Jahandar Lashaki, M. Fayaz, S. Niknaddaf, Z. Hashisho, Effect of the adsorbate kinetic diameter on the accuracy of the Dubinin–Radushkevich equation for modeling adsorption of organic vapors on activated carbon, Journal of Hazardous Materials 241–242 (2012) 154-163.

[45] H.-W. Hung, T.-F. Lin, Prediction of the adsorption capacity for volatile organic compounds onto activated carbons by the dubinin–radushkevich–langmuir model, Journal of the Air & Waste Management Association 57(4) (2007) 497-506.

[46] Q. Lu, G.A. Sorial, The role of adsorbent pore size distribution in multicomponent adsorption on activated carbon, Carbon 42(15) (2004) 3133-3142.

[47] C. Pelekani, V.L. Snoeyink, Competitive adsorption between atrazine and methylene blue on activated carbon: the importance of pore size distribution, Carbon 38(10) (2000) 1423-1436.

[48] M.-G. Lee, S.-W. Lee, S.-H. Lee, Comparison of vapor adsorption characteristics of acetone and toluene based on polarity in activated carbon fixed-bed reactor, Korean Journal of Chemical Engineering 23(5) (2006) 773-778.

[49] C. Yu-Chun, C. Pen-Chi, Effects of surface characteristics of activated carbons on voc adsorption, Journal of Environmental Engineering 127(1) (2001) 54.

[50] L. Li, Z. Sun, H. Li, T.C. Keener, Effects of activated carbon surface properties on the adsorption of volatile organic compounds, Journal of the Air & Waste Management Association 62(10) (2012) 1196-1202.

[51] N. Kawasaki, H. Kinoshita, T. Oue, T. Nakamura, S. Tanada, Study on adsorption kinetic of aromatic hydrocarbons onto activated carbon in gaseous flow method, Journal of Colloid and Interface Science 275(1) (2004) 40-43.

[52] E. Biron, M.J. Evans, Dynamic adsorption of water-soluble and insoluble vapours on activated carbon, Carbon 36(7) (1998) 1191-1197.

[53] Z.-H. Huang, F. Kang, K.-M. Liang, J. Hao, Breakthrough of methyethylketone and benzene vapors in activated carbon fiber beds, Journal of Hazardous Materials 98(1–3) (2003) 107-115.

[54] C.-L. Chuang, P.-C. Chiang, E.E. Chang, Kinetics of benzene adsorption onto activated carbon, Environmental Science and Pollution Research 10(1) (2003) 6-8.

[55] C.L. Chuang, P.C. Chiang, E.E. Chang, C.P. Huang, Adsorption-desorption rate of nonpolar volatile organic compounds onto activated carbon exemplified by C6H6 and CCl4, Practice Periodicals of Hazardous Toxic and Radioactive Waste Management 7 (2003) 148-155.

[56] Y.-C. Chiang, P.-C. Chiang, C.-P. Huang, Effects of pore structure and temperature on VOC adsorption on activated carbon, Carbon 39(4) (2001) 523-534.

[57] N. Mohan, G.K. Kannan, S. Upendra, R. Subha, N.S. Kumar, Breakthrough of toluene vapours in granular activated carbon filled packed bed reactor, Journal of Hazardous Materials 168(2–3) (2009) 777-781.

[58] A.J. Fletcher, Y. Yüzak, K.M. Thomas, Adsorption and desorption kinetics for hydrophilic and hydrophobic vapors on activated carbon, Carbon 44(5) (2006) 989-1004.

[59] F. Delage, P. Pré, P. Cloirec, Effects of moisture on warming of activated carbon bed during voc adsorption, Journal of Environmental Engineering 125(12) (1999) 1160-1167.

[60] W. Yazbek, P. Pré, A. Delebarre, Adsorption and desorption of volatile organic compounds in fluidized bed, Journal of Environmental Engineering 132(5) (2006) 442-452.

[61] M. Franz, H.A. Arafat, N.G. Pinto, Effect of chemical surface heterogeneity on the adsorption mechanism of dissolved aromatics on activated carbon, Carbon 38(13) (2000) 1807-1819.

[62] O.P. Mahajan, C. Moreno-castilla, P.L. Walker, Surface-treated activated carbon for removal of phenol from water, Separation Science and Technology 15(10) (1980) 1733-1752.

[63] P. Sullivan, M. Rood, K. Hay, S. Qi, Adsorption and electrothermal desorption of hazardous organic vapors, Journal of Environmental Engineering 127(3) (2001) 217-223.

[64] R.E. Sanders, Designs that lacked inherent safety: case histories, Journal of Hazardous Materials 104(1–3) (2003) 149-161.

[65] F. Delage, P. Pré, P. Le Cloirec, Mass transfer and warming during adsorption of high concentrations of vocs on an activated carbon bed: Experimental and Theoretical Analysis, Environmental Science & Technology 34(22) (2000) 4816-4821.

[66] Y.L. Ng, R. Yan, L.T.S. Tsen, L.C. Yong, M. Liu, D.T. Liang, Volatile organic compound adsorption in a gas-solid fluidized bed, Water Science and Technology 50(4) (2004) 233-240.

[67] A. Reichhold, H. Hofbauer, Internally circulating fluidized bed for continuous adsorption and desorption, Chemical Engineering and Processing: Process Intensification 34(6) (1995) 521-527.

[68] W. Song, D. Tondeur, L. Luo, J. Li, VOC adsorption in circulating gas fluidized bed, Adsorption 11(1) (2005) 853-858.

[69] A.M. Hamed, W.R. Abd El Rahman, S.H. El-Emam, Experimental study of the transient adsorption/desorption characteristics of silica gel particles in fluidized bed, Energy 35(6) (2010) 2468-2483.

[70] P.M. Álvarez, J.F. García-Araya, F.J. Beltrán, F.J. Masa, F. Medina, Ozonation of activated carbons: Effect on the adsorption of selected phenolic compounds from aqueous solutions, Journal of Colloid and Interface Science 283(2) (2005) 503-512.

[71] M. Popescu, J.P. Joly, J. Carré, C. Danatoiu, Dynamical adsorption and temperature-programmed desorption of VOCs (toluene, butyl acetate and butanol) on activated carbons, Carbon 41(4) (2003) 739-748.

[72] Z. Hashisho, M. Rood, L. Botich, Microwave-swing adsorption to capture and recover vapors from air streams with activated carbon fiber cloth, Environmental Science & Technology 39(17) (2005) 6851-6859.

[73] Ö. Aktaş, F. Çeçen, Competitive adsorption and desorption of a bi-solute mixture: effect of activated carbon type, Adsorption 13(2) (2007) 159-169.

[74] A. Dąbrowski, P. Podkościelny, Z. Hubicki, M. Barczak, Adsorption of phenolic compounds by activated carbon—a critical review, Chemosphere 58(8) (2005) 1049-1070.

[75] R.T. Yang, Adsorbents: fundamentals and applications, John Wiley & Sons Inc., Hoboken, NJ, USA, 2003.

[76] J. Rivera-Utrilla, M.A. Ferro-García, I. Bautista-Toledo, C. Sánchez-Jiménez, F. Salvador, M.D. Merchán, Regeneration of ortho-chlorophenol-exhausted activated carbons with liquid water at high pressure and temperature, Water Research 37(8) (2003) 1905-1911.

[77] A.A. Ahmad, A. Idris, Preparation and characterization of activated carbons derived from bio-solid: a review, ChemInform 45(42) (2014).

[78] J. Wang, S. Kaskel, KOH activation of carbon-based materials for energy storage, Journal of Materials Chemistry 22(45) (2012) 23710-23725.

[79] R.O. Grisdale, The properties of carbon contacts, Journal of Applied Physics 24(10) (1953) 1288-1296.

[80] G.R. Hennig, Surface oxides on graphite single crystals, Proceedings of the Fifth Conference on Carbon, Pergamon1962, pp. 143-146.

[81] A.P. Terzyk, The impact of carbon surface chemical composition on the adsorption of phenol determined at the real oxic and anoxic conditions, Applied Surface Science 253(13) (2007) 5752-5755.

[82] D.R. Yonge, T.M. Keinath, K. Poznanska, Z.P. Jiang, Single-solute irreversible adsorption on granular activated carbon, Environmental Science & Technology 19(8) (1985) 690-694.

[83] J.A. Mattson, H.B. Mark, M.D. Malbin, W.J. Weber, J.C. Crittenden, Surface chemistry of active carbon: Specific adsorption of phenols, Journal of Colloid and Interface Science 31(1) (1969) 116-130.

[84] P. Magne, P.L. Walker, Phenol adsorption on activated carbons: Application to the regeneration of activated carbons polluted with phenol, Carbon 24(2) (1986) 101-107.

[85] N. Soudani, S. Souissi-Najar, A. Ouederni, Influence of nitric acid concentration on characteristics of olive stone based activated carbon, Chinese Journal of Chemical Engineering 21(12) (2013) 1425-1430.

[86] S. Wang, Z.H. Zhu, A. Coomes, F. Haghseresht, G.Q. Lu, The physical and surface chemical characteristics of activated carbons and the adsorption of methylene blue from wastewater, Journal of Colloid and Interface Science 284(2) (2005) 440-446.

[87] A.-N.A. El-Hendawy, Influence of HNO3 oxidation on the structure and adsorptive properties of corncob-based activated carbon, Carbon 41(4) (2003) 713-722.

[88] Y. Gokce, Z. Aktas, Nitric acid modification of activated carbon produced from waste tea and adsorption of methylene blue and phenol, Applied Surface Science 313 (2014) 352-359.

[89] S. Wang, Z.H. Zhu, Effects of acidic treatment of activated carbons on dye adsorption, Dyes and Pigments 75(2) (2007) 306-314.

[90] H. Valdés, M. Sánchez-Polo, J. Rivera-Utrilla, C.A. Zaror, Effect of ozone treatment on surface properties of activated carbon, Langmuir 18(6) (2002) 2111-2116.

[91] M. Jahangiri, S.J. Shahtaheri, J. Adl, A. Rashidi, H. Kakooei, A.R. Forushani, M.R. Ganjali, A. Ghorbanali, The adsorption of benzene, toluene and xylenes (btx) on the carbon nanostructures: the study of different parameters, Fresenius Environmental Bulletin 20(4A) (2011) 1036-1045.

[92] A. Derylo-Marczewska, B. Buczek, A. Swiatkowski, Effect of oxygen surface groups on adsorption of benzene derivatives from aqueous solutions onto active carbon samples, Applied Surface Science 257(22) (2011) 9466-9472.

[93] F. Rodriguez-Reinoso, M. Molina-Sabio, M.A. Munecas, Effect of microporosity and oxygen surface groups of activated carbon in the adsorption of molecules of different polarity, The Journal of Physical Chemistry 96(6) (1992) 2707-2713.

[94] S. Furmaniak, Influence of activated carbon porosity and surface oxygen functionalities' presence on adsorption of acetonitrile as a simple polar volatile organic compound, Environmental Technology 36(15) (2015) 1984-1999.

[95] T. Bohli, A. Ouederni, Improvement of oxygen-containing functional groups on olive stones activated carbon by ozone and nitric acid for heavy metals removal from aqueous phase, Environmental Science & Pollution Research 23(16) (2016) 15852-15861.

[96] A. Gotzias, E. Tylianakis, G. Froudakis, T. Steriotis, Adsorption in micro and mesoporous slit carbons with oxygen surface functionalities, Microporous & Mesoporous Materials 209 (2015) 141-149.

[97] B. Ledesma, S. Román, A. Álvarez-Murillo, E. Sabio, J.F. González, Cyclic adsorption/thermal regeneration of activated carbons, Journal of Analytical and Applied Pyrolysis 106 (2014) 112-117.

[98] M.R. Cuervo, E. Asedegbega-Nieto, E. Díaz, A. Vega, S. Ordóñez, E. Castillejos-López, I. Rodríguez-Ramos, Effect of carbon nanofiber functionalization on the adsorption properties of volatile organic compounds, Journal of Chromatography A 1188(2) (2008) 264-273.

[99] Kureha Corporation. Website; http://www.kureha.com/pdfs/Kureha-BAC-Bead-Activated-Carbon.pdf., (accessed 27/10/2016.2016).

[100] J.P. Olivier, Improving the models used for calculating the size distribution of micropore volume of activated carbons from adsorption data, Carbon 36(10) (1998) 1469-1472.

[101] F. Salvador, N. Martin-Sanchez, R. Sanchez-Hernandez, M.J. Sanchez-Montero, C. Izquierdo, Regeneration of carbonaceous adsorbents. part I: thermal regeneration, Microporous and Mesoporous Materials 202 (2015) 259-276.

[102] H.P. Boehm, Some aspects of the surface chemistry of carbon blacks and other carbons, Carbon 32(5) (1994) 759-769.

[103] H.P. Boehm, E. Diehl, W. Heck, R. Sappok, Surface oxides of carbon, Angewandte Chemie International Edition in English 3(10) (1964) 669-677.

[104] H.P. Boehm, Surface oxides on carbon and their analysis: a critical assessment, Carbon 40(2) (2002) 145-149.

[105] D.M. Nevskaia, A. Santianes, V. Muñoz, A. Guerrero-Ruíz, Interaction of aqueous solutions of phenol with commercial activated carbons: an adsorption and kinetic study, Carbon 37(7) (1999) 1065-1074.

[106] G. de la Puente, J.J. Pis, J.A. Menéndez, P. Grange, Thermal stability of oxygenated functions in activated carbons, Journal of Analytical and Applied Pyrolysis 43(2) (1997) 125-138.

[107] A. Perrard, L. Retailleau, R. Berjoan, J.-P. Joly, Liquid phase oxidation kinetics of an ex-cellulose activated carbon cloth by NaOCl, Carbon 50(6) (2012) 2226-2234.

[108] A. Derylo-Marczewska, A. Swiatkowski, S. Biniak, M. Walczyk, Effect of properties of chemically modified activated carbon and aromatic adsorbate molecule on adsorption from liquid phase, Colloids and Surfaces A: Physicochemical and Engineering Aspects 327(1–3) (2008) 1-8.

[109] H. Guedidi, L. Reinert, J.-M. Lévêque, Y. Soneda, N. Bellakhal, L. Duclaux, The effects of the surface oxidation of activated carbon, the solution pH and the temperature on adsorption of ibuprofen, Carbon 54 (2013) 432-443.

[110] W. Tsang, The stability of alkyl radicals, Journal of the American Chemical Society 107(10) (1985) 2872-2880.

[111] K.E. McCulloh, V.H. Dibeler, Enthalpy of formation of methyl and methylene radicals of photoionization studies of methane and ketene, The Journal of Chemical Physics 64(11) (1976) 4445-4450.

[112] R.K. Rowe, T. Mukunoki, H.P. Sangam, Benzene, toluene, ethylbenzene, m&p-xylene, o-xylene diffusion and sorption for a geosynthetic clay liner at two temperatures, Journal of Geotechnical and Geoenvironmental Engineering 131(10) (2005) 1211-1221.

[113] M.A. Ferro-García, E. Utrera-Hidalgo, J. Rivera-Utrilla, C. Moreno-Castilla, J.P. Joly, Regeneration of activated carbons exhausted with chlorophenols, Carbon 31(6) (1993) 857-863.

APPENDIX A

Breakthrough curves

Adsorption of p-xylene

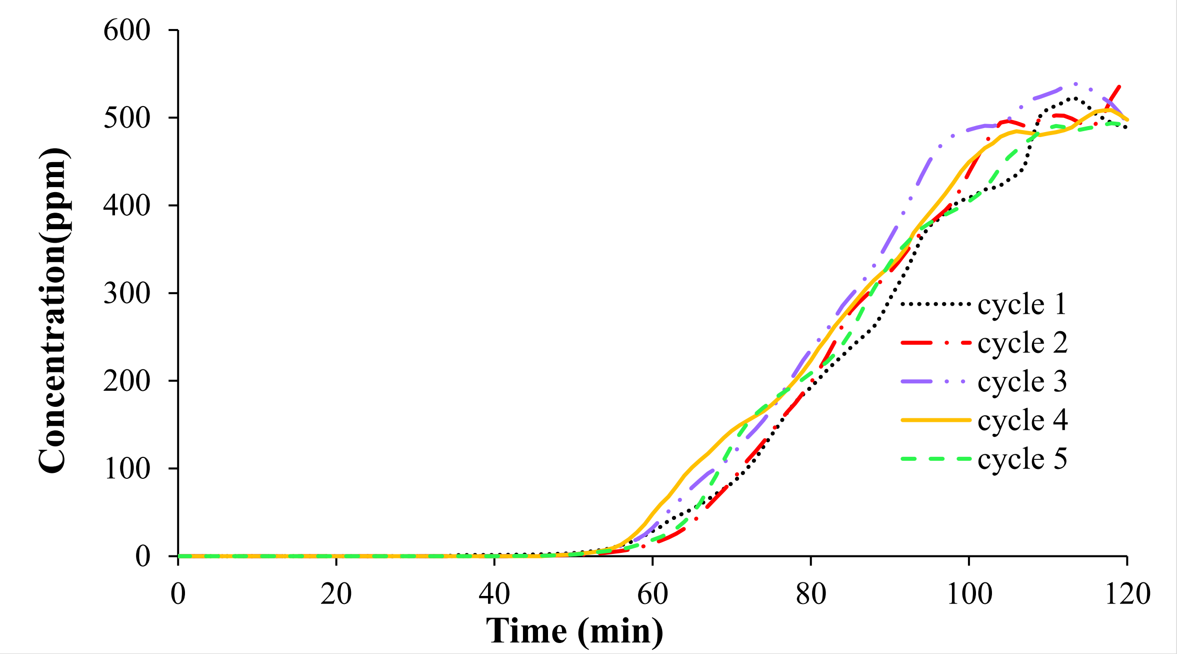

Figure A- 1. Breakthrough curves of p-xylene on heat treated BAC.

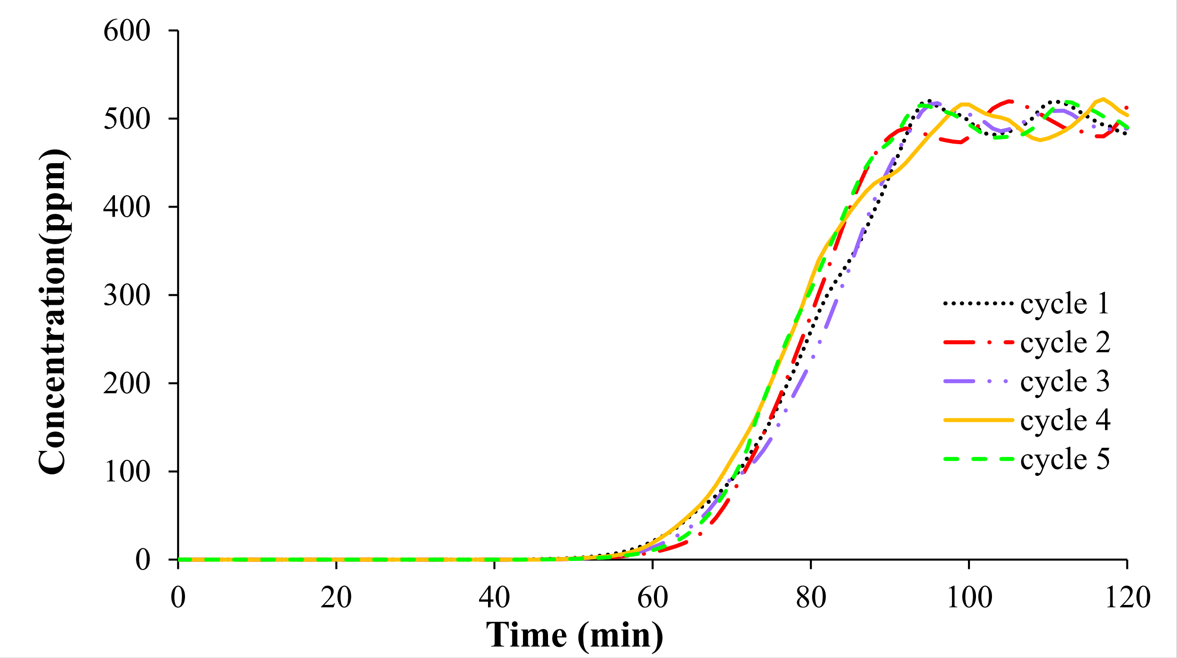

Figure A- 2. Breakthrough curves of p-xylene on hydrogen treated Kureha BAC.

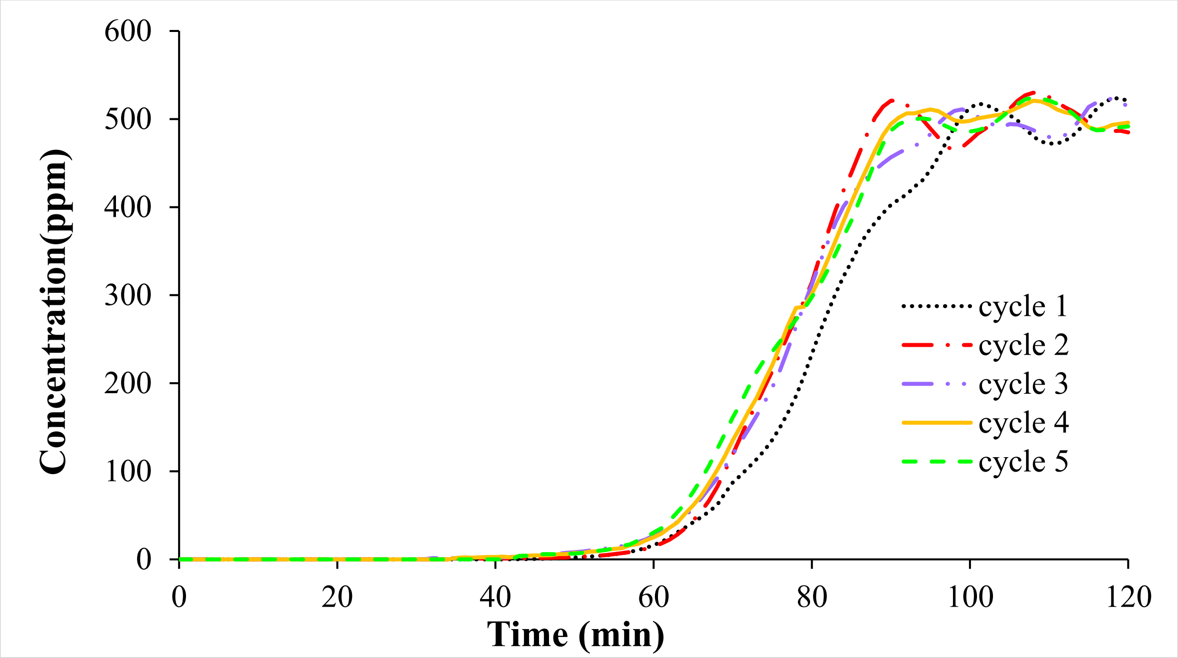

Figure A- 3. Breakthrough curves of p-xylene on acid treated Kureha BAC.

Adsorption of ethylbenzene

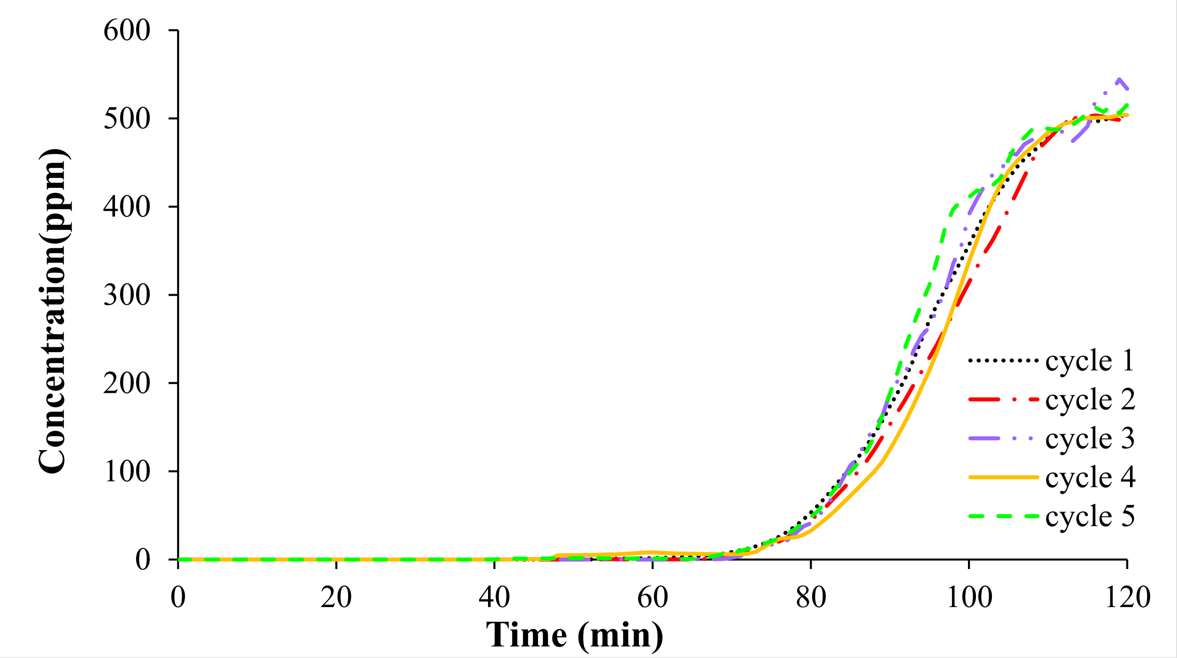

Figure A- 4. Breakthrough curves of ethylbenzene on heat treated BAC.

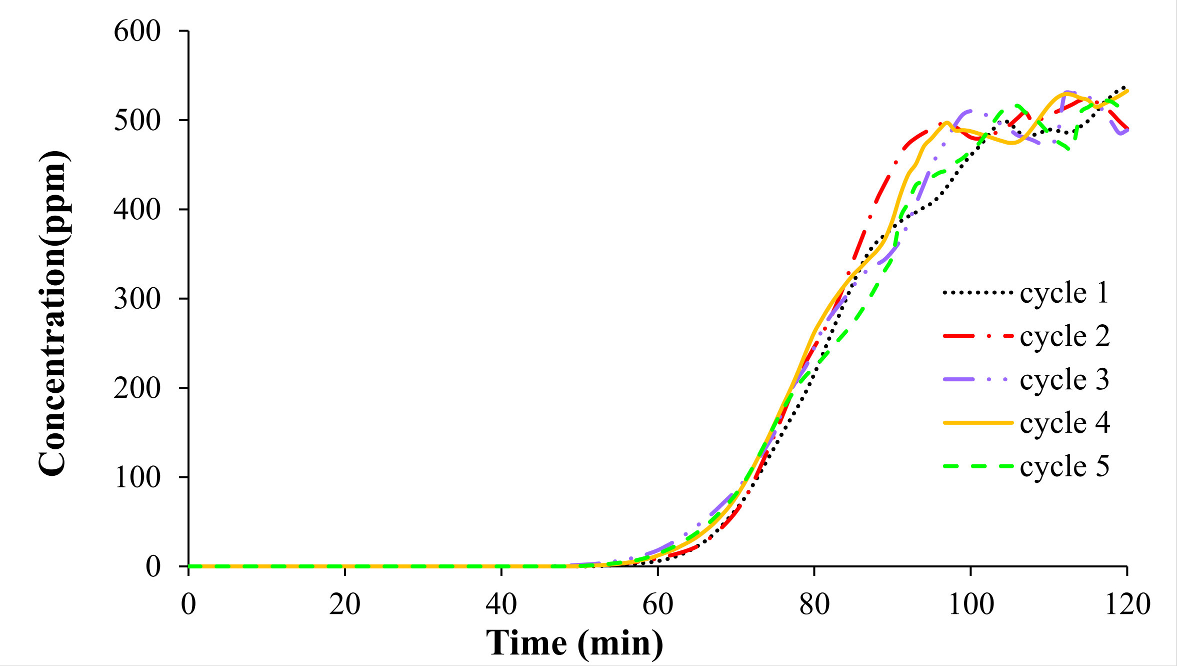

Figure A- 5. Breakthrough curves of ethylbenzene on hydrogen treated BAC.

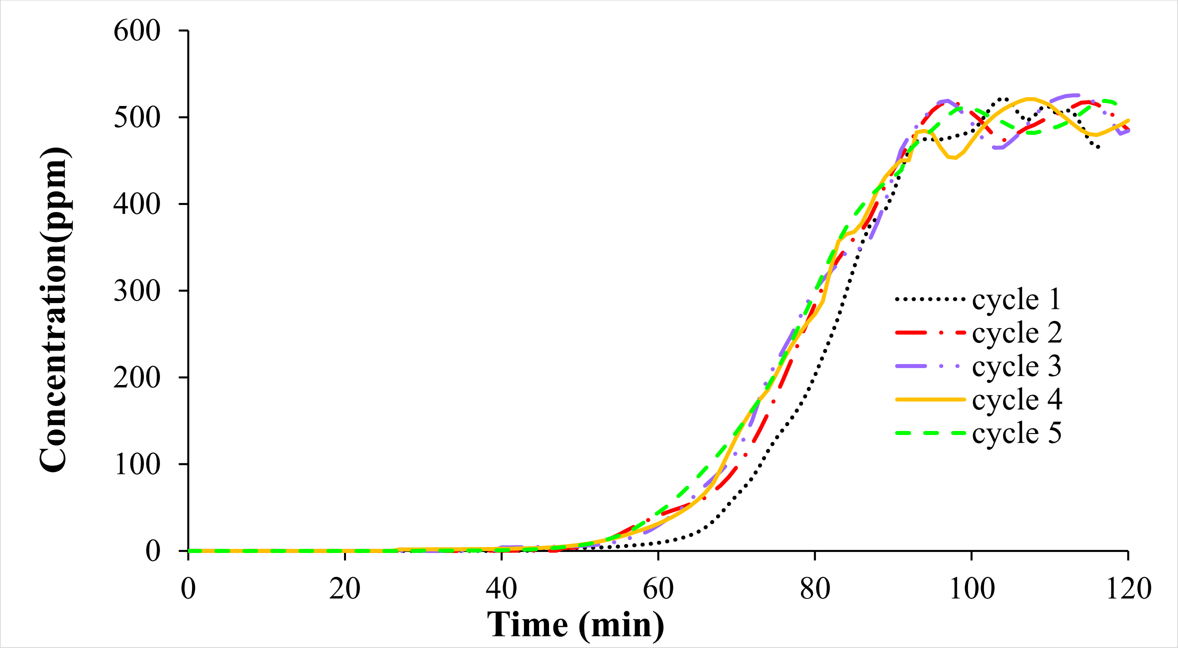

Figure A- 6. Breakthrough curves of ethylbenzene on acid treated BAC.

Adsorption of 1,2,4 trimethylbenzene

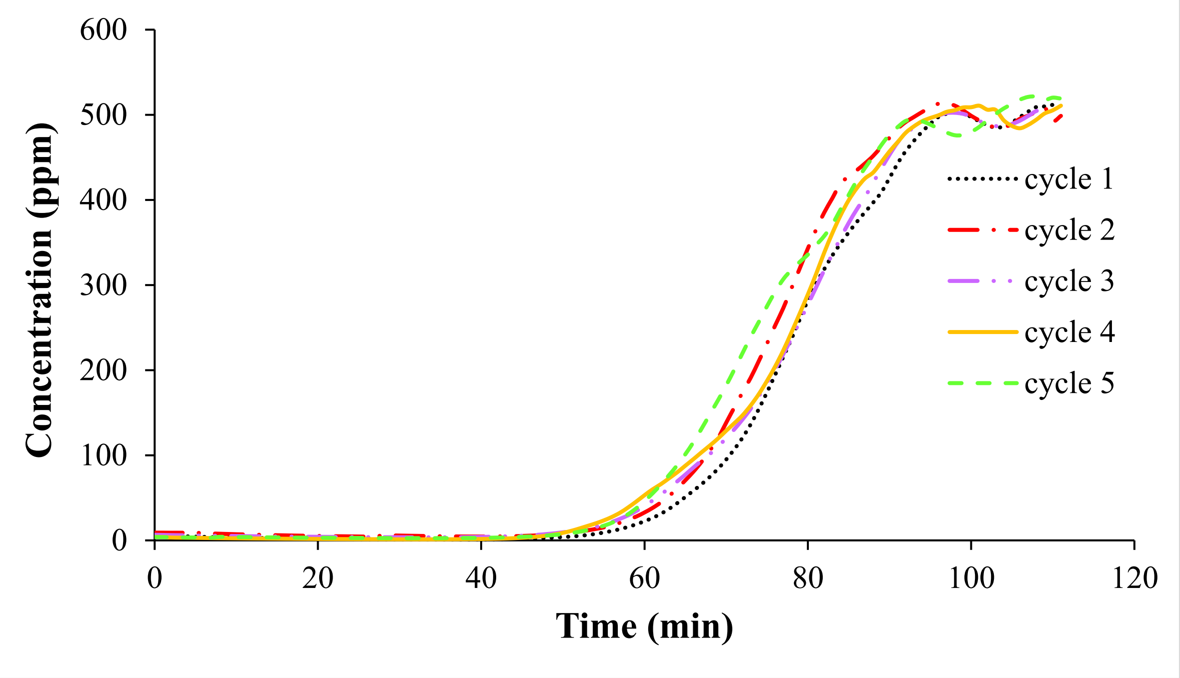

Figure A- 7. Breakthrough curves of 1, 2, 4 TMB on heat treated BAC.

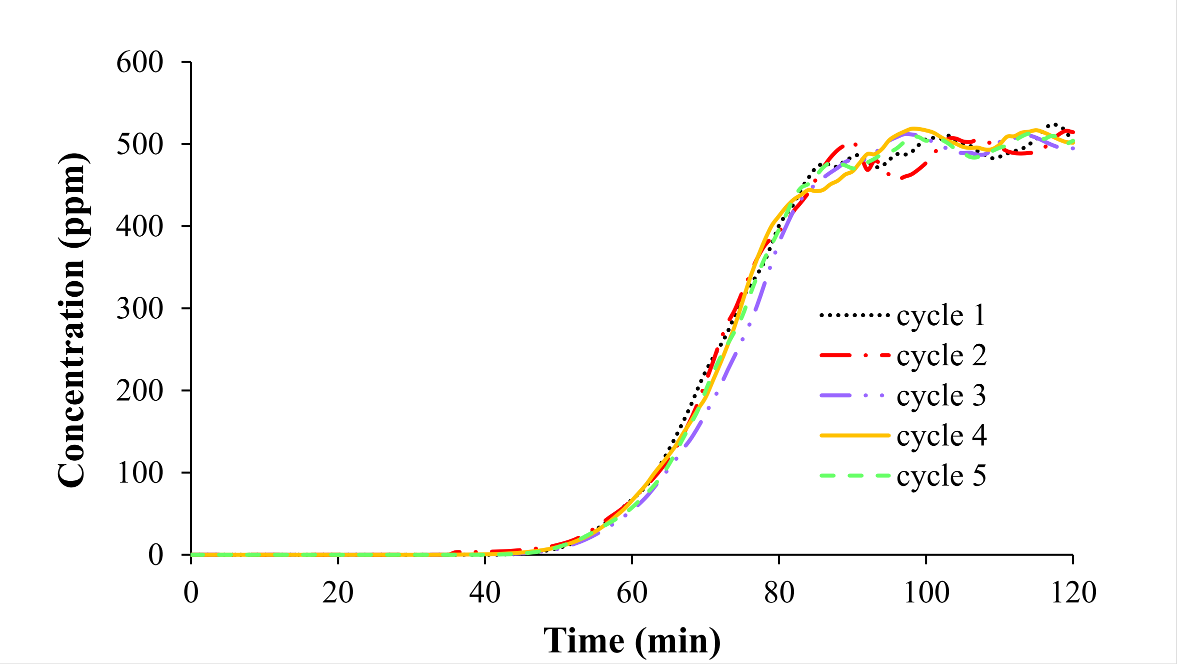

Figure A- 8. Breakthrough curves of 1, 2, 4 TMB on hydrogen treated BAC.

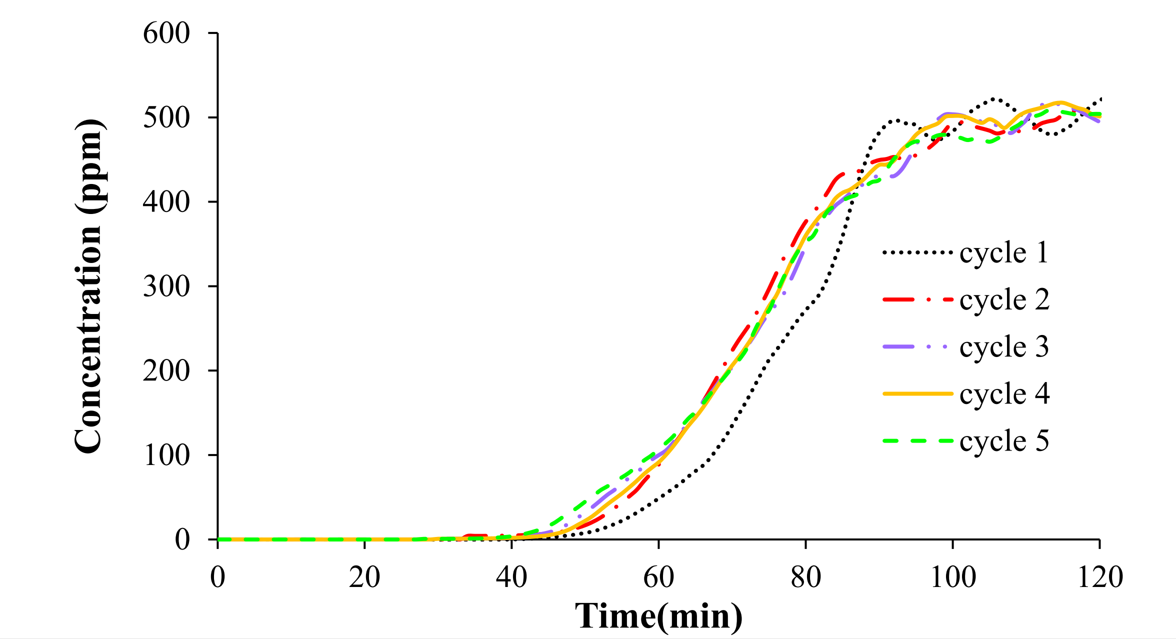

Figure A- 9. Breakthrough curves of 1, 2, 4 TMB on acid treated BAC.

Adsorption of butanol

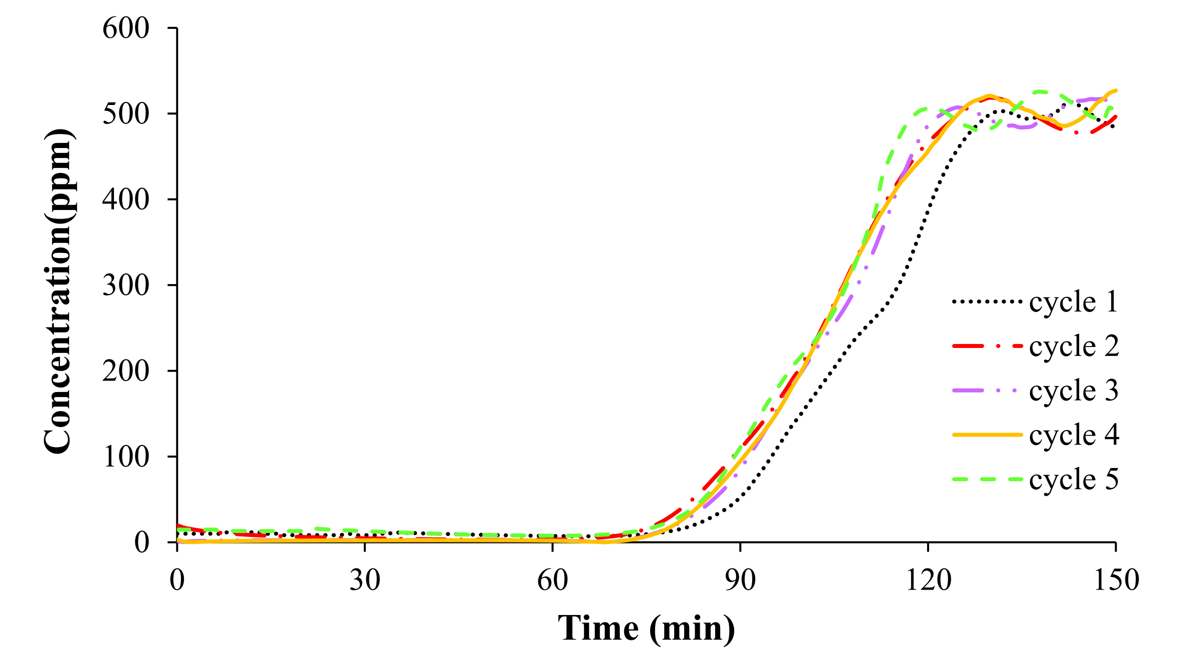

Figure A- 10. Breakthrough curves of n-butanol on heat treated BAC.

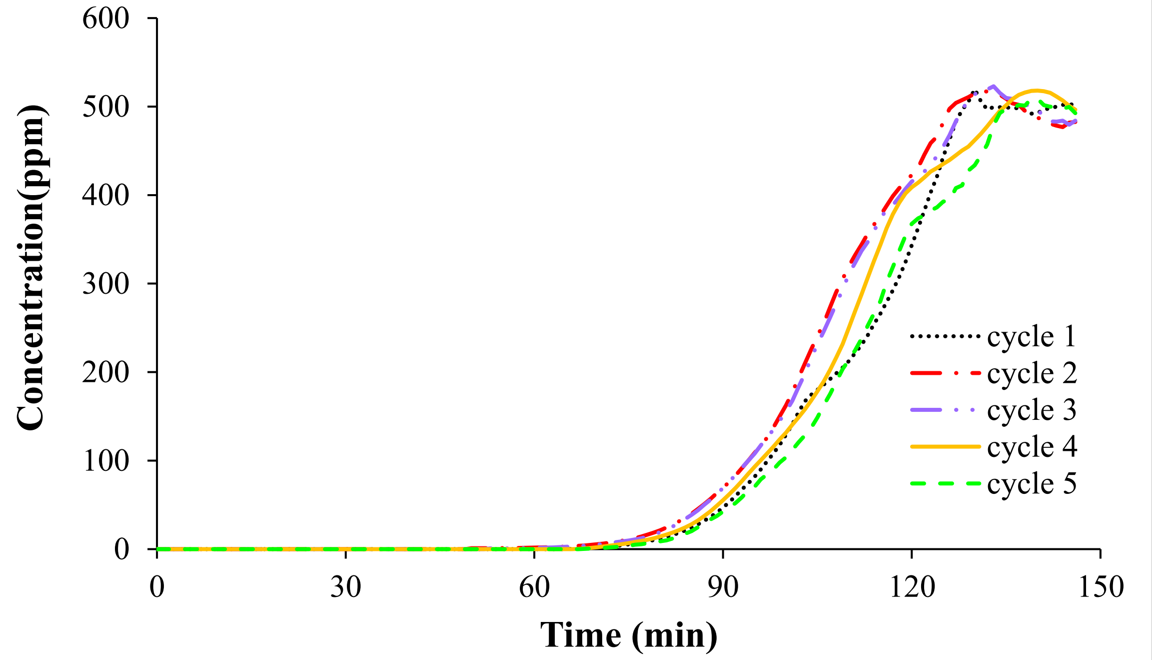

Figure A- 11. Breakthrough curves of n-butanol on hydrogen treated BAC.

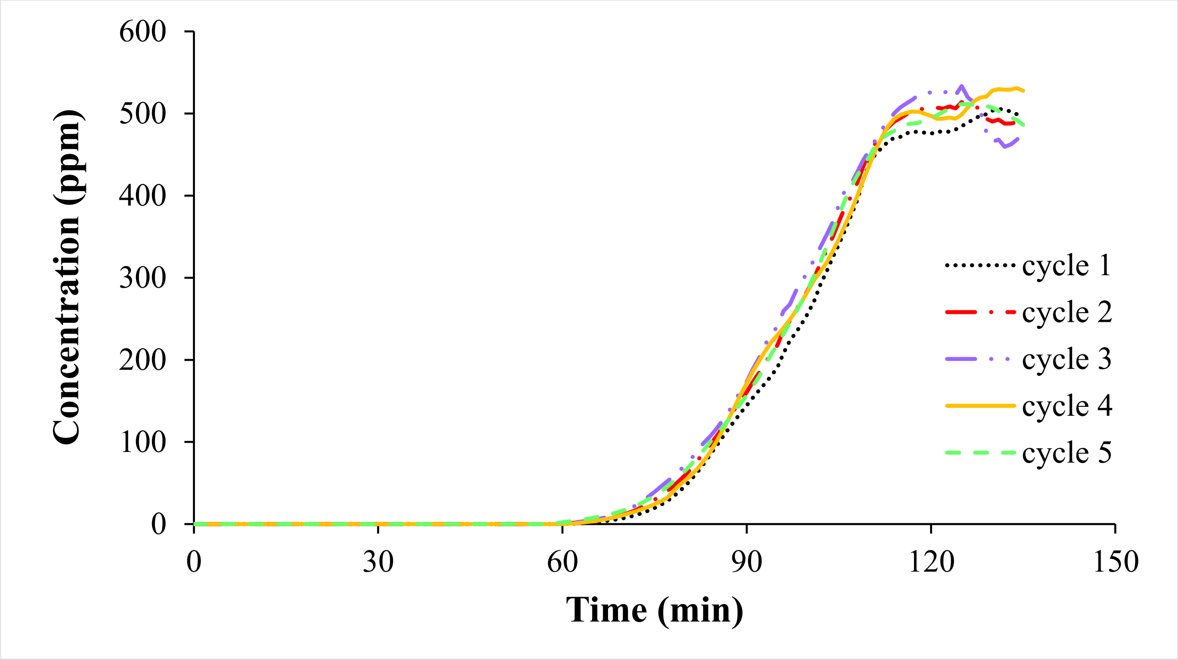

Figure A- 12. Breakthrough curves of n-butanol on acid treated BAC.

Adsorption of 2-butoxyethanol

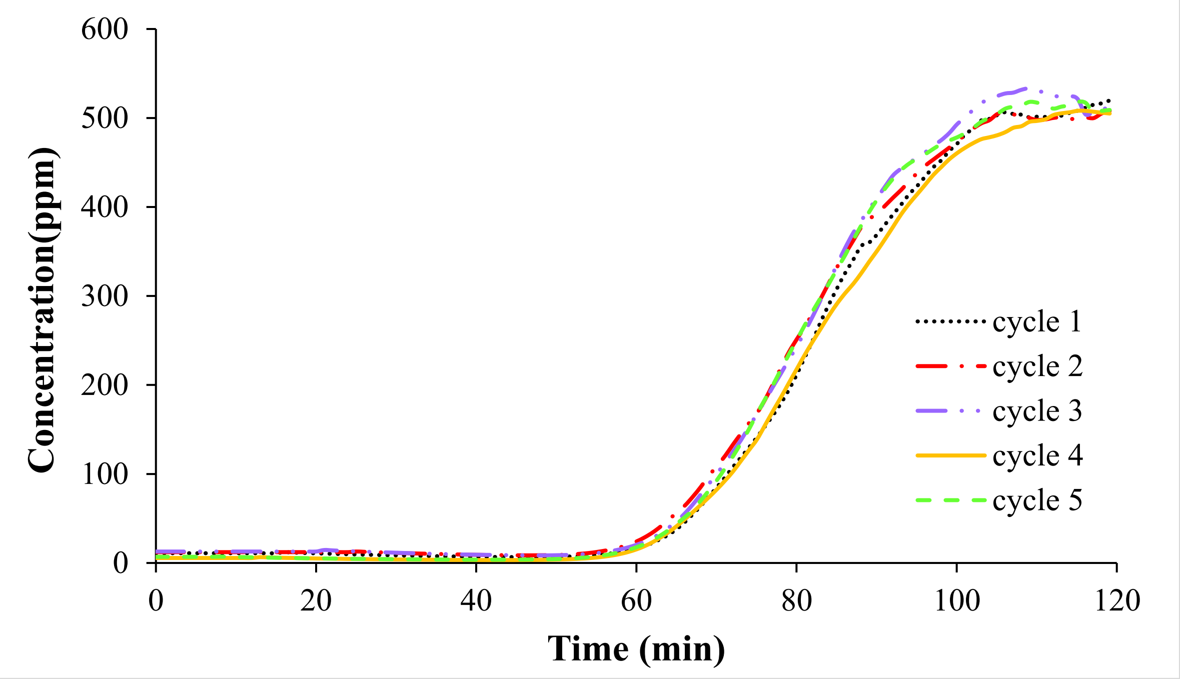

Figure A- 13. Breakthrough curves of 2-butoxyethanol on heat treated BAC.

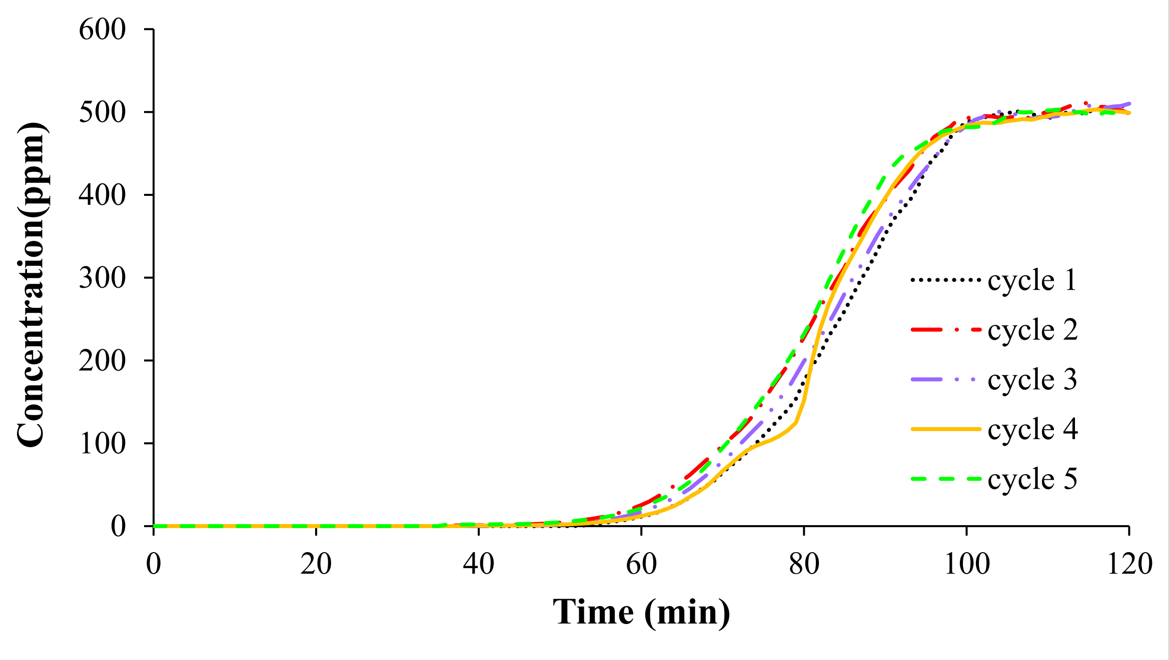

Figure A- 14. Breakthrough curves of 2-butoxyethanol on hydrogen treated BAC.

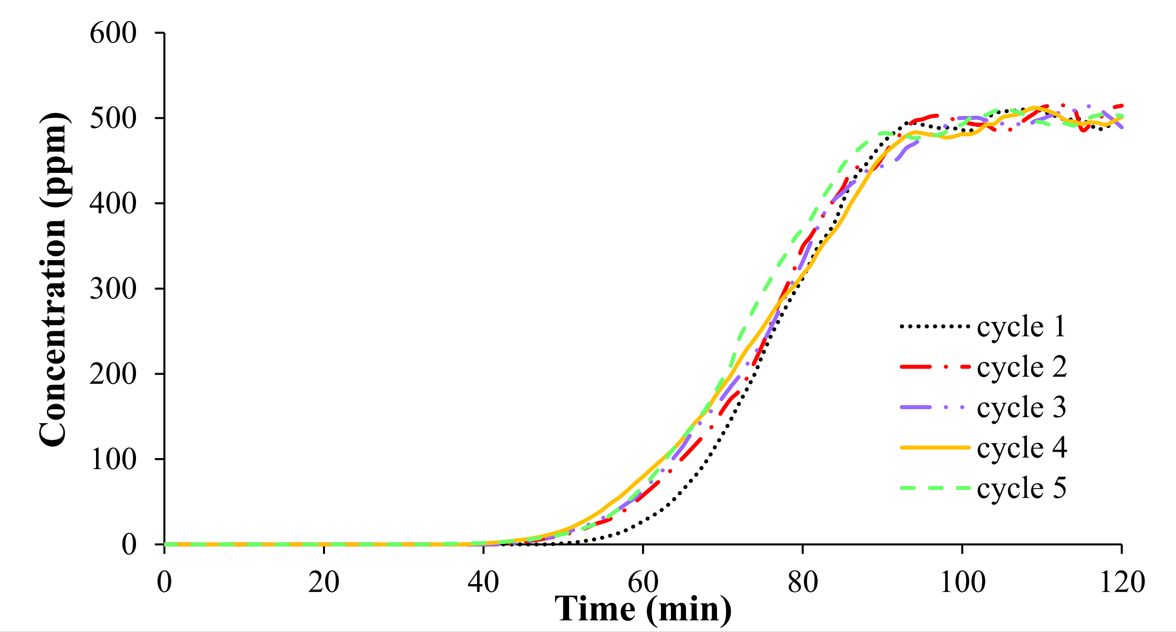

Figure A- 15. Breakthrough curves of 2-butoxyethanol on acid treated BAC.

Adsorption of n-decane

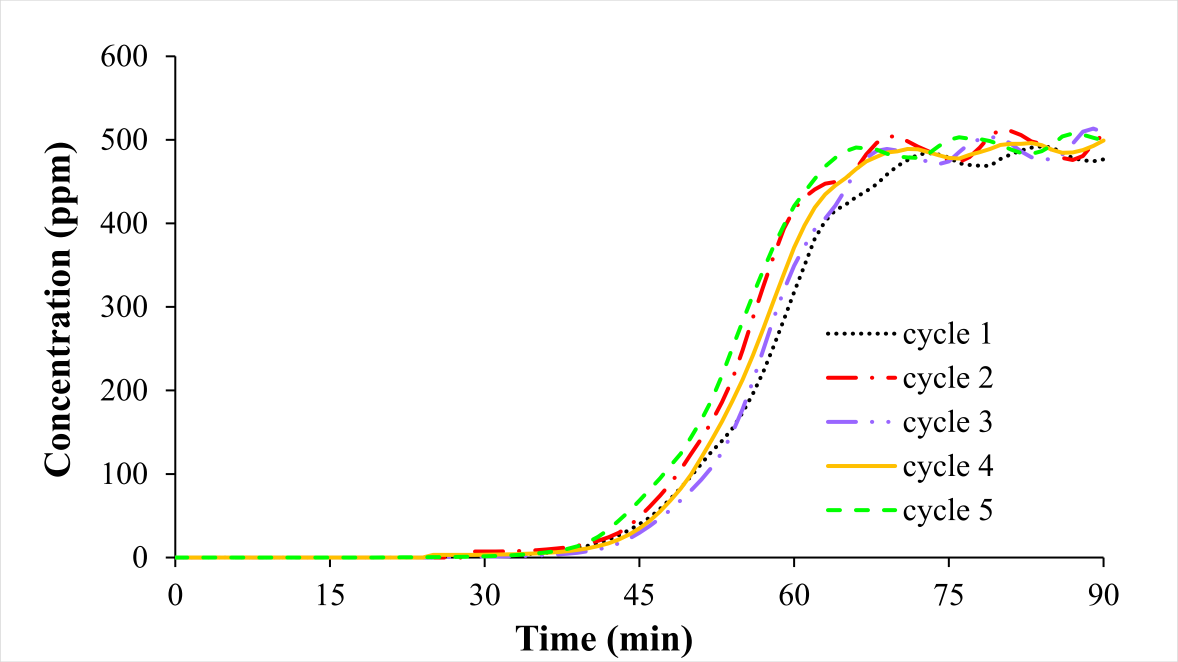

Figure A- 16. Breakthrough curves of n-decane on heat treated BAC.

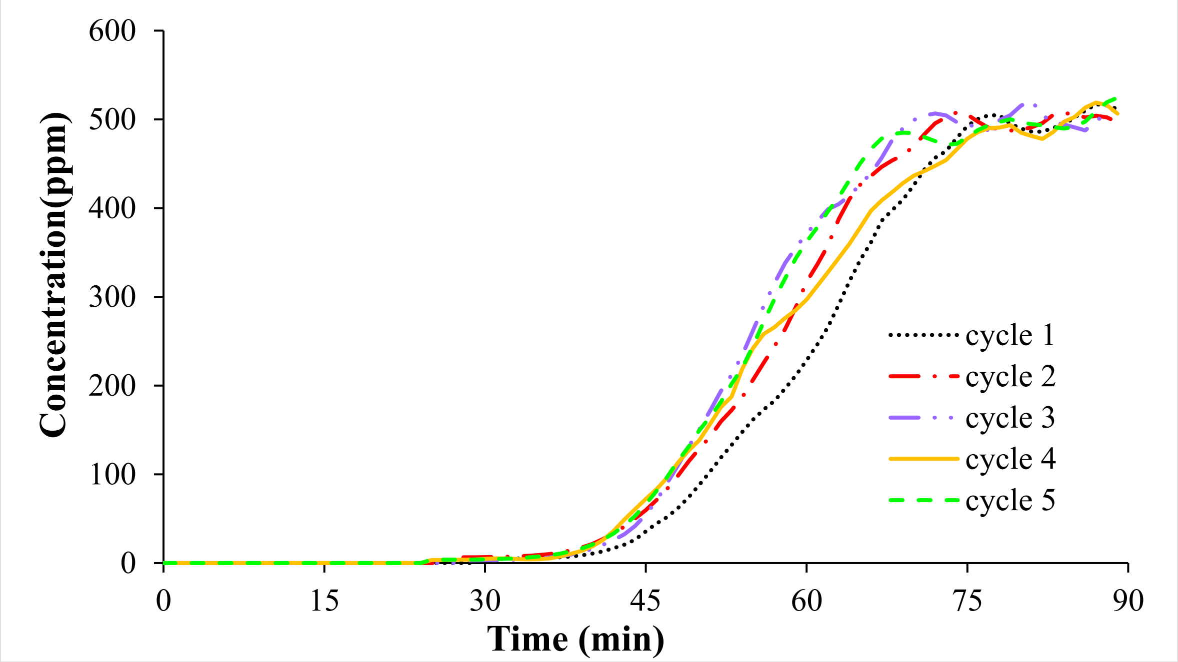

Figure A- 17. Breakthrough curves of n-decane on hydrogen treated BAC.

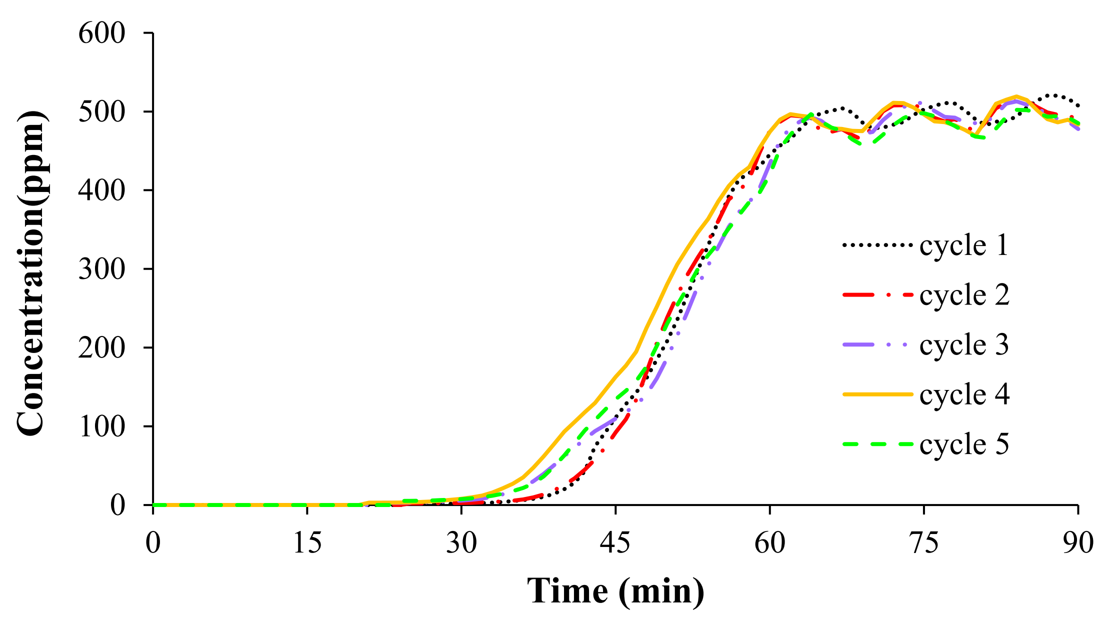

Figure A- 18. Breakthrough curves of n-decane on acid treated BAC.

Adsorption of 2-heptanone

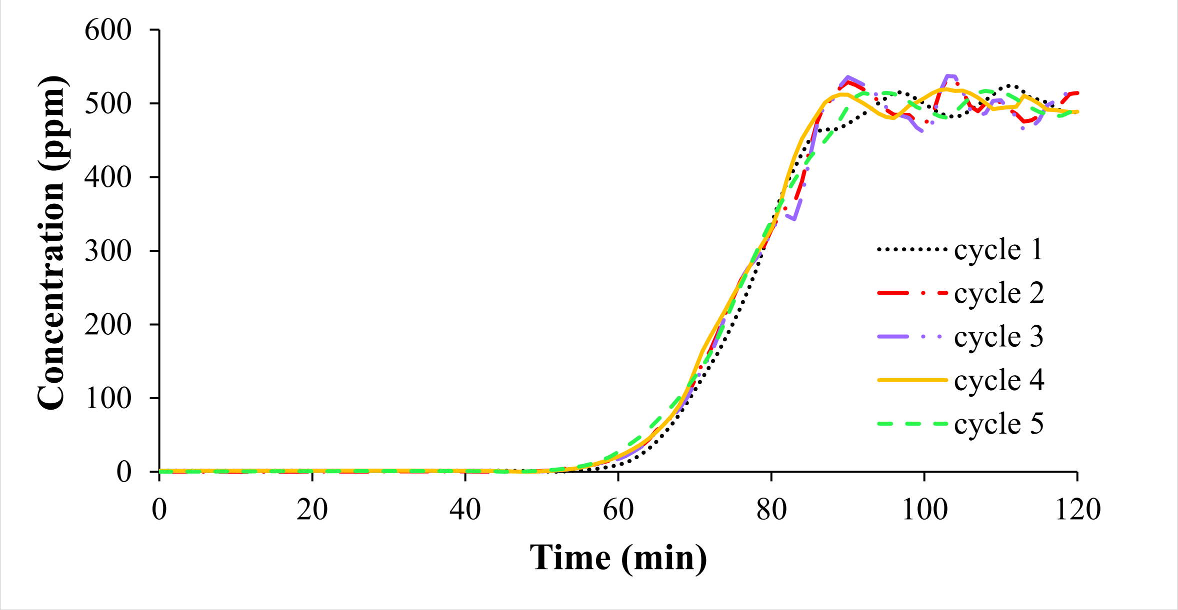

Figure A- 19. Breakthrough curves of 2-heptanone on heat treated BAC.

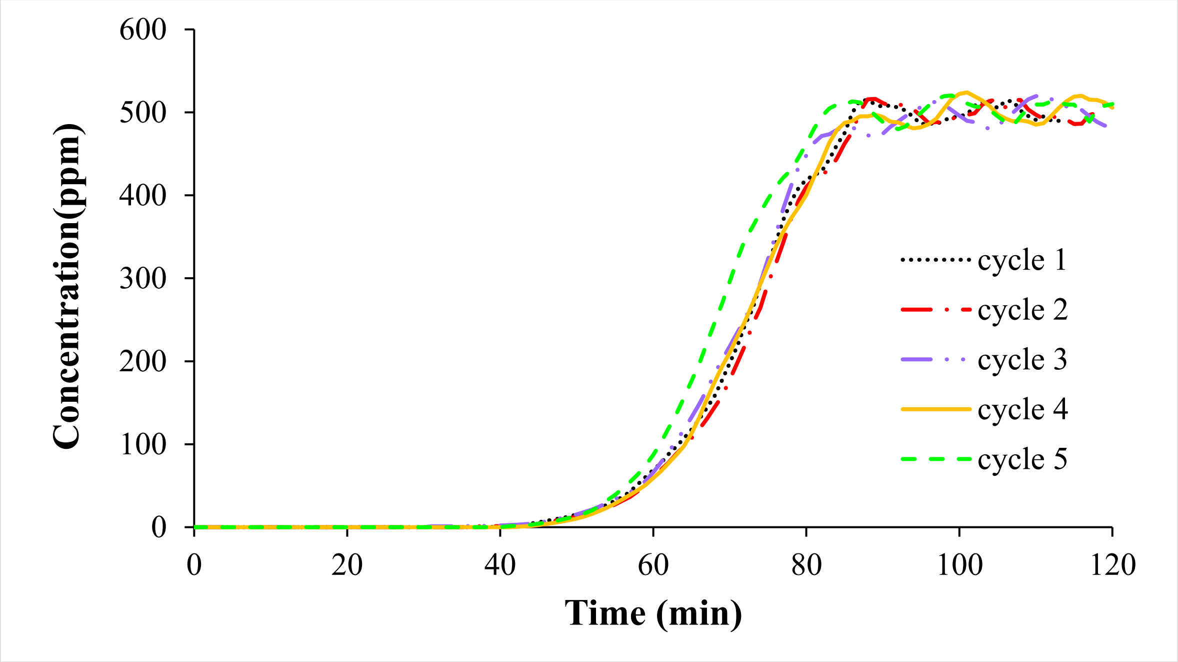

Figure A- 20. Breakthrough curves of 2-heptanone on hydrogen treated BAC.

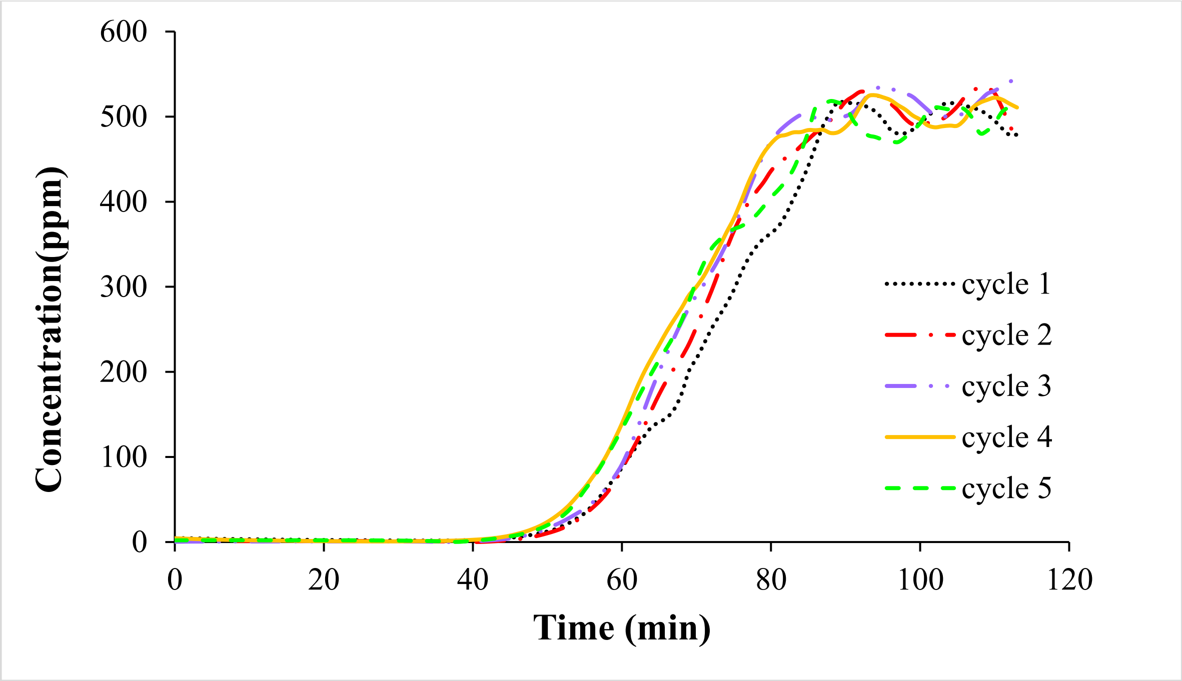

Figure A- 21. Breakthrough curves of 2-heptanone on acid treated BAC.

Adsorption of n-butyl acetate

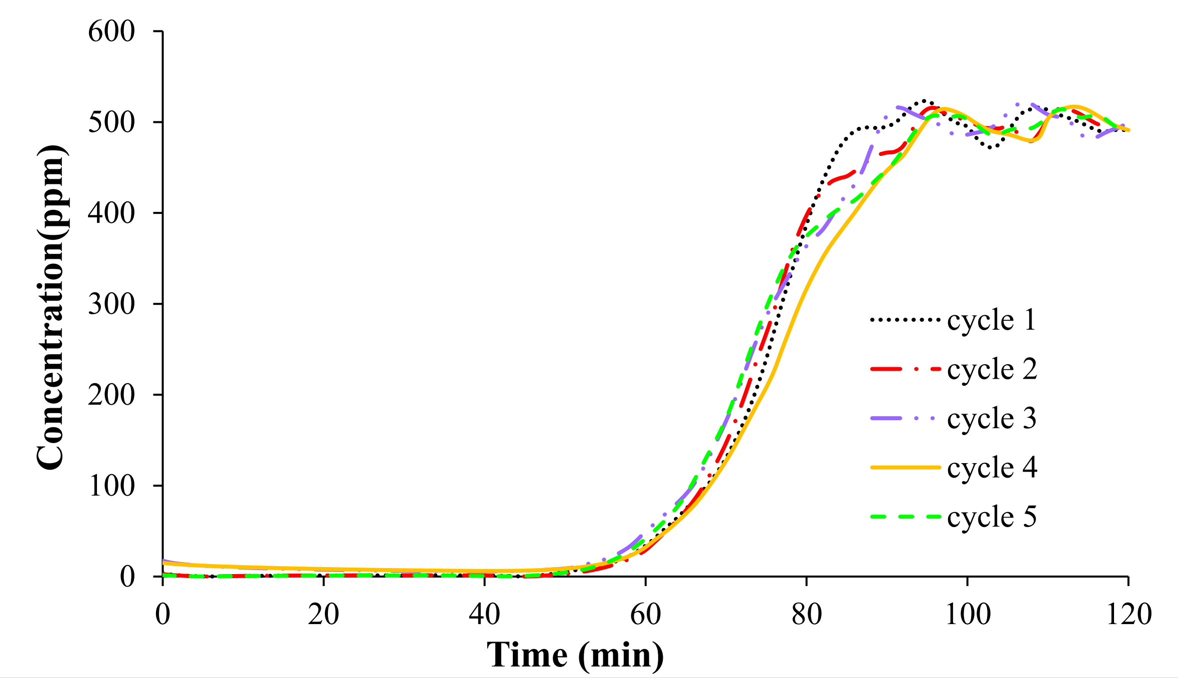

Figure A- 22. Breakthrough curves of n-butyl acetate on heat treated BAC.

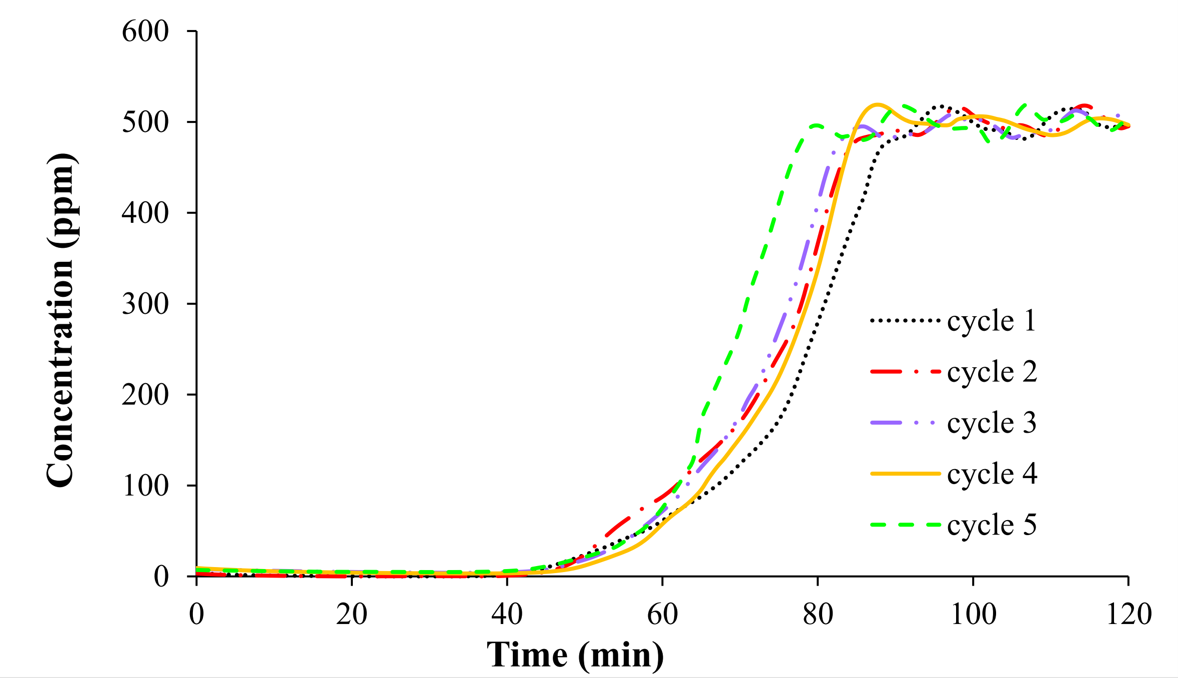

Figure A- 23. Breakthrough curves of n-butyl acetate on hydrogen treated BAC.

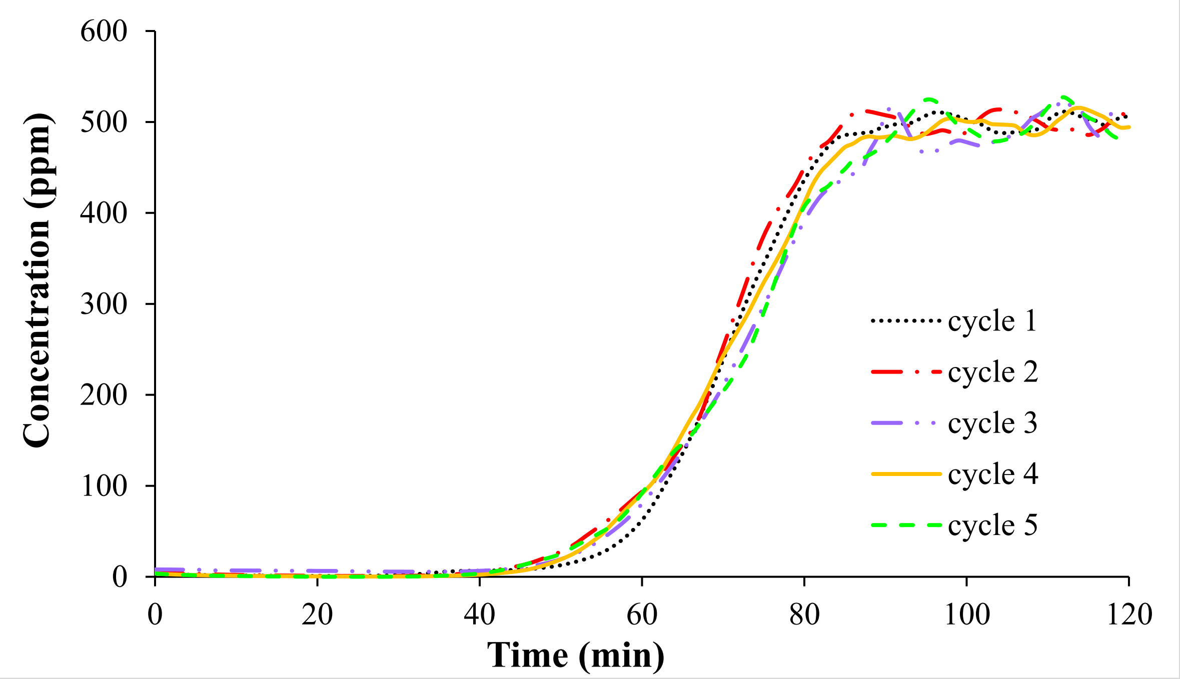

Figure A- 24. Breakthrough curves of n-butyl acetate on acid treated BAC.

APPENDIX B

Mass balance tables

Adsorption of p-xylene

Table B- 1. Mass balance for 5-cycle adsorption/desorption test of p-xylene on heat treated Kureha BAC

Cycle	Mass balance									Adsorption Time (min)
	BAC[1] (g)	Before Adsorption[2] (g)	After Adsorption[3] (g)	Adsorbed Adsorbate[4] (g)	Adsorption Capacity[5] (%)	After Regeneration [6] (g)	Heel[7] (g)	Total Heel[8] (g)	Total Heel[9] (%)	
1	4.066	329.940	331.629	1.689	41.5	329.945	0.005	0.005	0.1	120
2	-	329.945	331.623	1.678	41.3	329.954	0.009	0.014	0.3	120
3	-	329.954	331.617	1.663	40.9	329.955	0.001	0.015	0.4	120
4	-	329.955	331.603	1.648	40.5	329.957	0.002	0.017	0.4	120
5	-	329.957	331.613	1.656	40.7	329.956	-0.001	0.016	0.4	120

[1] Weight of dry bead activated carbon (Kureha)

[2] Weight of full reactor before adsorption

[3] Weight of full reactor after adsorption

[4] Weight of adsorbed adsorbate =
After Adsorption- Before Adsorption

[5] Adsorption capacity = Mass adsorbed*100/Mass of BAC

[6] Weight of full reactor after regeneration

[7] Weight of adsorbate remaining on the BAC after regeneration =
After Regeneration- Before Adsorption

[8] Weight of reactor after this regeneration test – weight of reactor before any adsorption

[9] Total heel*100/Mass of BAC

Table B- 2. Mass balance for 5-cycle adsorption/desorption test of p-xylene on hydrogen treated Kureha BAC

Cycle	Mass balance									Adsorption Time (min)
	BAC[1] (g)	Before Adsorption[2] (g)	After Adsorption[3] (g)	Adsorbed Adsorbate[4] (g)	Adsorption Capacity[5] (%)	After Regeneration [6] (g)	Heel[7] (g)	Total Heel[8] (g)	Total Heel[9] (%)	
1	4.066	329.870	331.477	1.607	39.5	329.887	0.017	0.017	0.4	120
2	-	329.887	331.462	1.575	38.7	329.890	0.003	0.020	0.5	120
3	-	329.890	331.458	1.568	38.6	329.890	0.000	0.020	0.5	120
4	-	329.890	331.454	1.564	38.5	329.893	0.003	0.023	0.6	120
5	-	329.893	331.456	1.563	38.4	329.895	0.002	0.025	0.6	120

[1] Weight of dry bead activated carbon (Kureha)

[2] Weight of full reactor before adsorption

[3] Weight of full reactor after adsorption

[4] Weight of adsorbed adsorbate =
After Adsorption- Before Adsorption

[5] Adsorption capacity = Mass adsorbed*100/Mass of BAC

[6] Weight of full reactor after regeneration

[7] Weight of adsorbate remaining on the BAC after regeneration =
After Regeneration- Before Adsorption

[8] Weight of reactor after this regeneration test – weight of reactor before any adsorption

[9] Total heel*100/Mass of BAC

Table B- 3. Mass balance for 5-cycle adsorption/desorption test of p-xylene on acid treated Kureha BAC

Cycle	Mass balance									Adsorption Time (min)
	BAC[1] (g)	Before Adsorption[2] (g)	After Adsorption[3] (g)	Adsorbed Adsorbate[4] (g)	Adsorption Capacity[5] (%)	After Regeneration [6] (g)	Heel[7] (g)	Total Heel[8] (g)	Total Heel[9] (%)	
1	4.060	329.972	331.572	1.600	39.4	330.033	0.061	0.061	1.5	120
2	-	330.033	331.559	1.526	37.6	330.052	0.019	0.080	2.0	120
3	-	330.052	331.573	1.521	37.5	330.070	0.018	0.098	2.4	120
4	-	330.070	331.555	1.485	36.6	330.086	0.016	0.114	2.8	120
5	-	330.086	331.569	1.483	36.5	330.105	0.019	0.133	3.3	120

[1] Weight of dry bead activated carbon (Kureha)

[2] Weight of full reactor before adsorption

[3] Weight of full reactor after adsorption

[4] Weight of adsorbed adsorbate =
After Adsorption- Before Adsorption

[5] Adsorption capacity = Mass adsorbed*100/Mass of BAC

[6] Weight of full reactor after regeneration

[7] Weight of adsorbate remaining on the BAC after regeneration =
After Regeneration- Before Adsorption

[8] Weight of reactor after this regeneration test – weight of reactor before any adsorption

[9] Total heel*100/Mass of BAC

Adsorption of ethylbenzene

Table B- 4. Mass balance for 5-cycle adsorption/desorption test of ethylbenzene on heat treated Kureha BAC

Cycle	Mass balance									Adsorption Time (min)
	BAC[1] (g)	Before Adsorption[2] (g)	After Adsorption[3] (g)	Adsorbed Adsorbate[4] (g)	Adsorption Capacity[5] (%)	After Regeneration [6] (g)	Heel[7] (g)	Total Heel[8] (g)	Total Heel[9] (%)	
1	4.047	330.503	332.165	1.662	41.1	330.506	0.003	0.003	0.1	120
2	-	330.506	332.169	1.663	41.1	330.507	0.001	0.004	0.1	120
3	-	330.507	332.154	1.647	40.7	330.506	-0.001	0.003	0.1	120
4	-	330.506	332.154	1.648	40.7	330.511	0.005	0.008	0.2	120
5	-	330.511	332.151	1.640	40.5	330.513	0.002	0.010	0.2	120

[1] Weight of dry bead activated carbon (Kureha)

[2] Weight of full reactor before adsorption

[3] Weight of full reactor after adsorption

[4] Weight of adsorbed adsorbate =
After Adsorption- Before Adsorption

[5] Adsorption capacity = Mass adsorbed*100/Mass of BAC

[6] Weight of full reactor after regeneration

[7] Weight of adsorbate remaining on the BAC after regeneration =
After Regeneration- Before Adsorption

[8] Weight of reactor after this regeneration test – weight of reactor before any adsorption

[9] Total heel*100/Mass of BAC

Table B- 5. Mass balance for 5-cycle adsorption/desorption test of ethylbenzene on hydrogen-treated Kureha BAC

Cycle	Mass balance									Adsorption Time (min)
	BAC[1] (g)	Before Adsorption[2] (g)	After Adsorption[3] (g)	Adsorbed Adsorbate[4] (g)	Adsorption Capacity[5] (%)	After Regeneration [6] (g)	Heel[7] (g)	Total Heel[8] (g)	Total Heel[9] (%)	
1	4.071	329.971	331.543	1.572	38.6	329.970	-0.001	-0.001	0.0	120
2	-	329.970	331.537	1.567	38.5	329.970	0.000	-0.001	0.0	120
3	-	329.970	331.536	1.566	38.5	329.970	0.000	-0.001	0.0	120
4	-	329.970	331.538	1.568	38.5	329.973	0.003	0.002	0.0	120
5	-	329.973	331.540	1.567	38.5	329.973	0.000	0.002	0.0	120

[1] Weight of dry bead activated carbon (Kureha)

[2] Weight of full reactor before adsorption

[3] Weight of full reactor after adsorption

[4] Weight of adsorbed adsorbate =
After Adsorption- Before Adsorption

[5] Adsorption capacity = Mass adsorbed*100/Mass of BAC

[6] Weight of full reactor after regeneration

[7] Weight of adsorbate remaining on the BAC after regeneration =
After Regeneration- Before Adsorption

[8] Weight of reactor after this regeneration test – weight of reactor before any adsorption

[9] Total heel*100/Mass of BAC

Table B- 6. Mass balance for 5-cycle adsorption/desorption test of ethylbenzene on acid-treated Kureha BAC

Cycle	Mass balance									Adsorption Time (min)
	BAC[1] (g)	Before Adsorption[2] (g)	After Adsorption[3] (g)	Adsorbed Adsorbate[4] (g)	Adsorption Capacity[5] (%)	After Regeneration [6] (g)	Heel[7] (g)	Total Heel[8] (g)	Total Heel[9] (%)	
1	4.108	332.843	334.460	1.617	39.4	332.878	0.035	0.035	0.9	120
2	-	332.878	334.468	1.590	38.7	332.892	0.014	0.049	1.2	120
3	-	332.892	334.462	1.570	38.2	332.898	0.006	0.055	1.3	120
4	-	332.898	334.469	1.571	38.2	332.899	0.001	0.056	1.4	120
5	-	332.899	334.465	1.566	38.1	332.901	0.002	0.058	1.4	120

[1] Weight of dry bead activated carbon (Kureha)

[2] Weight of full reactor before adsorption

[3] Weight of full reactor after adsorption

[4] Weight of adsorbed adsorbate =
After Adsorption- Before Adsorption

[5] Adsorption capacity = Mass adsorbed*100/Mass of BAC

[6] Weight of full reactor after regeneration

[7] Weight of adsorbate remaining on the BAC after regeneration =
After Regeneration- Before Adsorption

[8] Weight of reactor after this regeneration test – weight of reactor before any adsorption

[9] Total heel*100/Mass of BAC

Adsorption of TMB

Table B- 7. Mass balance for 5-cycle adsorption/desorption test of TMB on heat treated Kureha BAC

Cycle	Mass balance									Adsorption Time (min)
	BAC[1] (g)	Before Adsorption[2] (g)	After Adsorption[3] (g)	Adsorbed Adsorbate[4] (g)	Adsorption Capacity[5] (%)	After Regeneration[6] (g)	Heel[7] (g)	Total Heel[8] (g)	Total Heel[9] (%)	
1	3.946	332.972	334.751	1.779	45.1	332.981	0.009	0.009	0.2	120
2	-	332.981	334.751	1.770	44.9	332.986	0.005	0.014	0.4	120
3	-	332.986	334.779	1.793	45.4	332.997	0.011	0.025	0.6	120
4	-	332.997	334.781	1.784	45.2	332.998	0.001	0.026	0.7	120
5	-	332.998	334.779	1.781	45.1	333.001	0.003	0.029	0.7	120

[1] Weight of dry bead activated carbon (Kureha)

[2] Weight of full reactor before adsorption

[3] Weight of full reactor after adsorption

[4] Weight of adsorbed adsorbate = After Adsorption- Before Adsorption

[5] Adsorption capacity = Mass adsorbed*100/Mass of BAC

[6] Weight of full reactor after regeneration

[7] Weight of adsorbate remaining on the BAC after regeneration = After Regeneration- Before Adsorption

[8] Weight of reactor after this regeneration test – weight of reactor before any adsorption

[9] Total heel*100/Mass of BAC

Table B- 8. Mass balance for 5-cycle adsorption/desorption test of TMB on hydrogen-treated Kureha BAC

Cycle	Mass balance									Adsorption Time (min)
	BAC[1] (g)	Before Adsorption[2] (g)	After Adsorption[3] (g)	Adsorbed Adsorbate[4] (g)	Adsorption Capacity[5] (%)	After Regeneration[6] (g)	Heel[7] (g)	Total Heel[8] (g)	Total Heel[9] (%)	
1	4.034	331.818	333.496	1.678	41.6	331.818	0.000	0.000	0.0	120
2	-	331.818	333.497	1.679	41.6	331.822	0.004	0.004	0.1	120
3	-	331.822	333.502	1.680	41.6	331.824	0.002	0.006	0.1	120
4	-	331.824	333.493	1.669	41.4	331.825	0.001	0.007	0.2	120
5	-	331.825	333.501	1.676	41.5	331.831	0.006	0.013	0.3	120

[1] Weight of dry bead activated carbon (Kureha)

[2] Weight of full reactor before adsorption

[3] Weight of full reactor after adsorption

[4] Weight of adsorbed adsorbate =
After Adsorption- Before Adsorption

[5] Adsorption capacity = Mass adsorbed*100/Mass of BAC

[6] Weight of full reactor after regeneration

[7] Weight of adsorbate remaining on the BAC after regeneration =
After Regeneration- Before Adsorption

[8] Weight of reactor after this regeneration test – weight of reactor before any adsorption

[9] Total heel*100/Mass of BAC

Table B- 9. Mass balance for 5-cycle adsorption/desorption test of TMB on acid treated Kureha BAC

Cycle	Mass balance									Adsorption Time (min)
	BAC[1] (g)	Before Adsorption[2] (g)	After Adsorption[3] (g)	Adsorbed Adsorbate[4] (g)	Adsorption Capacity[5] (%)	After Regeneration [6] (g)	Heel[7] (g)	Total Heel[8] (g)	Total Heel[9] (%)	
1	4.029	333.456	335.244	1.788	44.4	333.570	0.114	0.114	2.8	120
2	-	333.570	335.217	1.647	40.9	333.585	0.015	0.129	3.2	120
3	-	333.585	335.223	1.638	40.7	333.603	0.018	0.147	3.6	120
4	-	333.603	335.225	1.622	40.3	333.620	0.017	0.164	4.1	120
5	-	333.620	335.242	1.622	40.3	333.631	0.011	0.175	4.3	120

[1] Weight of dry bead activated carbon (Kureha)

[2] Weight of full reactor before adsorption

[3] Weight of full reactor after adsorption

[4] Weight of adsorbed adsorbate =
After Adsorption- Before Adsorption

[5] Adsorption capacity = Mass adsorbed*100/Mass of BAC

[6] Weight of full reactor after regeneration

[7] Weight of adsorbate remaining on the BAC after regeneration =
After Regeneration- Before Adsorption

[8] Weight of reactor after this regeneration test – weight of reactor before any adsorption

[9] Total heel*100/Mass of BAC

Adsorption of n-butanol

Table B- 10. Mass balance for 5-cycle adsorption/desorption test of n-butanol on heat treated Kureha BAC

Cycle	Mass balance									Adsorption Time (min)
	BAC[1] (g)	Before Adsorption[2] (g)	After Adsorption[3] (g)	Adsorbed Adsorbate[4] (g)	Adsorption Capacity[5] (%)	After Regeneration[6] (g)	Heel[7] (g)	Total Heel[8] (g)	Total Heel[9] (%)	
1	4.047	328.135	329.610	1.475	36.4	328.135	0.000	0.000	0.0	150
2		328.135	329.602	1.467	36.2	328.140	0.005	0.005	0.1	150
3		328.140	329.572	1.432	35.4	328.135	-0.005	0.000	0.0	150
4		328.135	329.609	1.474	36.4	328.139	0.004	0.004	0.1	150
5		328.139	329.610	1.471	36.3	328.145	0.006	0.010	0.3	150

[1] Weight of dry bead activated carbon (Kureha)

[2] Weight of full reactor before adsorption

[3] Weight of full reactor after adsorption

[4] Weight of adsorbed adsorbate = After Adsorption- Before Adsorption

[5] Adsorption capacity = Mass adsorbed*100/Mass of BAC

[6] Weight of full reactor after regeneration

[7] Weight of adsorbate remaining on the BAC after regeneration = After Regeneration- Before Adsorption

[8] Weight of reactor after this regeneration test – weight of reactor before any adsorption

[9] Total heel*100/Mass of BAC

Table B- 11. Mass balance for 5-cycle adsorption/desorption test of n-butanol on hydrogen-treated Kureha BAC

Cycle	Mass balance									Adsorption Time (min)
	BAC[1] (g)	Before Adsorption[2] (g)	After Adsorption[3] (g)	Adsorbed Adsorbate[4] (g)	Adsorption Capacity[5] (%)	After Regeneration [6] (g)	Heel[7] (g)	Total Heel[8] (g)	Total Heel[9] (%)	
1	4.009	332.558	333.974	1.416	35.3	332.563	0.005	0.005	0.1	150
2	-	332.563	333.974	1.411	35.2	332.564	0.001	0.006	0.1	150
3	-	332.564	333.976	1.412	35.2	332.562	-0.002	0.004	0.1	150
4	-	332.562	333.971	1.409	35.2	332.565	0.003	0.007	0.2	150
5	-	332.565	333.977	1.412	35.2	332.570	0.005	0.012	0.3	150

[1] Weight of dry bead activated carbon (Kureha)

[2] Weight of full reactor before adsorption

[3] Weight of full reactor after adsorption

[4] Weight of adsorbed adsorbate =
After Adsorption- Before Adsorption

[5] Adsorption capacity = Mass adsorbed*100/Mass of BAC

[6] Weight of full reactor after regeneration

[7] Weight of adsorbate remaining on the BAC after regeneration =
After Regeneration- Before Adsorption

[8] Weight of reactor after this regeneration test – weight of reactor before any adsorption

[9] Total heel*100/Mass of BAC

Table B- 12. Mass balance for 5-cycle adsorption/desorption test of butanol on acid treated Kureha BAC

Cycle	Mass balance									Adsorption Time (min)
	BAC[1] (g)	Before Adsorption[2] (g)	After Adsorption[3] (g)	Adsorbed Adsorbate[4] (g)	Adsorption Capacity[5] (%)	After Regeneration [6] (g)	Heel[7] (g)	Total Heel[8] (g)	Total Heel[9] (%)	
1	4.032	332.383	333.785	1.402	34.8	332.393	0.010	0.010	0.2	150
2	-	332.393	333.776	1.383	34.3	332.402	0.009	0.019	0.5	150
3	-	332.402	333.779	1.377	34.2	332.403	0.001	0.020	0.5	150
4	-	332.403	333.778	1.375	34.1	332.400	-0.003	0.017	0.4	150
5	-	332.400	333.762	1.362	33.8	332.406	0.006	0.023	0.6	150

[1] Weight of dry bead activated carbon (Kureha)

[2] Weight of full reactor before adsorption

[3] Weight of full reactor after adsorption

[4] Weight of adsorbed adsorbate =
After Adsorption- Before Adsorption

[5] Adsorption capacity = Mass adsorbed*100/Mass of BAC

[6] Weight of full reactor after regeneration

[7] Weight of adsorbate remaining on the BAC after regeneration =
After Regeneration- Before Adsorption

[8] Weight of reactor after this regeneration test – weight of reactor before any adsorption

[9] Total heel*100/Mass of BAC

Adsorption of 2-butoxyethanol

Table B- 13. Mass balance for 5-cycle adsorption/desorption test of 2-butoxyethanol on heat treated Kureha BAC

Cycle	Mass balance									Adsorption Time (min)
	BAC[1] (g)	Before Adsorption[2] (g)	After Adsorption[3] (g)	Adsorbed Adsorbate[4] (g)	Adsorption Capacity[5] (%)	After Regeneration [6] (g)	Heel[7] (g)	Total Heel[8] (g)	Total Heel[9] (%)	
1	3.987	328.547	330.340	1.793	45.0	328.569	0.022	0.022	0.6	120
2		328.569	330.344	1.775	44.5	328.572	0.003	0.025	0.6	120
3		328.572	330.362	1.790	44.9	328.574	0.002	0.027	0.7	120
4		328.574	330.396	1.822	45.7	328.578	0.004	0.031	0.8	120
5		328.578	330.346	1.768	44.3	328.591	0.013	0.044	1.1	120

[1] Weight of dry bead activated carbon (Kureha)

[2] Weight of full reactor before adsorption

[3] Weight of full reactor after adsorption

[4] Weight of adsorbed adsorbate = After Adsorption- Before Adsorption

[5] Adsorption capacity = Mass adsorbed*100/Mass of BAC

[6] Weight of full reactor after regeneration

[7] Weight of adsorbate remaining on the BAC after regeneration = After Regeneration- Before Adsorption

[8] Weight of reactor after this regeneration test – weight of reactor before any adsorption

[9] Total heel*100/Mass of BAC

Table B- 14. Mass balance for 5-cycle adsorption/desorption test of 2-butoxyethanol on hydrogen-treated Kureha BAC

Cycle	Mass balance									Adsorption Time (min)
	BAC[1] (g)	Before Adsorption[2] (g)	After Adsorption[3] (g)	Adsorbed Adsorbate[4] (g)	Adsorption Capacity[5] (%)	After Regeneration [6] (g)	Heel[7] (g)	Total Heel[8] (g)	Total Heel[9] (%)	
1	4.045	332.586	334.299	1.713	42.3	332.591	0.005	0.005	0.1	120
2	-	332.591	334.330	1.739	42.9	332.595	0.004	0.009	0.2	120
3	-	332.595	334.296	1.701	42.1	332.608	0.013	0.022	0.5	120
4	-	332.608	334.296	1.688	41.7	332.614	0.006	0.028	0.7	120
5	-	332.614	334.294	1.680	41.5	332.616	0.002	0.030	0.7	120

[1] Weight of dry bead activated carbon (Kureha)

[2] Weight of full reactor before adsorption

[3] Weight of full reactor after adsorption

[4] Weight of adsorbed adsorbate =
After Adsorption- Before Adsorption

[5] Adsorption capacity = Mass adsorbed*100/Mass of BAC

[6] Weight of full reactor after regeneration

[7] Weight of adsorbate remaining on the BAC after regeneration =
After Regeneration- Before Adsorption

[8] Weight of reactor after this regeneration test – weight of reactor before any adsorption

[9] Total heel*100/Mass of BAC

Table B- 15. Mass balance for 5-cycle adsorption/desorption test of 2-butoxyethanol on acid treated Kureha BAC

Cycle	Mass balance									Adsorption Time (min)
	BAC[1] (g)	Before Adsorption[2] (g)	After Adsorption[3] (g)	Adsorbed Adsorbate[4] (g)	Adsorption Capacity[5] (%)	After Regeneration [6] (g)	Heel[7] (g)	Total Heel[8] (g)	Total Heel[9] (%)	
1	4.077	331.666	333.402	1.736	42.6	331.701	0.035	0.035	0.9	120
2	-	331.701	333.399	1.698	41.6	331.713	0.012	0.047	1.2	120
3	-	331.713	333.389	1.676	41.1	331.715	0.002	0.049	1.2	120
4	-	331.715	333.385	1.670	41.0	331.723	0.008	0.057	1.4	120
5	-	331.723	333.391	1.668	40.9	331.732	0.009	0.066	1.6	120

[1] Weight of dry bead activated carbon (Kureha)

[2] Weight of full reactor before adsorption

[3] Weight of full reactor after adsorption

[4] Weight of adsorbed adsorbate =
After Adsorption- Before Adsorption

[5] Adsorption capacity = Mass adsorbed*100/Mass of BAC

[6] Weight of full reactor after regeneration

[7] Weight of adsorbate remaining on the BAC after regeneration =
After Regeneration- Before Adsorption

[8] Weight of reactor after this regeneration test – weight of reactor before any adsorption

[9] Total heel*100/Mass of BAC

Adsorption of n-decane

Table B- 16. Mass balance for 5-cycle adsorption/desorption test of n-decane on heat treated Kureha BAC

Cycle	Mass balance									Adsorption Time (min)
	BAC[1] (g)	Before Adsorption[2] (g)	After Adsorption[3] (g)	Adsorbed Adsorbate[4] (g)	Adsorption Capacity[5] (%)	After Regeneration [6] (g)	Heel[7] (g)	Total Heel[8] (g)	Total Heel[9] (%)	
1	4.051	332.370	333.856	1.486	36.7	332.394	0.024	0.024	0.6	90
2	-	332.394	333.858	1.464	36.1	332.390	-0.004	0.020	0.5	90
3	-	332.390	333.857	1.467	36.2	332.393	0.003	0.023	0.6	90
4	-	332.393	333.857	1.464	36.1	332.396	0.003	0.026	0.6	90
5	-	332.396	333.861	1.465	36.2	332.399	0.003	0.029	0.7	90

[1] Weight of dry bead activated carbon (Kureha)

[2] Weight of full reactor before adsorption

[3] Weight of full reactor after adsorption

[4] Weight of adsorbed adsorbate =
After Adsorption- Before Adsorption

[5] Adsorption capacity = Mass adsorbed*100/Mass of BAC

[6] Weight of full reactor after regeneration

[7] Weight of adsorbate remaining on the BAC after regeneration =
After Regeneration- Before Adsorption

[8] Weight of reactor after this regeneration test – weight of reactor before any adsorption

[9] Total heel*100/Mass of BAC

Table B- 17. Mass balance for 5-cycle adsorption/desorption test of n-decane on hydrogen-treated Kureha BAC

Cycle	Mass balance									Adsorption Time (min)
	BAC[1] (g)	Before Adsorption[2] (g)	After Adsorption[3] (g)	Adsorbed Adsorbate[4] (g)	Adsorption Capacity[5] (%)	After Regeneration [6] (g)	Heel[7] (g)	Total Heel[8] (g)	Total Heel[9] (%)	
1	4.061	332.300	333.733	1.433	35.3	332.328	0.028	0.028	0.7	90
2	-	332.328	333.736	1.408	34.7	332.324	-0.004	0.024	0.6	90
3	-	332.324	333.722	1.398	34.4	332.322	-0.002	0.022	0.5	90
4	-	332.322	333.732	1.410	34.7	332.330	0.008	0.030	0.7	90
5	-	332.330	333.732	1.402	34.5	332.329	-0.001	0.029	0.7	90

[1] Weight of dry bead activated carbon (Kureha)

[2] Weight of full reactor before adsorption

[3] Weight of full reactor after adsorption

[4] Weight of adsorbed adsorbate =
After Adsorption- Before Adsorption

[5] Adsorption capacity = Mass adsorbed*100/Mass of BAC

[6] Weight of full reactor after regeneration

[7] Weight of adsorbate remaining on the BAC after regeneration =
After Regeneration- Before Adsorption

[8] Weight of reactor after this regeneration test – weight of reactor before any adsorption

[9] Total heel*100/Mass of BAC

Table B- 18. Mass balance for 5-cycle adsorption/desorption test of n-decane on acid treated Kureha BAC

Cycle	Mass balance									Adsorption Time (min)
	BAC[1] (g)	Before Adsorption[2] (g)	After Adsorption[3] (g)	Adsorbed Adsorbate[4] (g)	Adsorption Capacity[5] (%)	After Regeneration [6] (g)	Heel[7] (g)	Total Heel[8] (g)	Total Heel[9] (%)	
1	4.021	332.191	333.608	1.417	35.2	332.215	0.024	0.024	0.6	90
2	-	332.215	333.591	1.376	34.2	332.225	0.010	0.034	0.8	90
3	-	332.225	333.588	1.363	33.9	332.227	0.002	0.036	0.9	90
4	-	332.227	333.589	1.362	33.9	332.239	0.012	0.048	1.2	90
5	-	332.239	333.590	1.351	33.6	332.241	0.002	0.050	1.2	90

[1] Weight of dry bead activated carbon (Kureha)

[2] Weight of full reactor before adsorption

[3] Weight of full reactor after adsorption

[4] Weight of adsorbed adsorbate = After Adsorption- Before Adsorption

[5] Adsorption capacity = Mass adsorbed*100/Mass of BAC

[6] Weight of full reactor after regeneration

[7] Weight of adsorbate remaining on the BAC after regeneration = After Regeneration- Before Adsorption

[8] Weight of reactor after this regeneration test – weight of reactor before any adsorption

[9] Total heel*100/Mass of BAC

Adsorption of 2-heptanone

Table B- 19. Mass balance for 5-cycle adsorption/desorption test of 2-heptanone on heat treated Kureha BAC

Cycle	Mass balance									Adsorption Time (min)
	BAC[1] (g)	Before Adsorption[2] (g)	After Adsorption[3] (g)	Adsorbed Adsorbate[4] (g)	Adsorption Capacity[5] (%)	After Regeneration [6] (g)	Heel[7] (g)	Total Heel[8] (g)	Total Heel[9] (%)	
1	4.106	332.380	334.033	1.653	40.3	332.387	0.007	0.007	0.2	120
2	-	332.387	334.006	1.619	39.4	332.386	-0.001	0.006	0.1	120
3	-	332.386	333.999	1.613	39.3	332.389	0.003	0.009	0.2	120
4	-	332.389	334.003	1.614	39.3	332.392	0.003	0.012	0.3	120
5	-	332.392	334.010	1.618	39.4	332.399	0.007	0.019	0.5	120

[1] Weight of dry bead activated carbon (Kureha)

[2] Weight of full reactor before adsorption

[3] Weight of full reactor after adsorption

[4] Weight of adsorbed adsorbate =
After Adsorption- Before Adsorption

[5] Adsorption capacity = Mass adsorbed*100/Mass of BAC

[6] Weight of full reactor after regeneration

[7] Weight of adsorbate remaining on the BAC after regeneration =
After Regeneration- Before Adsorption

[8] Weight of reactor after this regeneration test – weight of reactor before any adsorption

[9] Total heel*100/Mass of BAC

Table B- 20. Mass balance for 5-cycle adsorption/desorption test of 2-heptanone on hydrogen-treated Kureha BAC

Cycle	Mass balance									Adsorption Time (min)
	BAC[1] (g)	Before Adsorption[2] (g)	After Adsorption[3] (g)	Adsorbed Adsorbate[4] (g)	Adsorption Capacity[5] (%)	After Regeneration [6] (g)	Heel[7] (g)	Total Heel[8] (g)	Total Heel[9] (%)	
1	4.043	332.600	334.139	1.539	38.1	332.609	0.009	0.009	0.2	120
2	-	332.609	334.123	1.514	37.4	332.612	0.003	0.012	0.3	120
3	-	332.612	334.125	1.513	37.4	332.612	0.000	0.012	0.3	120
4	-	332.612	334.123	1.511	37.4	332.612	0.000	0.012	0.3	120
5	-	332.612	334.103	1.491	36.9	332.613	0.001	0.013	0.3	120

[1] Weight of dry bead activated carbon (Kureha)

[2] Weight of full reactor before adsorption

[3] Weight of full reactor after adsorption

[4] Weight of adsorbed adsorbate =
After Adsorption- Before Adsorption

[5] Adsorption capacity = Mass adsorbed*100/Mass of BAC

[6] Weight of full reactor after regeneration

[7] Weight of adsorbate remaining on the BAC after regeneration =
After Regeneration- Before Adsorption

[8] Weight of reactor after this regeneration test – weight of reactor before any adsorption

[9] Total heel*100/Mass of BAC

Table B- 21. Mass balance for 5-cycle adsorption/desorption test of 2-heptanone on acid treated Kureha BAC

Cycle	Mass balance									Adsorption Time (min)
	BAC[1] (g)	Before Adsorption[2] (g)	After Adsorption[3] (g)	Adsorbed Adsorbate[4] (g)	Adsorption Capacity[5] (%)	After Regeneration [6] (g)	Heel[7] (g)	Total Heel[8] (g)	Total Heel[9] (%)	
1	4.034	332.315	333.857	1.542	38.2	332.350	0.035	0.035	0.9	120
2	-	332.350	333.847	1.497	37.1	332.371	0.021	0.056	1.4	120
3	-	332.371	333.850	1.479	36.7	332.374	0.003	0.059	1.5	120
4	-	332.374	333.838	1.464	36.3	332.390	0.016	0.075	1.9	120
5	-	332.390	333.840	1.450	35.9	332.403	0.013	0.088	2.2	120

[1] Weight of dry bead activated carbon (Kureha)

[2] Weight of full reactor before adsorption

[3] Weight of full reactor after adsorption

[4] Weight of adsorbed adsorbate = After Adsorption- Before Adsorption

[5] Adsorption capacity = Mass adsorbed*100/Mass of BAC

[6] Weight of full reactor after regeneration

[7] Weight of adsorbate remaining on the BAC after regeneration = After Regeneration- Before Adsorption

[8] Weight of reactor after this regeneration test – weight of reactor before any adsorption

[9] Total heel*100/Mass of BAC

Adsorption of n-butyl acetate

Table B- 22. Mass balance for 5-cycle adsorption/desorption test of n-butyl acetate on heat treated Kureha BAC

Cycle	Mass balance									Adsorption Time (min)
	BAC[1] (g)	Before Adsorption[2] (g)	After Adsorption[3] (g)	Adsorbed Adsorbate[4] (g)	Adsorption Capacity[5] (%)	After Regeneration [6] (g)	Heel[7] (g)	Total Heel[8] (g)	Total Heel[9] (%)	
1	4.013	330.349	332.017	1.668	41.6	330.350	0.001	0.001	0.0	120
2	-	330.350	332.019	1.669	41.6	330.353	0.003	0.004	0.1	120
3	-	330.353	332.018	1.665	41.5	330.357	0.004	0.008	0.2	120
4	-	330.357	332.018	1.661	41.4	330.356	-0.001	0.007	0.2	120
5	-	330.356	332.020	1.664	41.5	330.356	0.000	0.007	0.2	120

[1] Weight of dry bead activated carbon (Kureha)

[2] Weight of full reactor before adsorption

[3] Weight of full reactor after adsorption

[4] Weight of adsorbed adsorbate = After Adsorption- Before Adsorption

[5] Adsorption capacity = Mass adsorbed*100/Mass of BAC

[6] Weight of full reactor after regeneration

[7] Weight of adsorbate remaining on the BAC after regeneration = After Regeneration- Before Adsorption

[8] Weight of reactor after this regeneration test – weight of reactor before any adsorption

[9] Total heel*100/Mass of BAC

Table B- 23. Mass balance for 5-cycle adsorption/desorption test of n-butyl acetate on hydrogen-treated Kureha BAC

Cycle	Mass balance									Adsorption Time (min)
	BAC[1] (g)	Before Adsorption[2] (g)	After Adsorption[3] (g)	Adsorbed Adsorbate[4] (g)	Adsorption Capacity[5] (%)	After Regeneration [6] (g)	Heel[7] (g)	Total Heel[8] (g)	Total Heel[9] (%)	
1	4.075	330.900	332.530	1.630	40.0	330.901	0.001	0.001	0.0	120
2	-	330.901	332.530	1.629	40.0	330.901	0.000	0.001	0.0	120
3	-	330.902	332.529	1.627	39.9	330.902	0.001	0.002	0.0	120
4	-	330.903	332.514	1.611	39.5	330.902	0.000	0.002	0.0	120
5	-	330.903	332.520	1.617	39.7	330.903	0.001	0.003	0.1	120

[1] Weight of dry bead activated carbon (Kureha)

[2] Weight of full reactor before adsorption

[3] Weight of full reactor after adsorption

[4] Weight of adsorbed adsorbate =
After Adsorption- Before Adsorption

[5] Adsorption capacity = Mass adsorbed*100/Mass of BAC

[6] Weight of full reactor after regeneration

[7] Weight of adsorbate remaining on the BAC after regeneration =
After Regeneration- Before Adsorption

[8] Weight of reactor after this regeneration test – weight of reactor before any adsorption

[9] Total heel*100/Mass of BAC

Table B- 24. Mass balance for 5-cycle adsorption/desorption test of n-butyl acetate on acid-treated Kureha BAC

Cycle	Mass balance									Adsorption Time (min)
	BAC[1] (g)	Before Adsorption[2] (g)	After Adsorption[3] (g)	Adsorbed Adsorbate[4] (g)	Adsorption Capacity[5] (%)	After Regeneration [6] (g)	Heel[7] (g)	Total Heel[8] (g)	Total Heel[9] (%)	
1	4.001	329.905	331.490	1.585	39.6	329.909	0.004	0.004	0.1	120
2	-	329.909	331.484	1.575	39.4	329.916	0.007	0.011	0.3	120
3	-	329.916	331.489	1.573	39.3	329.914	-0.002	0.009	0.2	120
4	-	329.914	331.482	1.568	39.2	329.918	0.004	0.013	0.3	120
5	-	329.918	331.484	1.566	39.1	329.920	0.002	0.015	0.4	120

[1] Weight of dry bead activated carbon (Kureha)

[2] Weight of full reactor before adsorption

[3] Weight of full reactor after adsorption

[4] Weight of adsorbed adsorbate =
After Adsorption- Before Adsorption

[5] Adsorption capacity = Mass adsorbed*100/Mass of BAC

[6] Weight of full reactor after regeneration

[7] Weight of adsorbate remaining on the BAC after regeneration =
After Regeneration- Before Adsorption

[8] Weight of reactor after this regeneration test – weight of reactor before any adsorption

[9] Total heel*100/Mass of BAC